NUREG/IA-0028

International Agreement Report

Review of LOFT Large Break Experiments

OECD LOFT Project

Prepared by
S. M. Modro
Austrian Research Center Seibersdorf

S. N. Aksan
Paul Scherrer Institute

V. T. Berta
Idaho National Engineering Laboratory

A. B. Wahba
Gesellschaft fuer Reaktorsicherheit

Office of Nuclear Regulatory Research
U.S. Nuclear Regulatory Commission
Washington, DC 20555

October 1989

Prepared as part of
The Agreement on Research Participation and Technical Exchange
under the International Thermal-Hydraulic Code Assessment
and Application Program (ICAP)

Published by
U.S. Nuclear Regulatory Commission

NOTICE

This report was prepared under an international cooperative agreement for the exchange of technical information. Neither the United States Government nor any agency thereof, or any of their employees, makes any warranty, expressed or implied, or assumes any legal liability or responsibility for any third party's use, or the results of such use, of any information, apparatus product or process disclosed in this report, or represents that its use by such third party would not infringe privately owned rights.

Available from

Superintendent of Documents
U.S. Government Printing Office
P.O. Box 37082
Washington, D.C. 20013-7082

and

National Technical Information Service
Springfield, VA 22161

NUREG/IA-0028

International Agreement Report

Review of LOFT Large Break Experiments

OECD LOFT Project

Prepared by
S. M. Modro
Austrian Research Center Seibersdorf

S. N. Aksan
Paul Scherrer Institute

V. T. Berta
Idaho National Engineering Laboratory

A. B. Wahba
Gesellschaft fuer Reaktorsicherheit

Office of Nuclear Regulatory Research
U.S. Nuclear Regulatory Commission
Washington, DC 20555

October 1989

Prepared as part of
The Agreement on Research Participation and Technical Exchange
under the International Thermal-Hydraulic Code Assessment
and Application Program (ICAP)

Published by
U.S. Nuclear Regulatory Commission

NOTICE

This report documents work performed under the joint sponsorship of the Austrian Research Center Seibersdorf, Austria, the Paul Scherrer Institute, Switzerland, the Idaho National Engineering Laboratory, USA, and the Gesellschaft fuer Reaktorsicherheit (GRS), Federal Republic of Germany. The information in this report has been provided to the USNRC under the terms of an information exchange agreement between the United States and the Swiss Federal Office of Energy (BEW) (Agreement on Research Participation and Technical Exchange Between the United States Nuclear Regulatory Commission and the Swiss Federal Office of Energy (BEW) for and on Behalf of the Government of Switzerland in the USNRC Thermal Hydraulic Transients Program and the ECCS-Reflood Program of the Swiss Federal Institute for Reactor Research (EIR) Covering a Four-Year Period, May 2, 1984), and an information exchange agreement between the United States and the Federal Republic Republic of Germany (Technical Exchange and Cooperation Arrangement Between the United States Nuclear Regulatory Commission and the Bundesminister Fuer Forschung und Technologie of the Federal Republic of Germany in the field of reactor safety research and development, April 30, 1981). The BEW and GRS have consented to the publication of this report as a USNRC document in order that it may receive the widest possible circulation among the reactor safety community. Neither the United States Government nor the BEW nor the GRS or any agency thereof, or any of their employees, makes any warranty, expressed or implied, or assumes any legal liability of responsibility for any third party's use, or the results of such use, of any information, apparatus, product or process disclosed in this report, or represents that its use by such third party would not infringe privately owned rights.

ABSTRACT

Six non-nuclear and five nuclear large break loss-of-coolant experiments were performed in the Loss-of-Fluid Test (LOFT) PWR facility at the Idaho National Engineering Laboratory. These experiments provided a large amount of data necessary for evaluation and refinement of reactor system computer codes and had major impact on the understanding of large break loss-of-coolant accidents. An overview of these nuclear large break experiments performed under NRC and OECD LOFT programs is given and the major research results are presented.

EXECUTIVE SUMMARY

One of the most prominent reactor safety research facilities in the world was the Loss-of-Fluid Test (LOFT) facility. This unique facility, located at the Idaho National Engineering Laboratory, was a 50 MW(th) pressurized water reactor which was designed on the principal of volume scaling to simulate the major components and system responses of a four-loop commercial PWR during a hypothetical loss-of-coolant accident. Extensive research programs were conducted at the LOFT facility under the sponsorship of the U.S. NRC and later under the auspices of the Organization for Economic Cooperation and Development (OECD) with funding from a consortium of ten countries.

Forty-four experiments were completed over a nine year period ending with a severe fuel damage experiment in July 1985. These experiments were conducted at typical initial and boundary conditions associated with loss of coolant accidents and anticipated transients in commercial PWRs. The research program included six nuclear large break LOCA experiments the primary objective of which was to obtain data on LOCA phenomena and system response for a range of initial and boundary conditions which could be used for reactor system code development and assessment. The objectives, design, and principal results of the nuclear large break experiments are described. The important thermal-hydraulic phenomena measured in the large break transients and their significance are discussed in the principal areas of analysis that have been undertaken.

The sequence of large break LOCA experiments was conducted with increasing transient severity wherein the initial and boundary conditions increasingly approached licensing limits. The L2-2 Experiment was the first nuclear experiment conducted in the LOFT facility. This experiment was conducted with a maximum linear heat generation rate of 26.2 kW/m and with continuous primary coolant pump operation. Subsequent experiments were conducted with larger power densities and variations in primary coolant pump operating boundary conditions extending to an immediate trip at break initiation with a decoupling of the flywheels. The emergency core cooling

system (ECCS) operating conditions incorporated various degrees of degradation such as loss of ECC in the broken loop, as an example. The principal finding from the large break experiments is that, for the degrees of severity in initial and boundary conditions, the measured fuel cladding temperatures remained well below the peak cladding licensing limit temperatures.

The data obtained from the LOFT large break LOCA experiments provided new insight into phenomena associated with large break LOCA. One of the most important phenomena, observed for first time in the LOFT transients, is fuel cladding cooling/quench during blowdown. This phenomenon is very important to the degree of transient severity because it removes a large part of the stored energy from the fuel early in the transient. Extensive research was conducted to investigate the source and magnitude of the phenomenon. The cooling/quench phenomena was determined to be caused by system hydraulics in response to the operational characteristics of the primary coolant pumps relative to the transition from subcooled to saturated choked flow at the break. Two of the large break experiments, L2-5 and LP-LB-1, incorporated pump characteristics, by design, which did not produce the cooling/quench phenomena. The cooling/quench phenomena was allowed to occur by intent in other experiments, in order to quantify the phenomena and provide proof of the source. The significant finding was that the cooling/quench phenomena would occur in all conditions except for a pump trip concurrent with break initiation and decoupling from the flywheels. Similar limiting conditions are expected to be required to suppress the phenomena in commercial PWRs.

Because of the significance of this early cooling/quench phenomenon and because the systems codes at the state of development at that time were not able to calculate this phenomenon accurately, several specific investigations were conducted to determine quantitatively the effect of the LOFT cladding thermocouples on the measured cooling phenomena. The concern was that these thermocouples, by providing additional surface to the fuel cladding (fin effect), could affect the heat transfer characteristics and also may measure only very localized phenomena. Separate effect experiments in other facilities and analysis of LOFT data showed conclusively that the blowdown

cooling/quench in LOFT large break LOCA experiments is real. However, the thermocouples do reduce the blowdown peak cladding temperature because of an induced delay to DNB. Fin cooling subsequent to DNB was not found to adversely affect measurement accuracy. In contrast, surface cladding thermocouples are recognized to accelerate reflood quenching which occurs at much slower rates and lower pressure compared to the observed quenching during blowdown.

Examination of the LOFT large break LOCA experiments provided important insight on emergency core cooling (ECC) performance during large break transients. In general, the experiment results have shown that the ECCS operation even in degraded conditions was effective in core quench and transient recovery. The hot wall delay time was at most 2 s. Only a small part of the ECC water is lost through downcomer bypass to the broken loop cold leg indicating that the "downcomer bypass", which is one of the concerns in licensing, is not of concern. Cooling phenomena during blowdown can reduce the time to final quench by about 30% because the reflood quench is strongly dependent on cladding temperature levels at the end of the refill phase. Experiment LP-FP-1 which included upper plenum ECC injection showed that ECCS mode as being highly effective and that relatively small amounts of water can quench the core.

Predictions of the LOFT large break LOCA experiments were performed using older generations of computer codes such as RELAP4/MOD6. Newer codes such as RELAP5/MOD2 and TRAC-PF1/MOD1 are in the process of being assessed using LOFT data. Review of several recent calculations indicates that the hydraulic conditions in the LOFT experiments are calculated relatively well. However, cooling/quench phenomena associated with blowdown and reflood are not well calculated. The calculations do not correspond to measured cladding temperatures during blowdown even though the hydraulics appear to be reasonably calculated. These results indicate the need for acquiring better understanding of the early cooling/quench phenomena and consequent improvement in post-CHF heat transfer modeling.

In summary, the LOFT experiments showed that the core thermal response in a large break LOCA is much less severe than initially anticipated, and the ECCS as designed is effective in plant recovery.

ABBREVIATIONS AND ACRONYMS

BWR	Boiling Water Reactor
CCFL	Counter Current Flow Limitation
CFM	Central Fuel Module
CHF	Critical Heat Flux
COUPLE	General purpose heat conduction computer code
DNB	Departure from Nucleate Boiling
ECC	Emergency Core Coolant
ECCS	Emergency Core Coolant System
FEBA	Solid type electric heater rod
FRAP	Computer code for analysis of LWR fuel under transient condition
FRG	Federal Republic of Germany
GRS	Gesellschaft fuer Reaktorsicherheit mbH.
HPIS	High Pressure Injection System
ILCL	Intact Loop Cold Leg
INEL	Idaho National Engineering Laboratory
KFK	Kernforschungszentrum Karlsruhe
LANL	Los Alamos National Laboratory
LB	Large Break
LOCA	Loss-of-Coolant Accident
LOCE	Loss-of-Coolant Experiment
LOFT	Loss-of-Fluid Test
LPIS	Low Pressure Injection System
LTSF	LOFT Test Support Facility
LWR	Light Water Reactor
MLHGR	Maximum Linear Heat Generation Rate
NEPTUN	Reflood test facility - Paul Scherrer Institute, Switzerland
NRC	Nuclear Regulatory Commission
OECD	Organization for Economic Cooperation and Development
PBF	Power Burst Facility
PCP	Primary Coolant Pump
PPS	Plant Protection System
PSI	Paul Scherrer Institute (previously EIR (Switzerland))
PSS	Pressure Suppression System

ABBREVIATIONS AND ACRONYMS
(Continued)

PWR	Pressurized Water Reactor
QOBV	Quick-Opening Blowdown Valve
RCP	Reactor Coolant Pump
REBEKA	Cartridge type electric heater rod
RELAP	Thermal-hydraulic computer system code for LWR transient and LOCA analysis - INEL
RCS	Reactor Coolant System
RNB	Return to Nucleate Boiling
SG	Steam Generator
SPND	Self Powered Neutron Detectors
TC	Thermocouple
T/H	Thermal-Hydraulic
TRAC	Thermal-hydraulic computer system code for PWR transient and LOCA analysis, three-dimensional capability - LANL

ABBREVIATIONS AND ACRONYMS

BWR	Boiling Water Reactor
CCFL	Counter Current Flow Limitation
CFM	Central Fuel Module
CHF	Critical Heat Flux
COUPLE	General purpose heat conduction computer code
DNB	Departure from Nucleate Boiling
ECC	Emergency Core Coolant
ECCS	Emergency Core Coolant System
FEBA	Solid type electric heater rod
FRAP	Computer code for analysis of LWR fuel under transient condition
FRG	Federal Republic of Germany
GRS	Gesellschaft fuer Reaktorsicherheit mbH.
HPIS	High Pressure Injection System
ILCL	Intact Loop Cold Leg
INEL	Idaho National Engineering Laboratory
KFK	Kernforschungszentrum Karlsruhe
LANL	Los Alamos National Laboratory
LB	Large Break
LOCA	Loss-of-Coolant Accident
LOCE	Loss-of-Coolant Experiment
LOFT	Loss-of-Fluid Test
LPIS	Low Pressure Injection System
LTSF	LOFT Test Support Facility
LWR	Light Water Reactor
MLHGR	Maximum Linear Heat Generation Rate
NEPTUN	Reflood test facility - Paul Scherrer Institute, Switzerland
NRC	Nuclear Regulatory Commission
OECD	Organization for Economic Cooperation and Development
PBF	Power Burst Facility
PCP	Primary Coolant Pump
PPS	Plant Protection System
PSI	Paul Scherrer Institute (previously EIR (Switzerland))
PSS	Pressure Suppression System

ABBREVIATIONS AND ACRONYMS
(Continued)

PWR	Pressurized Water Reactor
QOBV	Quick-Opening Blowdown Valve
RCP	Reactor Coolant Pump
REBEKA	Cartridge type electric heater rod
RELAP	Thermal-hydraulic computer system code for LWR transient and LOCA analysis - INEL
RCS	Reactor Coolant System
RNB	Return to Nucleate Boiling
SG	Steam Generator
SPND	Self Powered Neutron Detectors
TC	Thermocouple
T/H	Thermal-Hydraulic
TRAC	Thermal-hydraulic computer system code for PWR transient and LOCA analysis, three-dimensional capability - LANL

CONTENTS

FIGURES

TABLES

REVIEW OF LOFT LARGE BREAK EXPERIMENTS

1. INTRODUCTION

The Loss-of-Fluid Test (LOFT) facility in its form during the U.S. Nuclear Regulatory Commission (NRC) sponsored experimental program and during the OECD sponsored experimental program, had its beginnings in May 1967. At that time the basic mission of LOFT was changed to be in compliance with the developing emphasis in the nuclear industry to include engineered safeguards in nuclear plant designs which would bring a nuclear plant to safe shutdown condition following a loss-of-coolant accident (LOCA). Over the succeeding two years the LOFT program objectives [1] and the facility design required to meet those program objectives [2] were developed and finalized. The LOFT program objectives were:

1. Provide data required to evaluate the adequacy of and improve the analytical methods currently used to predict:

   a. The LOCA response of large Pressurized Water Reactors (PWRs)
   b. The performance of engineered safety features with particular emphasis on Emergency Core Cooling Systems (ECCSs)
   c. The quantitative margins of safety inherent in the performance of the engineered safety features.

2. Identify and investigate any unexpected events or threshold(s) in the response of either the plant or the engineered safety features and develop analytical techniques that adequately describe and account for the unexpected behavior(s).

3. Provide experience in the application of standards from the Division of Reactor Development and Technology, and other standards and codes generally applicable to large PWRs by their use and evaluation by the LOFT Program. This objective was satisfied during design and construction of the LOFT facility.

The new facility design was required, therefore, to model, as nearly as possible, a "typical current generation large PWR primary coolant system, reactor system, and ECCS."

The LOFT PWR design was based on the contention at that time that the large break LOCA (double-ended offset shear of a primary coolant pipe) in a cold leg of a PWR primary coolant system would provide the most severe test of the ECCS. Consequently, the LOFT PWR design incorporated the intact loop-broken loop concept wherein the intact loop was an operating loop with active components and the broken loop was a "simulator loop" with inactive components which simulated pressure differentials only [2].

Technology available to understand and calculate LOCA phenomena and performance of the ECCS was extremely limited at the time LOFT became operational. There were few other experimental facilities to aid in the evaluation of ECCS performance and available computer codes were too simplified to calculate complex LOCA phenomena that were theorized to occur. The LOFT experimental program, therefore, was based on a step-wise approach to an "integral" system large break LOCA with the core at typical commercial plant power densities and with a fully operational ECCS at typical commercial plant set points. The experimental approach to this LOCA is summarized in Table 1. The integral system LOCA at typical PWR operating conditions was achieved in Experiment L2-3. Subsequent large break LOCA experiments, also listed in Table 1, were conducted to study LOCA phenomena and system response for other sets of initial and boundary conditions, and to provide wide range data for code development and application to commercial plant designs. The six LOFT large break nuclear experiments, and the LOCA phenomena and ECCS behavior in them, comprise the subject of this report. More detailed information on the approach to the LBLOCA and the results of the NRC sponsored experiments is contained in References 1 and 3. A summary of each of the nuclear experiments is given in Section 3.

TABLE 1. LOFT EXPERIMENTAL APPROACH TO A LARGE BREAK LOCA AT TYPICAL PWR CONDITIONS AND SUBSEQUENT NUCLEAR LARGE BREAK EXPERIMENTS

Experiments	Objectives (summarization)	Significant Plant Characteristics/Parameters
Nonnuclear L0 Series	Qualify components and operational procedures for valves simulating a pipe break.	Vent submergence variations from 13.5 cm to 56.2 cm.
L0-2 L0-3 L0-3A L0-3B L0-3C L0-4 L0-5 L0-8 L0-9 L0-10	Verify pressure suppression system capability to withstand structural loading. Provide data to determine maximum vent submergence in the pressure suppression tank for complete RCS blowdown	Coolant injection limited to 0.048 m^3 through each of two quick-opening blowdown valves (QOBVs). Experiments included either one or both valve openings. Injected mass is sufficient to test dynamic loading capacity of the PSS. Injected coolant temperature typical of PWR steady state cold leg temperature.
Nonnuclear L1 Series		
L1-1	Verification of system and component performance at less than maximum severity blowdown conditions. Evaluate QOBV and PSS performance.	Core simulator in place for pressure drop simulations. Break size reduced to one-half maximum size for double-ended offset shear. Primary coolant at typical PWR pressure and cold leg temperature.
L1-2	Provide thermal-hydraulic data for an isothermal LOCA with maximum break area and no ECCS operation.	High intact loop flow resistance. ECCS initiated after system thermal stabilization to obtain data on hot wall effects. Core simulator in place.

TABLE 1. (Continued)

Experiments	Objectives (summarization)	Significant Plant Characteristics/Parameters
LI-3 LI-3A	Provide thermal-hydraulic data for an isothermal LOCA with ECCS injection into the lower plenum.	Low intact loop flow resistance. Core simulator in place.
	Provide data on intact loop flow resistance for comparison to LI-2.	
LI-4	Provide thermal-hydraulic data for an isothermal LOCA with ECCS injection into the cold leg.	Low intact flow resistance. Core simulator in place.
	Provide data on PCS operation and rapid depressurization with borated water.	Borated water used for the first time.
	Provide data on ECC bypass and mixing (in conjunction with LI-3A).	
LI-5	Evaluate core mechanical response to LOCA depressurization loads.	Nuclear core installed, all control rods in and coolant boration > 3000 ppm.
	Evaluate system data with nuclear core installed.	Low intact loop resistance. This condition maintained for all subsequent nuclear large break LOCA experiments.
	Provide isothermal base case LOCA for comparison for nuclear LOCAs.	Pressure and temperature conditions typical of PWR hot stand by conditions.
	Provide operator training and operating procedure verification for nuclear test control with the reactor shutdown.	Unpressurized fuel rods.
	Provide thermal-hydraulic data for ECCS injection into the cold leg.	

TABLE 1. (Continued)

Experiments	Objectives (summarization)	Significant Plant Characteristics/Parameters
Nuclear L2 Series	Provide data to analyze.	Configuration identical to L1-5 except for nuclear core power generation and system initial conditions in the core-to-SG inlet region.
L2-2	1. DNB and RNB 2. Post-CHF heat transfer 3. Fuel rod thermal MLHGR of 26.2 kW/m 4. Thermal-hydraulic for 67% nominal hot-leg-to-cold leg DT. 5. ECCS performance and system refill, reflood, and core quench.	
L2-3	Provide data on core-wide and spatial variations of fuel rod cladding thermal response.	System configuration identical to L2-2 except for reactor power increase to a MLHGR of 39.4 kW/m.
Integral system large break LOCA at typical PWR conditions.	Provide thermal-hydraulic data for a large break LOCA at typical PWR steady state operating conditions to identify phenomena and effects on fuel rod cladding thermal response. Provide data on ECCS performance, system refill and reflood, and core quench for these LOCA conditions.	
L2-5	Provide data to determine conservatisms in Appendix K assumptions for LOCA from typical PWR operating conditions and for the case of early ANB suppression.	System configuration identical to L2-2 except for reactor power MLHGR of 40.1 kW/m. Early PCP trip with flywheels disconnected for rapid coastdown.

TABLE 1. (Continued)

Experiments	Objectives (summarization)	Significant Plant Characteristics/Parameters
OECD-LOFT Program		
LP-02-6	Provide T/H data on LOCA with design basis boundary conditions on both unpressurized and prepressurized fuel rods to determine safety margins in ECC licensing.	System configuration identical to L2-2 except for CFM which had all but outer row fuel rods prepressurized to 2.41 MPa. Boundary conditions included loss-of-offsite power coincident with LOCA initiation and United States minimum ECC injection assumptions.
LP-LB-1	Maximize the fraction of the core that has not rewet by the end of blowdown. Provide system and core thermal-hydraulic data for a LOCA under these conditions. Provide data on reflood initiation of high temperature and significant downcomer head conditions.	System configuration identical to L2-2. MLHGR of ~52 kW/m. Boundary conditions included loss-of-offsite power coincident with LOCA initiation and United Kingdom (UK) minimum safeguard ECC injection. PCP trip and flywheel disconnect within 1s of LOCA initiation.
LP-FP-1	Obtain data on the release of fission products form the fuel cladding gap both into the vapor environment in the core during heatup and into water after the subsequent reflood. Obtain data on fission product transport through and out of the reactor coolant system in the vapor environment.	System configuration identical to L-2 except for: (1) Special CFM containing 24 6-wt% enriched fuel rods (all others standard enriched; 22 of the 6-wt% rods pressurized) and a flow shroud to channel fission product release. (2) Addition of an upper plenum ECC injection nozzle. (3) ECCS designed and scaled to FRG KWU 1300-MWe reference plant ECCS. (4) Addition of a special fission product sampling and measurement system. ECCS delayed until fuel cladding ballooning and rupture occurred on 6% enriched fuel rods. Fission product transport path was the broken loop hot leg. Broken loop cold leg closed after

The large break loss-of-coolant accident (LBLOCA) data from the LOFT experimental program represents the only integral system data from a facility that has a nuclear core. As such, the LOFT data is instrumental in the current USNRC effort to quantify calculational uncertainty for the thermal-hydraulic system codes. The LOFT system response to the simulation of a LBLOCA revealed phenomena which had not previously been observed. Specifically, the first nuclear experiment, L2-2, showed significant fuel cladding cooling during blowdown which included a complete quench. Subsequent analyses, the results of which were experimentally confirmed, showed that this phenomena was linked to system hydraulics inclusive of the operating characteristics of the primary coolant pumps. Section 4 includes an analysis of this phenomena.

Also included in Section 4 is an extensive review of separate effects experiment results in concert with the evaluation of a spectrum of LOFT LBLOCA experimental data which addresses the question of the validity of the observed blowdown cooling phenomena. Questions arose concerning this data because (1) current generation codes cannot predict the degree of cooling observed during blowdown, (2) externally mounted cladding thermocouples are known to introduce fin cooling effects, and (3) the LOFT nuclear rod temperature data differed significantly from electric heat rod data. In summary, analyses of the available data have led to the conclusion that the observed blowdown cooling phenomena in the LOFT LBLOCA experiments actually occurred. Further, the externally mounted thermocouples do have some bias that results in lower measured temperatures relative to bare fuel rod cladding temperature. An appropriate correction must be applied to both blowdown and reflood cladding temperature data. Finally, the external thermocouples did influence but did not mask the fuel cladding temperature response to the system hydraulics. The appropriate correction factors to be applied to the temperature data have not been resolved as yet; however, in view of the conclusions reached, the LOFT LBLOCA experiments and the phenomena within them are discussed in Section 3 using measured fuel cladding temperature data. Determination of the correction factors will not affect the interpretation of the phenomena observed.

2. THE LOFT FACILITY

The LOFT Experimental Facility was a 50 MW (th) pressurized water reactor system designed to simulate the major components and system responses of a commercial PWR during postulated loss-of-coolant accidents (LOCA) and anticipated transients. The LOFT Experimental Facility shown in Figure 1 is described in detail in Reference 2. The facility consisted of five major systems: the Reactor System with the nuclear core (Figure 2); Primary Coolant System; Blowdown Suppression System; Emergency Core Cooling System; and a Secondary Coolant System. These systems were instrumented to measure the behavior of system parameters during the experiments.

The Reactor System included a nuclear 1.68 m long core arranged in nine fuel rod bundles (four triangular and five square). The LOFT fuel was designed to have the same physical, chemical and metallurgical properties as commercial fuel.

The Primary Coolant System consisted of an operating loop (with a steam generator, two primary coolant pumps in parallel, pressurizer and connecting piping) representing three intact loops of a four loop PWR, and a "broken loop" which simulated the broken loop of a four loop PWR during LOCA conditions. The broken loop consisted of hot and cold legs which connect the Reactor System to the Pressure Suppression System, and are equipped with steam generator and pump simulators and quick-opening blowdown valves. The piping arrangement was variable to simulate hot or cold leg breaks.

The LOFT Blowdown Suppression System was designed to simulate the containment back pressure in large PWRs during LOCA events. It consisted of a large pressure suppression tank, downcomers and a header connected to the primary system via the quick-opening blowdown valves.

The emergency core cooling system (ECCS) consists of the same three systems currently in commercial PWRs -- the high pressure injection system (HPIS), the accumulator, and the low pressure injection system (LPIS). The systems are actuated similarly to their generic counterparts and inject

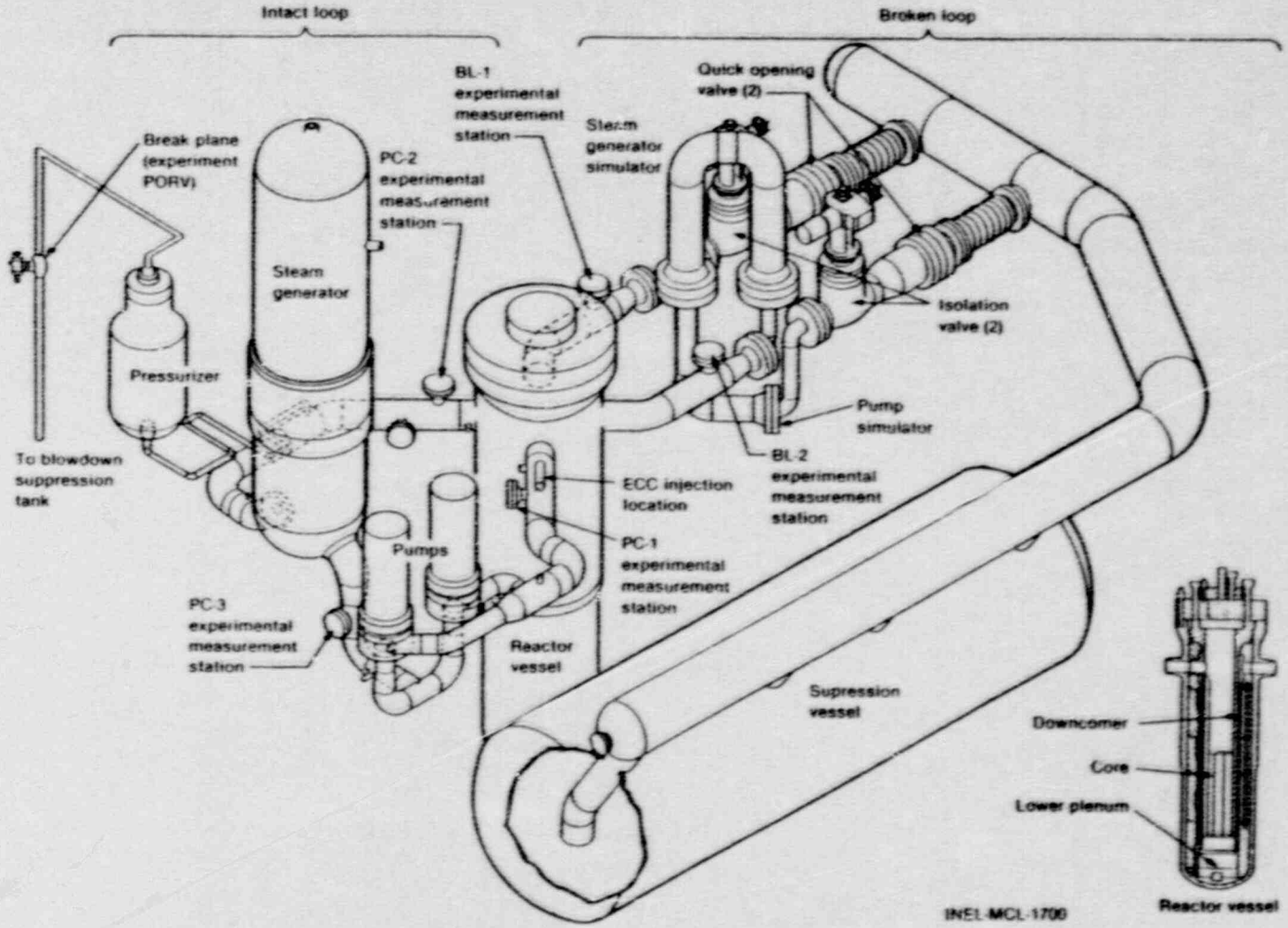

Figure 1. Axonometric projection of LOFT system configuration for Experiment L2-2.

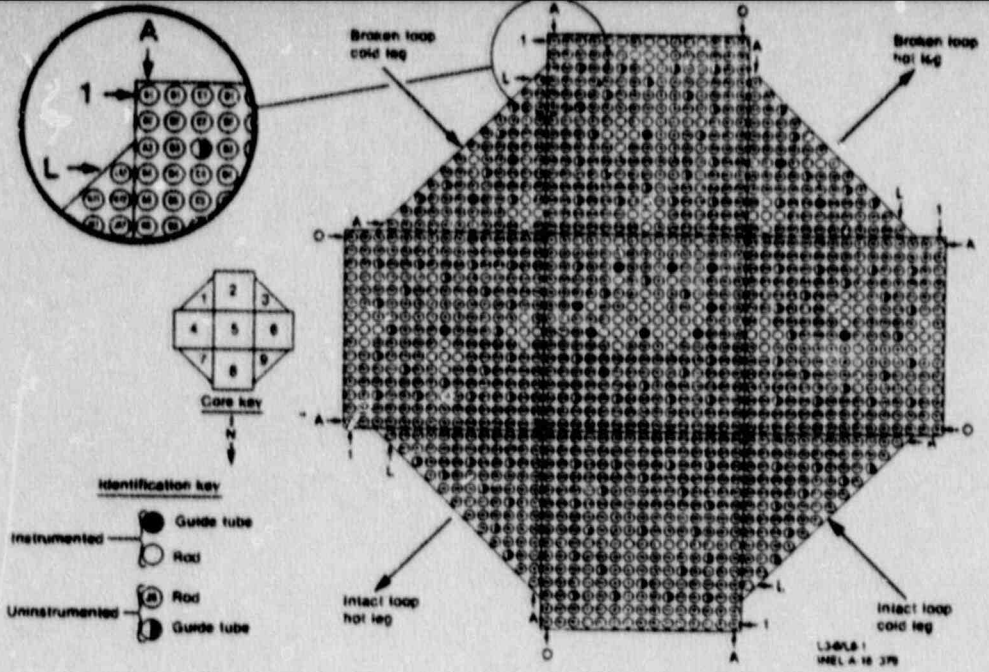

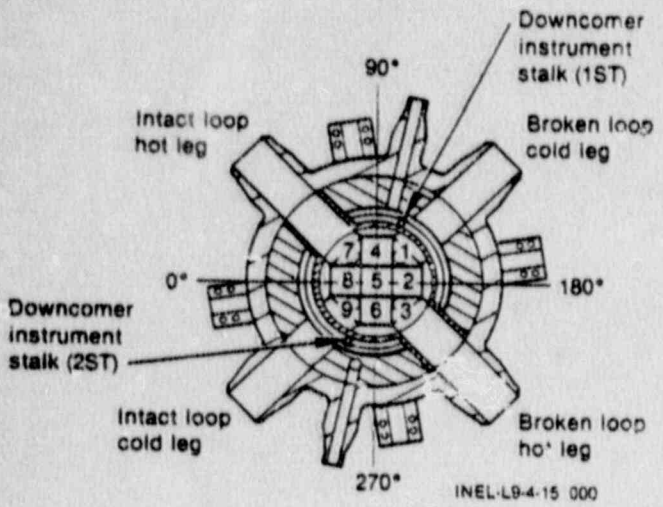

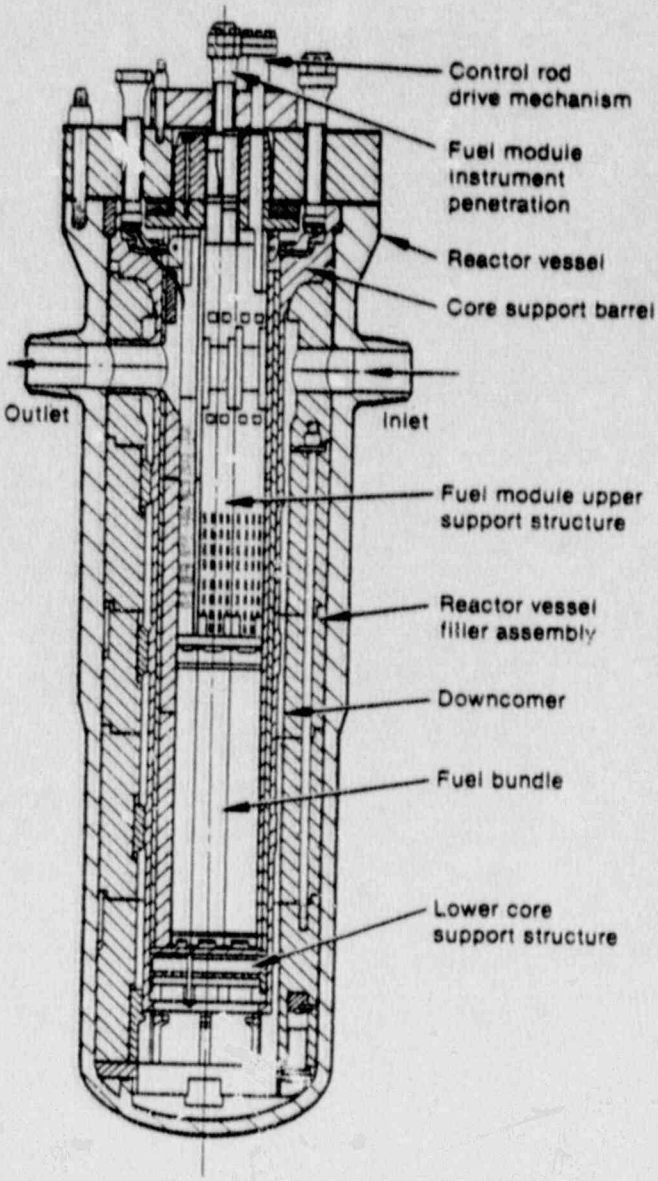

Figure 2. LOFT reactor vessel and core.

scaled amounts of emergency core coolant (ECC) typical of the ECC delivery behavior in commercial PWRs. The LOFT ECCS has the capability of injecting ECC to any of several locations including the intact loop hot or cold legs, and the reactor vessel downcomer, lower plenum, or upper plenum. An identical backup ECCS is also available which functions separately from the ECCS used in a LOCE.

The LOFT Secondary System was designed to remove the heat transferred into the steam generator to the environment. This system however could not be controlled for full simulation of secondary system response in large PWRs.

The component and system volumes of the Reactor and Primary Coolant Systems were designed proportional to their respective volumes in a commercial PWR with the ratio of the two system powers as the proportionality factor [4]. The design objective for the LOFT facility was to produce the significant thermal hydraulic phenomena with approximately the same conditions and sequence of events that could occur during postulated accidents in commercial PWR systems. The LOFT scale model of the generic PWR that resulted is summarized in Table 2 which contains comparisons of geometric and physical parameters between LOFT and commercial PWRs. The physical parameters listed are nominal operating conditions in the Westinghouse 4-loop ZION PWR and in the LOFT system prior to the LOCE designated L2-3.

The LOFT reactor core is about one-half the length of typical reactor cores in commercial plants. However, this is the only compromise made in the nuclear fuel for the LOFT core. PWR 15x15 array fuel rod assemblies are used in the geometry shown in Figure 2. The triangular corner assemblies are partial square assemblies for simulation of a more circular core. The outer four square fuel assemblies have reactor control rods in the guide tubes. The center fuel assembly is the most heavily instrumented assembly with instruments placed in the vacant guide tubes as well as on the fuel rods. The LOFT fuel assemblies are complete with upper and lower end boxes and fuel rod spacer grids at five elevations.

TABLE 2. LOFT - COMMERCIAL PWR COMPARISONS

Item	LOFT		TROJAN	
	Volume (m^3)	% Total	% Total	Volume (m^3)
Reactor Vessel				
Outlet Plenum	0.95	12.51	15.95	55.47
Core and Bypass	0.31	4.12	7.50	26.05
Lower Plenum	0.71	9.32	8.58	29.73
Downcomer and Inlet Annulus	0.69	9.00	5.89	20.42
Subtotal		34.95	37.95	
Intact Loop[a]				
Hot Leg Pipe	0.35	4.60	1.94	6.71
Cold Leg Pipe	0.37	4.85	2.08	7.22
Pump Suction Pipe	0.33	4.38	3.09	10.70
Steam Generator	1.45	18.97	26.40	91.49
Pump	0.20	2.60	1.96	6.80
Subtotal		35.40	35.47	
Broken Loop				
Cold Leg to Break[b]	0.16	2.16	1.72	5.97
Vessel to Steam generator	0.15	1.98	0.65	2.24
Steam Generator	0.52	6.88	8.80	30.50
Pump	0.05	0.72	0.65	2.27
Additional Volume Part of Outlet Plenum	0.19	2.46	N/A	N/A
Additional Volume Part of Inlet Plenum	0.22	2.83	N/A	N/A
Subtotal		17.03	11.17	
Pressurizer	0.96	12.62	14.7	50.97
Total	7.63	100.00	100.00	346.60

TABLE 2. (Continued)

Item	LOFT	ZION
Core (Loft L2-3, ZION nominal conditions included)		
Fuel rod number	1300	39372
Length (m)	1.68	3.68
Inlet flow area (m^2)	0.16	4.96
Coolant volume (m^3)	0.295	20.227
Maximum linear heat generation rate (KW/m)	39.4	39.4
Coolant temperature rise (K)	32.2	32.2
Power (MW)	36.7	3540.5
Peaking Factor	2.34	1.60
Power/coolant volume (MW/m^3)	124.4	175.0
Core volume/system volume	.038	.057
Mass flux ($Kg/s\text{-}m^2$)	1248.8	3707.3
Core mass flow/system volume ($Kg/s\text{-}m^3$)	25.6	51.7

a. TROJAN values are for three loops combined
b. Includes pump suction piping

The LOFT facility is augmented with an extensive "experimental" measurements system (2) in addition to the normal PWR instrument systems for reactor operation and control. State measurements of the coolant in the primary system provide the capability of following the redistribution of mass and energy in the primary coolant system following the initiation of a transient. Extensive thermal measurements in the nuclear core provide detailed information on the thermal response of the fuel cladding. Nuclear measurements in the core assist in determining the initial or steady state energy distribution. The philosophy followed on measurement locations in the nuclear core, as shown in Figure 2, was to instrument one-half of the core on a circular symmetry basis with emphasis on the center fuel assembly.

3. LOFT NUCLEAR LARGE BREAK EXPERIMENTS

Six nuclear large break LOCA experiments were conducted in the LOFT facility as described in Table 1. Three of the experiments, L2-2, L2-3 and L2-5 were conducted as a part of the U.S. NRC LOFT Program. The other three experiments, LP-02-6, LP-LB-1, LP-FP-1 were conducted as part of the international OECD LOFT Program. The principal phenomena and events in these large break LOCA transients are summarized in this section. The initial conditions for these experiments are summarized in Table 3. Additionally to these six experiments we will discuss the experiment LP-FP-1A. This was aborted experiment LP-FP-1. Although it was only short blowdown, data of this experiment were very valuable to understand the thermal-hydraulic processes in the actual experiment LP-FP-1.

Along with the experiment description, a review of experiment predictions and post-experiment calculations are presented. Appendix A summarizes some recent code analyses of the LOFT large break LOCA experiments and gives a brief description of the three codes used in these analysis: RELAP5, TRAC and DRUFAN.

3.1 Experiment L2-2

The basic objective of this first nuclear large break experiment [5], which was conducted in December 1978, was to provide integrated system data on thermal-hydraulics and fuel behavior during a 200% cold leg break (double-ended offset pipe shear) LOCA. The configuration of the facility for this experiment is shown in Figure 1. The experiment was conducted from 50% power (25 MW, 26.38 kW/m maximum linear heat generation rate), a specification that resulted from the planned stepwise approach to the large break LOCA at typical PWR operating conditions. Prior to experiment initiation, the reactor was operated at steady state to build in decay heat equivalent to approximately 90 percent of that for infinite operation at the initial condition power level. This criteria was used for all LOFT nuclear experiments.

TABLE 3. LOFT PWR OPERATING CONDITIONS PRIOR TO THE LARGE BREAK EXPERIMENTS

Parameter	L2-2	L2-3	L2-5	LP-02-6	LP-LB-1	LP-FP-1
Primary Coolant System						
Mass flow rate (kg/s)	194.2	199 ± 6.3	192.4 ± 7.8	248.7 ± 2.6	305.8 ± 2.6	486.7 ± 2.5
Pressure (MPa)	15.64	15.06 ± 0.03	14.94 ± 0.06	15.09 ± 0.08	14.90 ± 0.08	14.77 ± 0.07
Cold leg temperature (K)	557.7	560.7 ± 1.8	556.6 ± 4.0	555.9 ± 1.1	556 ± 1	563.2 ± 1.1
Hot leg temperature (K)	580.4	592.9 ± 1.8	589.7 ± 1.6	589.0 ± 1.0	587.8 ± 1.2	577.6 ± 0.8
Boron concentration (ppm)	838	679 ± 4	668 ± 15	512 ± 15	513 ± 15	612 ± 15
Reactor Vessel						
Power level (MW)	24.88	36.0 ± 1.0	36.0 ± 1.2	46.0 ± 1.2	49.3 ± 1.2	37.0 ± 1.2
Maximum linear heat generation rate (kW/m)	26.37	39.0 ± 3.0	40.1 ± 3.0	48.8 ± 3.6	51.7 ± 3.6	51.2 ± 3.6
Control rod position (above full-in position, (m)	1.37	1.37 ± 0.01	1.376 ± 0.010	1.381 ± 0.0002	1.455 ± 0.0002	1.38 ± 0.002
Pressurizer						
Steam volume (m^3)	0.353	0.293 ± 0.008	0.32 ± 0.02	0.39 ± 0.02	0.37 ± 0.02	0.27 ± 0.02
Water volume (m^3)	0.607	0.670 ± 0.008	0.61 ± 0.02	0.607 ± 0.02	0.56 ± 0.02	0.66 ± 0.02
Water temperature (K)	619	615.3 ± 3.0	615.0 ± 0.3	615.6 ± 5.8	615 ± 5.8	616.2 ± 5.8
Pressure (MPa)	15.62	15.06 ± 0.03	1.14 ± 0.3	15.3 ± 0.11	14.92 ± 0.11	14.73 ± 0.11
Liquid level (m)	1.089	1.19 ± 0.01	(a)	1.04 ± 0.04	1.04 ± 0.04	1.23 ± 0.04
Broken Loop						
Hot leg temperature (K)	561.2	565.5 ± 1.8	561.9 ± 4.3	560 ± 6	561 ± 6	564.8 ± 1.8
Cold leg temperature (K)	555	554.3 ± 1.8	554.3 ± 4.2	553 ± 6	552 ± 6	561.4 ± 1.5
Steam Generator Secondary Side						
Water level (m)	3.14	3.11 ± 0.025	(a)	3.28 ± 0.6	3.19 ± 0.02	3.10 ± 0.06
Water temperature (K)	553	482.1 ± 3	547.1 ± 0.6	538 ± 1.5	528 ± 1.5	548.5 ± 1.5
Pressure (MPa)	6.25	6.18 ± 0.08	5.85 ± 0.06	5.63 ± 0.2	5.53 ± 0.02	6.41 ± 0.08
Mass flow rate (kg/s)	12.67	19.5 ± 0.4	19.1 ± 0.4	24.3 ± 0.4	25.4 ± 0.4	19.0 ± 0.4

(a) Measurement failed.

The experiment was initiated by opening the quick-opening blowdown valves. The reactor was scrammed automatically on low system pressure in 1.7 s. The ECC flow was directed into the intact loop cold leg, beginning with HPIS flow at 12 s after blowdown initiation and accumulator injection at 18 s at 4.2 MPa primary system pressure. The primary coolant pumps were operating during the blowdown and were tripped at 200s. Detailed experiment results are presented in Reference 6.

While the hydraulic behavior of the system was approximately as predicted, the thermal behavior of the core was surprising. The cladding temperature rose initially as predicted but an unpredicted core wide cooling started at about 5.5 s leading to a complete core quench. The maximum core temperature of 789K was reached during the initial temperature rise. Figure 3 shows the measured and predicted fuel cladding temperatures for the center fuel module.

The early rewet was caused by resumption of positive core flow when the broken loop cold leg break flow transitioned from subcooled to saturated critical at about 3.4 s which resulted in a decrease of the mass flow rate. At this time the cold leg coolant in the operating loop was still under subcooled conditions with pumps operating. This condition resulted in an increase in reactor vessel coolant inventory as more coolant flowed into the vessel than flowed out (Figure 4). This additional fluid was carried, due to the positive core flow, through the core causing a complete fuel rod rewet at 5.5 s.

The large difference between the predicted and measured core thermal behavior was concluded to be caused by at least one and possibly all of the following:

- inadequate modeling of initial fuel stored energy
- inadequate heat transfer models
- insufficiently accurate system hydraulic calculations
- presence of thermocouples on the surface of fuel cladding

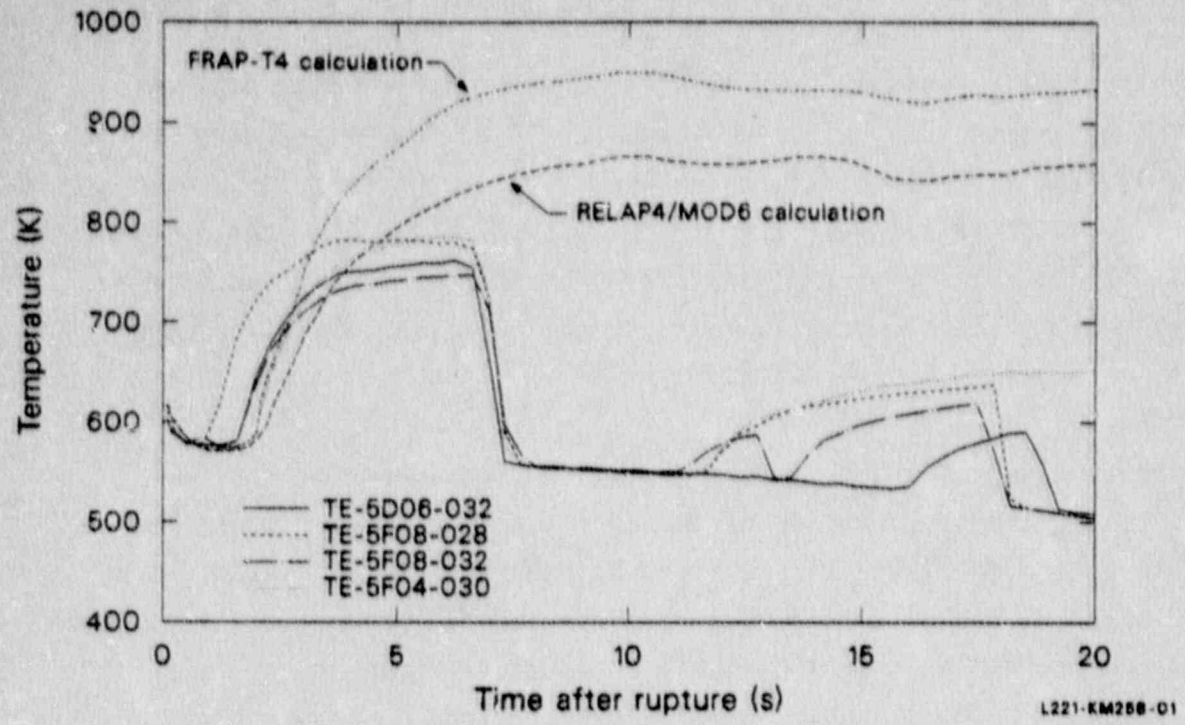

Figure 3. Predicted and measured fuel rod cladding temperature near midplane of center fuel module for Experiment L2-2.

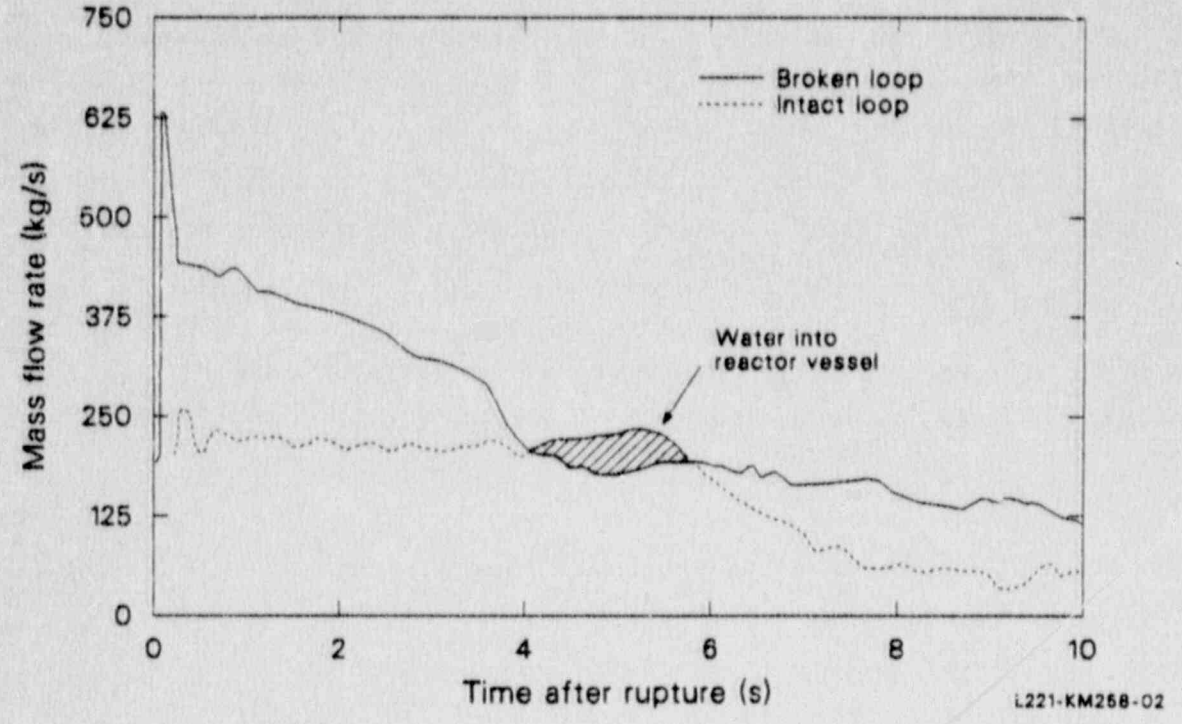

Figure 4. Mass flow rates in cold legs of intact and broken loops during Experiment L2-2.

The problem of inadequate modeling of initial fuel stored energy was eliminated as a possibility after inspection of the experiment data which showed that the difference was primarily caused by heat removal mechanisms rather than the heat supply mechanisms.

Detailed examination [7] of the predictions revealed that the code calculated in the 3 to 10 s interval a stagnation at the core outlet, whereas the experiment data indicated strong upward flow. Comparisons made of the predicted and measured mass flow rates in the intact loop cold leg showed reasonable agreement between prediction and calculations. The comparison of break mass flow rate showed however strong overprediction of the cold leg break flow by as much as 120 kg/s. Overprediction of the break flow was responsible for miscalculation of core hydraulics.

3.2 Experiment L2-3

Experiment L2-3, the second nuclear large break LOCA experiment, was performed in May 1979. The major objective [5] of this experiment was to measure thermal-hydraulic phenomena and effects on fuel rod cladding thermal response for a higher initial power level. The LOFT system configuration for this experiment was identical to the configuration for experiment L2-2 with the exception that the power was increased to 36.7 MW (39.4 kW/m maximum linear heat generation rate). The core power density, the core coolant temperature rise and the system pressure corresponded to typical operating conditions in a pressurized water reactor power plant.

The experiment was initiated by opening the quick-opening blowdown valves. Reactor scram was completed 1.7 seconds later, HPIS injection was initiated at 14 s, accumulator injection at 17 s at 4.18 MPa system pressure, and LPIS injection at 29 s. The core was reflooded at 55 s. During this experiment, as in experiment L2-2, the primary coolant pumps operated throughout the experiment and were tripped at 200 s. Detailed results of this experiment are presented in Reference 8. The core thermal response in this experiment was similar to the core thermal response in the Experiment L2-2, (Figure 5). The differences in the temperature magnitudes

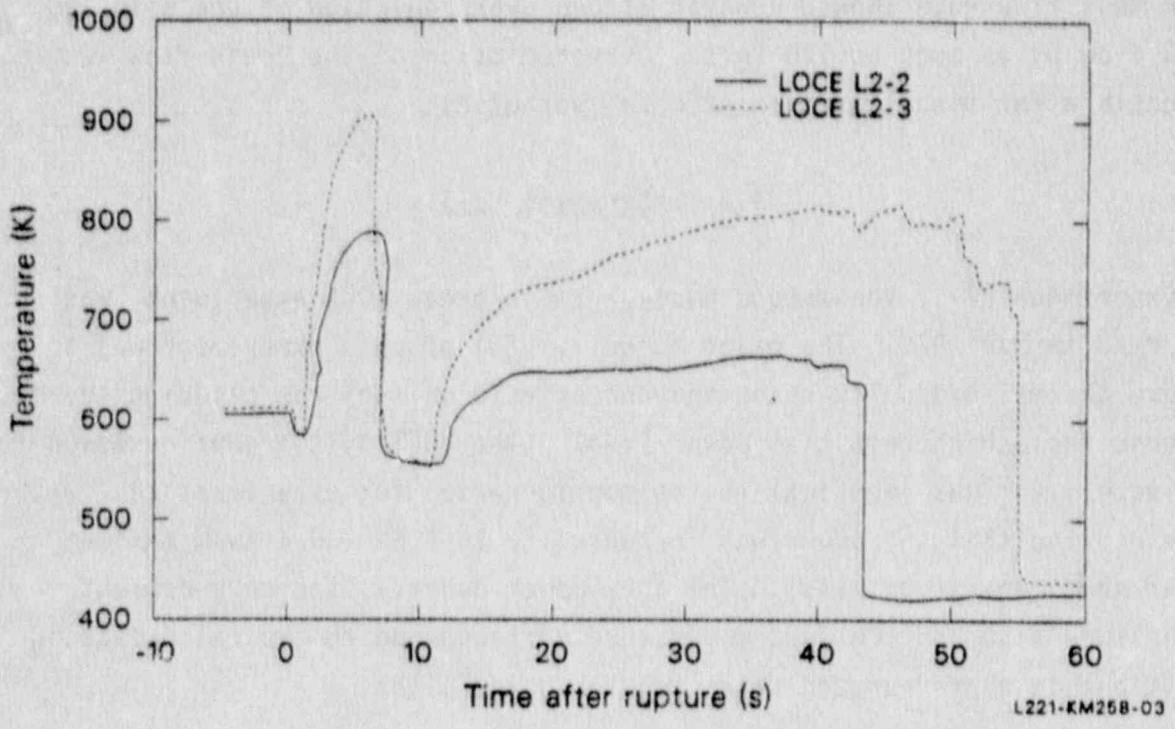

Figure 5. Temperature of fuel rod cladding during Experiments L2-2 and L2-3.

and event occurrence times is consistent with the core power and initial core fluid temperature rise. Measured peak cladding temperature was 789K in Experiment L2-2 and 914K in Experiment L2-3. In both experiments the maximum peak cladding temperature occurred during the blowdown phase. In both experiments an early cladding rewet was observed which was caused by the same phenomena. As in Experiment L2-2 the transition from subcooled to saturated critical flow in the broken loop cold leg occurred about 2 s earlier than the fluid saturation in the cold leg of the operating loop resulting in more coolant being delivered to the downcomer than removed. This additional coolant traversed the core from bottom to top and caused fuel cladding rewet for a short period of time.

The experience from the sensitivity studies performed after Experiment L2-2 was applied to the prediction of the Experiment L2-3, however the early rewet again was not predicted (Figure 6). Analyses [9] have shown that the difference between the predicted and measured fuel cladding temperatures is a result of post-critical heat transfer modeling in the core. The analyses indicated that the critical heat flux (CHF) correlation used in RELAP4/MOD6 is not suitable for LOFT cases where the rewet occurred at core coolant mass fluxes of 10C to 600kg/s m^2. An alternate approach, the Biasi CHF correlation which covered the mass flux ranges from 100 to 6000kg/s m^2, was built into RELAP4/MOD6. The calculation with this correlation, with measured initial conditions, keeping all other modeling the same as for the predictions showed better agreement with experimental data. Figure 6 shows the prediction and posttest calculation of cladding temperature compared with the measured cladding temperature.

The calculated maximum peak cladding temperature was approximately 70K higher than measured in the experiment. Further study indicated that lack of a fuel cracking model (from power ramping) in the RELAP code results in a larger fuel gap width and consequently in higher stored energy and higher peak cladding temperature. Calculations with the FRAP-T5 code, which contains a fuel relocation model, using boundary conditions from RELAP4/MOD6 calculations, showed excellent agreement of calculated with measured cladding temperature.

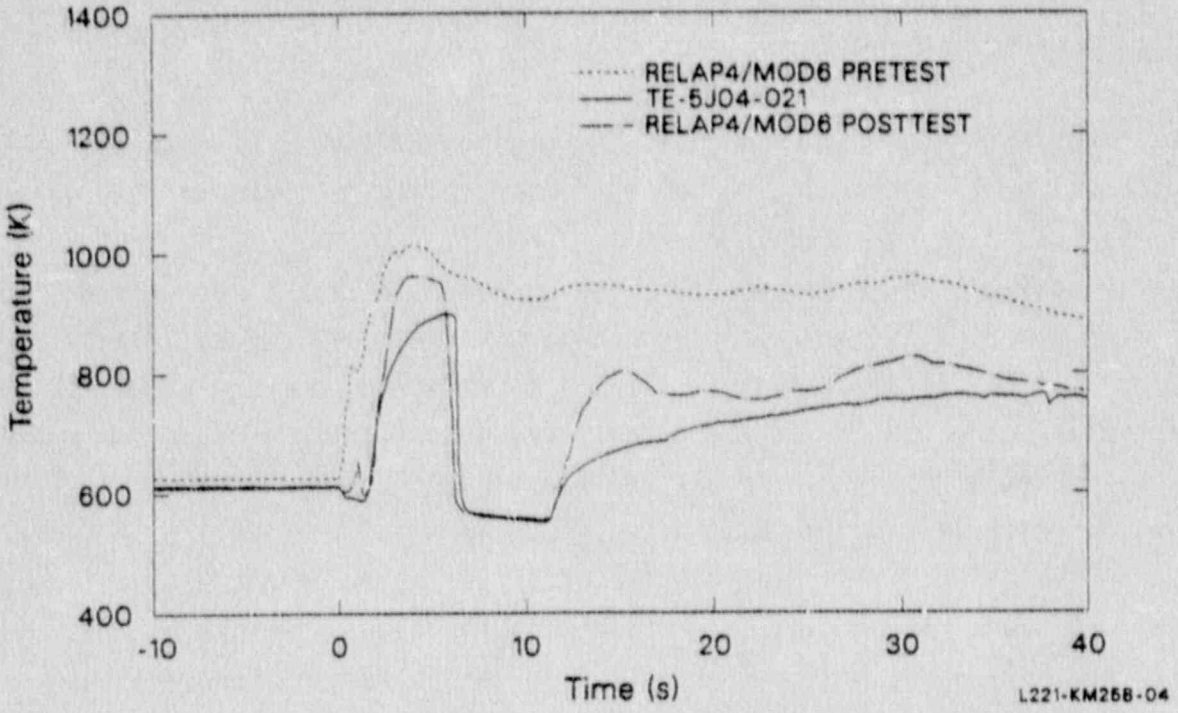

Figure 6. Calculated and measured cladding temperature on fuel rod 5J4 at 0.53 m above bottom of the core for Experiment L2-3.

3.3 Experiment L2-5

The third large break LOCA experiment was performed in June 1982. This experiment, designated L2-5, simulated a 200% break in the cold leg piping of a commercial PWR simultaneous with loss of offsite power. This experiment was designed to provide experimental data to demonstrate that Appendix K assumptions result in a conservative prediction of peak cladding temperature, even without early rewet. The configuration of the facility was identical to the configuration used in experiments L2-2 and L2-3. The core steady state power level was 36 MW (40.1 kW/m maximum linear heating rate). The reactor was scrammed on a low pressure signal at 0.34 s. Following the scram, the operators tripped the primary coolant pumps at 0.94 s. The pumps were not connected to the flywheels in this experiment. This was done in order to provide an early rapid pump coastdown which would prevent the early core rewet phenomena and result in higher fuel cladding temperatures. Reference 10 provides detailed experimental results for this experiment.

The core thermal response was quite different, and more complex, than in Experiments L2-2 and L2-3. Figure 7 shows typical cladding temperature in the lower half of the central fuel bundle compared to cladding temperature measured in this region during the L2-3 experiment. The cladding temperatures in L2-5 increased quickly in response to degraded cooling as in the previous large break experiments. At about 5 s the temperature rise rate decreased, and about 10 s after reaching approximately 1050K the cladding temperature began to decrease slowly. 20 s after experiment initiation the temperature increased again and reached a maximum of 1077K at about 30 s. From this time on a gradual cooling of the cladding occurred in response to the injection of ECC water. The fuel rod cladding was completely quenched by 65 s.

In the upper part of the central fuel bundle and high power regions of the peripheral bundle the measured thermal response was quite different from that in the high power region. As shown in Figure 8, initially the cladding temperatures increased similarly to the high power region. However, at about 15 s after experiment initiation a strong top-down quench was measured which

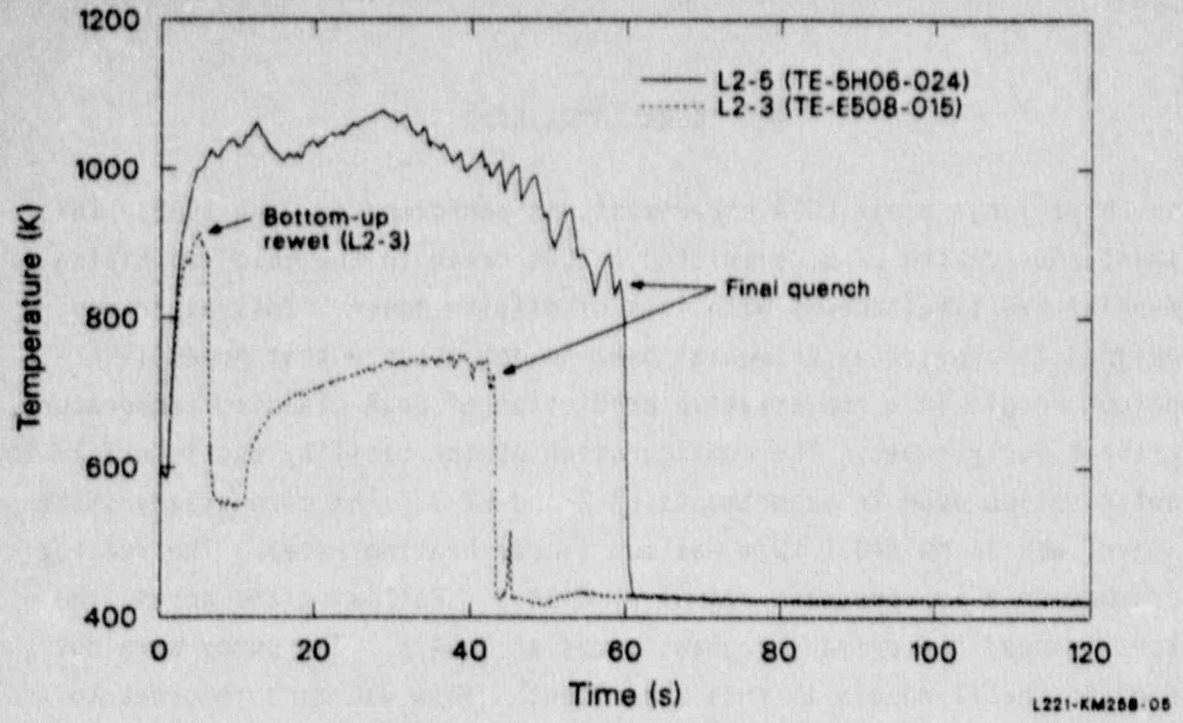

Figure 7. Maximum temperature on fuel rod cladding during Experiments L2-3 and L2-5.

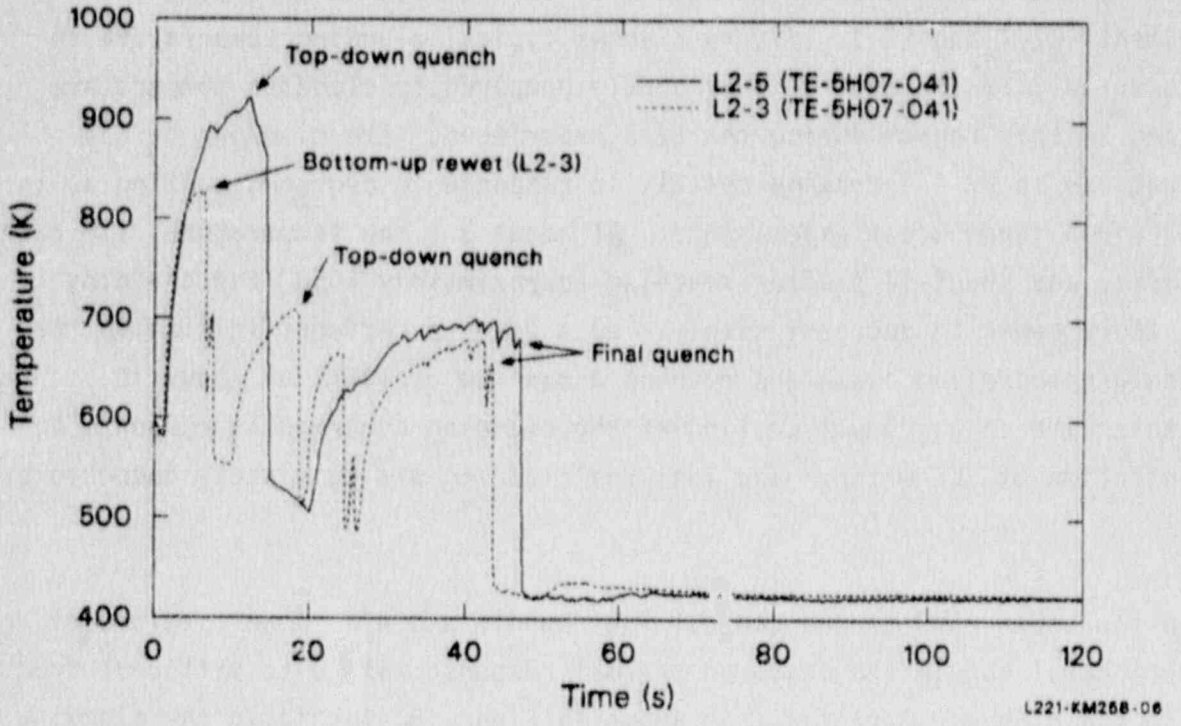

Figure 8. Temperature of fuel rod cladding in upper half of central fuel assembly during Experiments L2-3 and L2-5.

lasted for a few seconds followed by another temperature excursion. Subsequently, during reflood these core regions were quenched in the same manner as the high power region.

The fuel cladding thermal behavior in the lower power regions of the peripheral fuel bundles was also unique. The cooling was sufficient in these regions to maintain the cladding at saturation until about 20 s (Figure 9). This part of the core behaved similarly in L2-3 and L2-5 and experienced only relatively small temperature excursions before final quench occurred from ECCS reflood.

In summary the core thermal behavior in Experiment L2-5 was similar to the core thermal behavior in Experiment L2-3 with the exception of the early bottom-up core wide rewet which occurred in Experiment L2-3. This difference was caused by the mode of primary pump operation and demonstrates the sensitivity of fuel cladding temperature on hydraulic phenomena attributable to primary pump operation.

Predictions for Experiment L2-5 [11] were performed using the RELAP5/MOD1 code. Figure 10 shows the predicted and measured maximum temperature of the fuel rod cladding in the core. The calculated maximum peak cladding temperature was 1082 K in comparison to the measured maximum peak cladding temperature of 1077 K; however, the maximum was calculated to be much earlier than measured. This is in part due to the failure of the code to calculate the top down quench which was measured in the upper regions of the core. Also the later heatup in the peripheral fuel bundles was not calculated.

In the post L2-5 recovery phase, a potential reactor operating procedure was studied wherein the reactor vessel liquid level was to be maintained below the reactor vessel nozzles and above the core. The reactor operators were required to cycle the HPIS and LPIS flows to control the coolant level based on observation of temperature measurements at several elevations in the upper plenum. Temperatures observed by the operators and also the coolant temperature measured at the core exit are shown in Figure 11. These temperature measurements did not indicate that core heatup, or inadequate

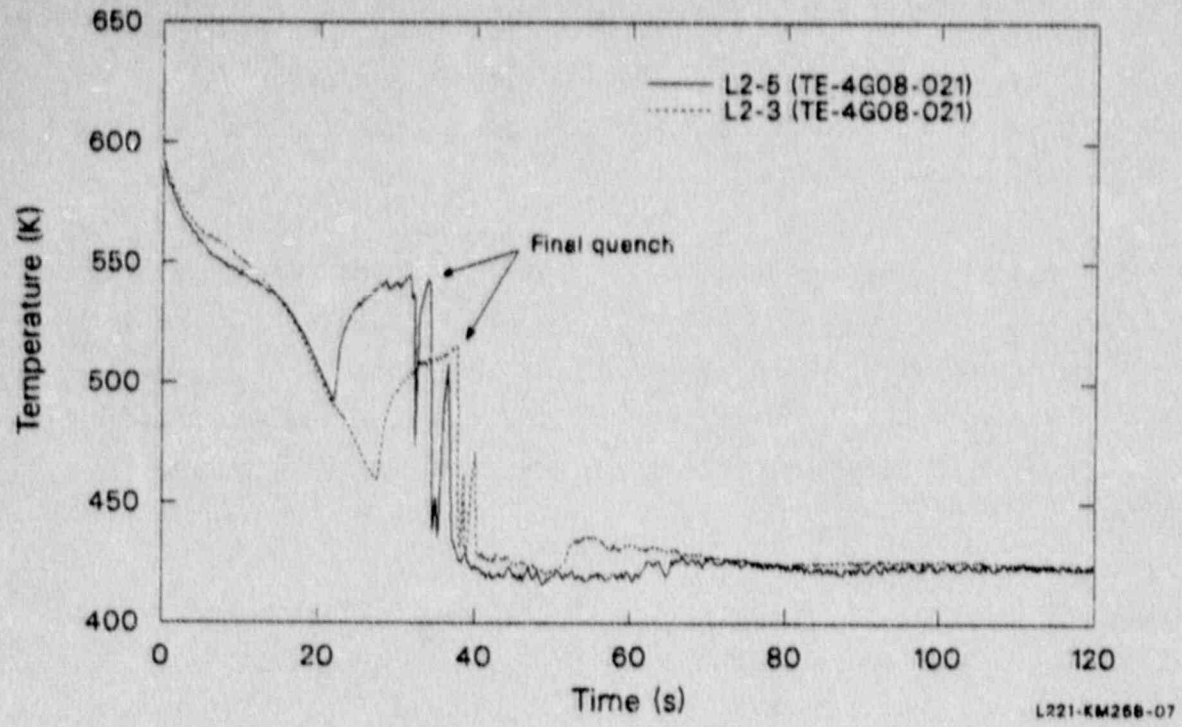

Figure 9. Temperature of fuel rod cladding in a peripheral fuel assembly during Experiments L2-3 and L2-5.

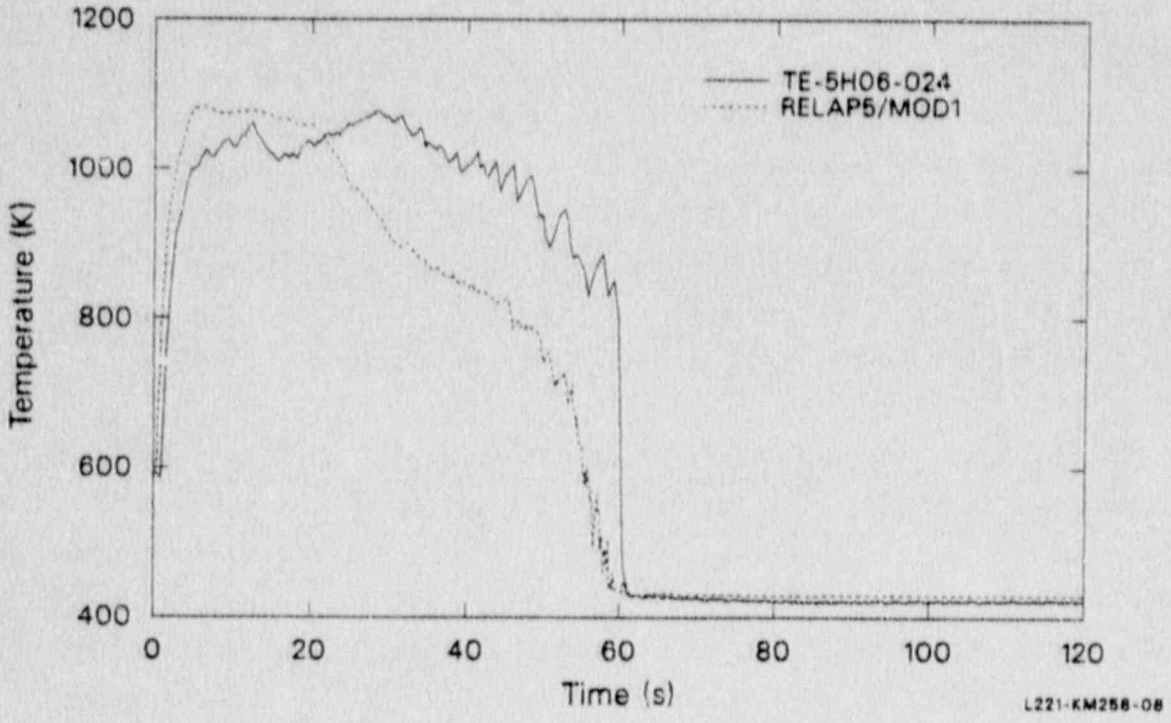

Figure 10. Predicted and measured maximum temperature of fuel rod cladding for experiment L2-5.

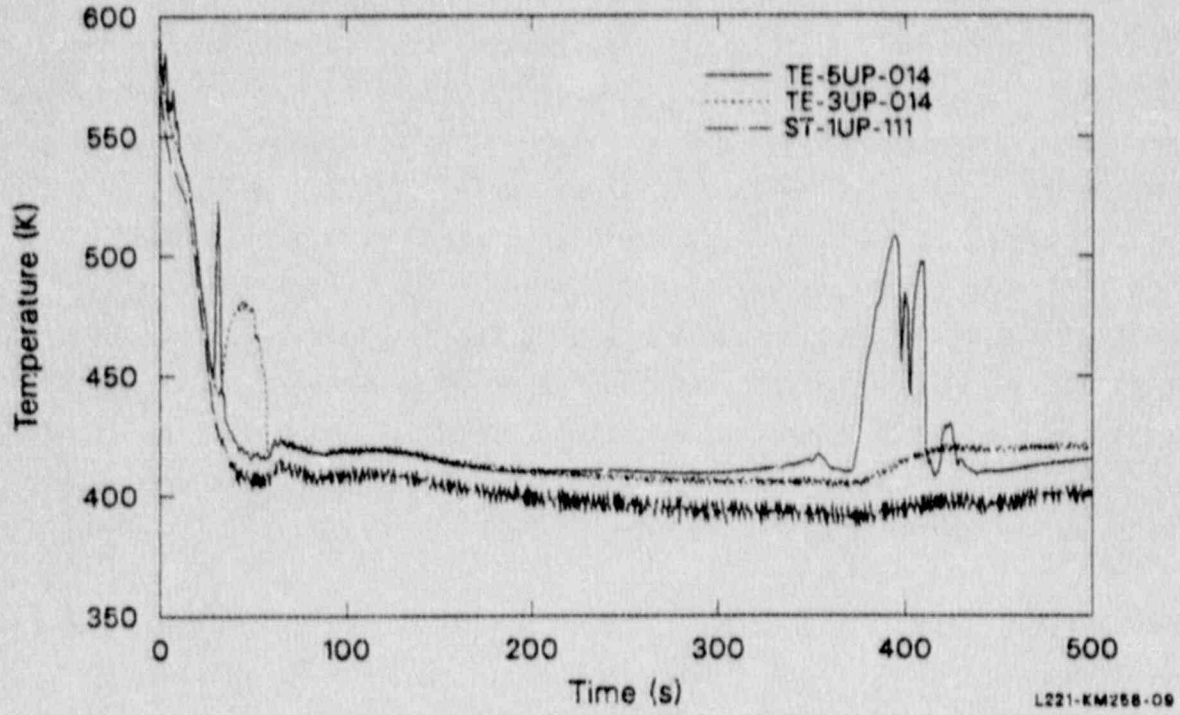

Figure 11. Core exit and upper plenum fluid temperatures compared with saturation temperature during Experiment L2-5.

core cooling, had occurred until about 370 s. Figure 12 shows that inadequate core cooling occurred before 200 s and that the core was in significant heatup prior to 370 s. These results clearly show that upper plenum coolant temperature measurements are not adequate for liquid level control and maintenance of adequate core cooling.

3.4 Experiment LP-C2-6

Experiment LP-02-6, the fourth nuclear large break experiment was conducted in October 1983. The major objective of this experiment was to provide data to assess the capability of computer codes to predict PWR system response during a design basis accident [12] . This experiment simulated a double ended offset shear of a commercial PWR main cold leg coolant pipe. The initial conditions for this experiment were representative of USNRC licensing limits in commercial PWR and included loss of offsite power coincident with LOCA initiation and minimum United States emergency core coolant injection. The experiment was initiated from a power level of 46MW (49kW/m maximum linear heat generation rate). Prepressurized fuel was used in this experiment in the central fuel assembly. Results of this experiment are discussed in Reference 13.

The experiment was initiated by opening the quick-opening blowdown valves in the broken hot and cold legs. The reactor scrammed automatically when the hot leg pressure reached 14.8MPa at 0.1 s. The primary coolant pumps were tripped and allowed to coast down until 16.5 s, when they were disconnected from the flywheels. The flow in the core reversed almost instantaneously with experiment initiation, and the fuel rod cladding experienced DNB within 1 s after experiment initiation. The cladding temperature increased until about 5 s when the positive core flow was reestablished. Figure 13 shows cladding temperatures at four different elevations in the core CFM for the first 60 s of the transient. The data show that in the first 10 s the fuel cladding was quenched in the lower 2/3 of the core while the upper part of the core was cooled but not quenched. This is quite different core thermal response from that observed during experiment L2-5 in the same time frame. The difference in thermal response is the result of different pump operation

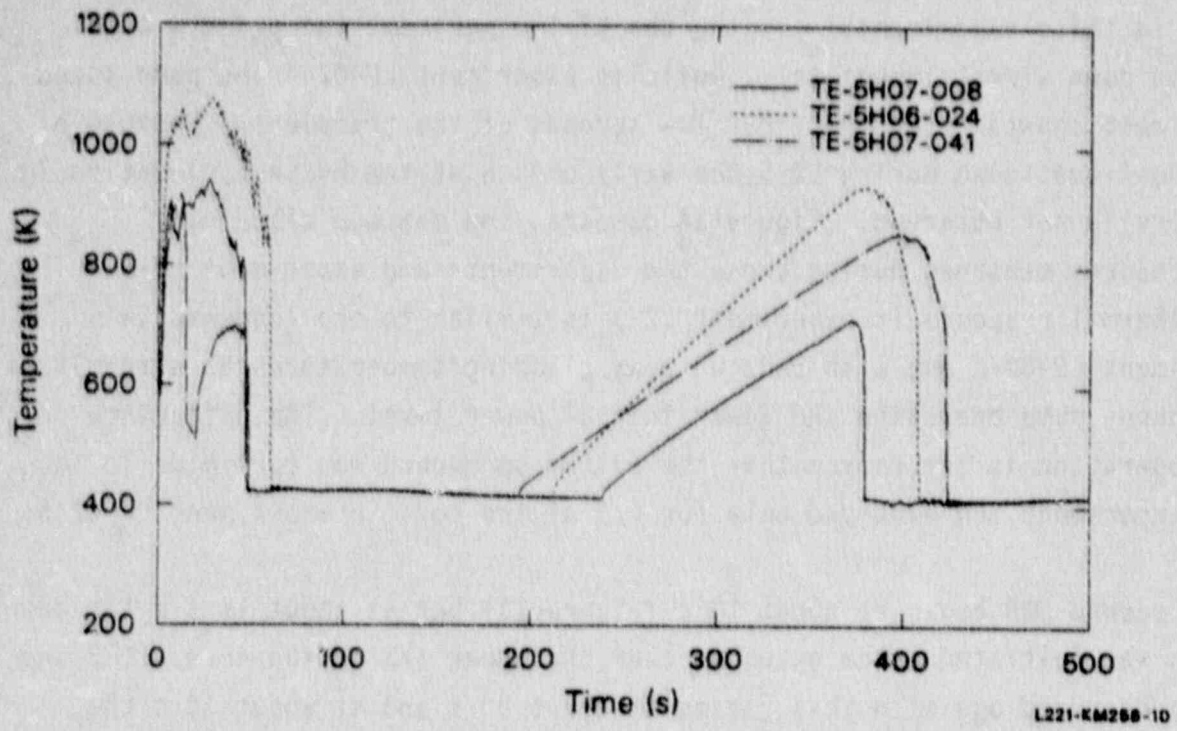

Figure 12. Temperature of fuel rod cladding at different elevations during the second core heatup in Experiment L2-5.

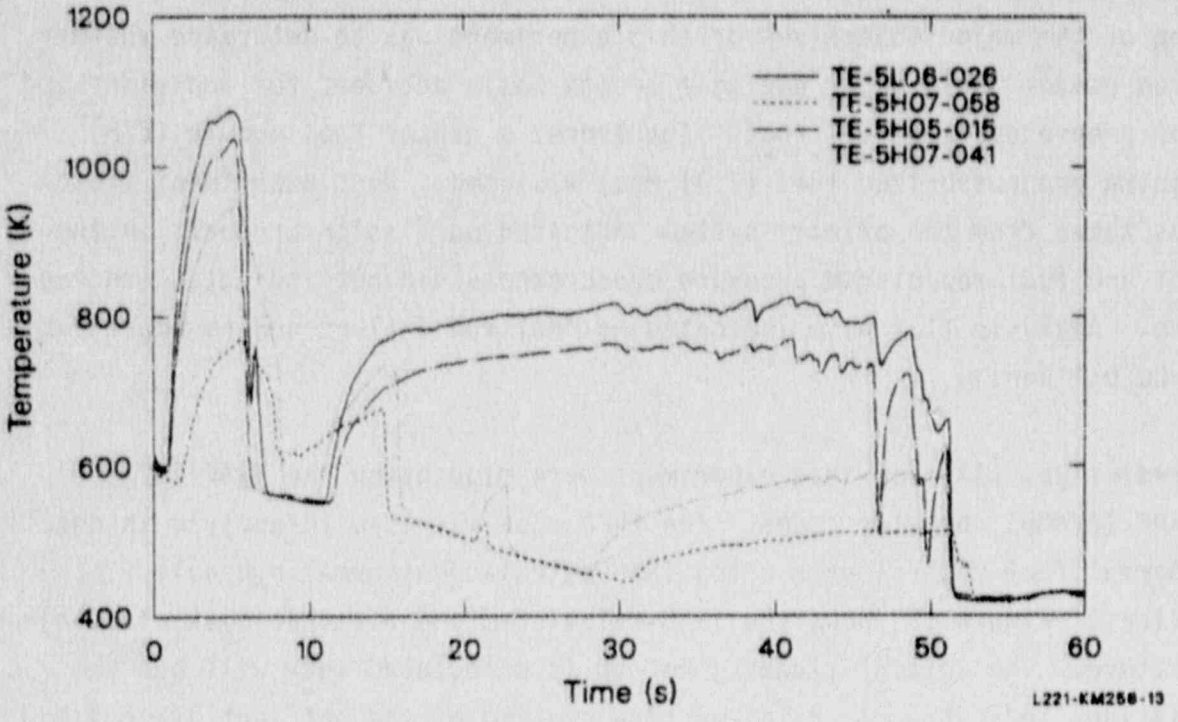

Figure 13. Fuel rod cladding temperatures at different elevations in the center fuel module during Experiment LP-02-6.

modes in these experiments. During the L2-5 experiment the primary pumps coasted down almost immediately, while in experiment LP-02-6 the pump speed was almost constant for the first few seconds of the transient. Because of the short coastdown during L2-5 the early quench at the hottest elevation in the core is not observed. Figure 14 compares the maximum cladding temperatures measured during these two experiments and experiment L2-3. The core thermal response in experiment L2-3 is similar to the response in experiment LP-02-6 but with reduced peak cladding temperatures as a result of continuous pump operation and lower initial power level. The difference in pump operation is the reason that the bottom up quench was core wide in the L2-3 experiment and extended only for 2/3 of the core in experiment LP-02-6.

A second DNB began at about 10 s (Figure 13) but at about 15 s a top down quench was initiated which extended over the upper 1/3 of the core. CHF and heatup occurred again in this region at about 20 s and at about 30 s the entire core was above saturation temperature. ECCS reflood quenched the core at 56 s. The maximum cladding temperature reached during the reflood phase was 840K.

One of the major objectives of this experiment was to determine whether fuel rod damage would occur during a design basis accident for unpressurized and for prepressurized fuel rods. Therefore, a center fuel module (CFM) containing prepressurized fuel (2.41 Mpa) was used. Post-experiment fluid samples taken from the primary system indicated no fission products in the coolant and fuel rod plenum pressure measurements did not indicate cladding rupture. Analysis [13] also indicated no fuel rod failure and no appreciable fuel rod ballooning.

Predictions [14] for this experiment were made using the TRAC-PD2/MOD1 and FRAP-T6/MOD1 computer codes. The FRAP code was used to analyze in detail the thermal fuel rod response using TRAC-calculated thermal-hydraulic conditions. Figure 15 shows the TRAC-calculated and measured peak cladding temperature. The initial cladding heatup is calculated very well but the calculations indicate only relative slow cooling of the hot spot after 5 s whereas the data show a rapid quench. The lack of a quench in the calculation is responsible for higher peak temperatures after blowdown and

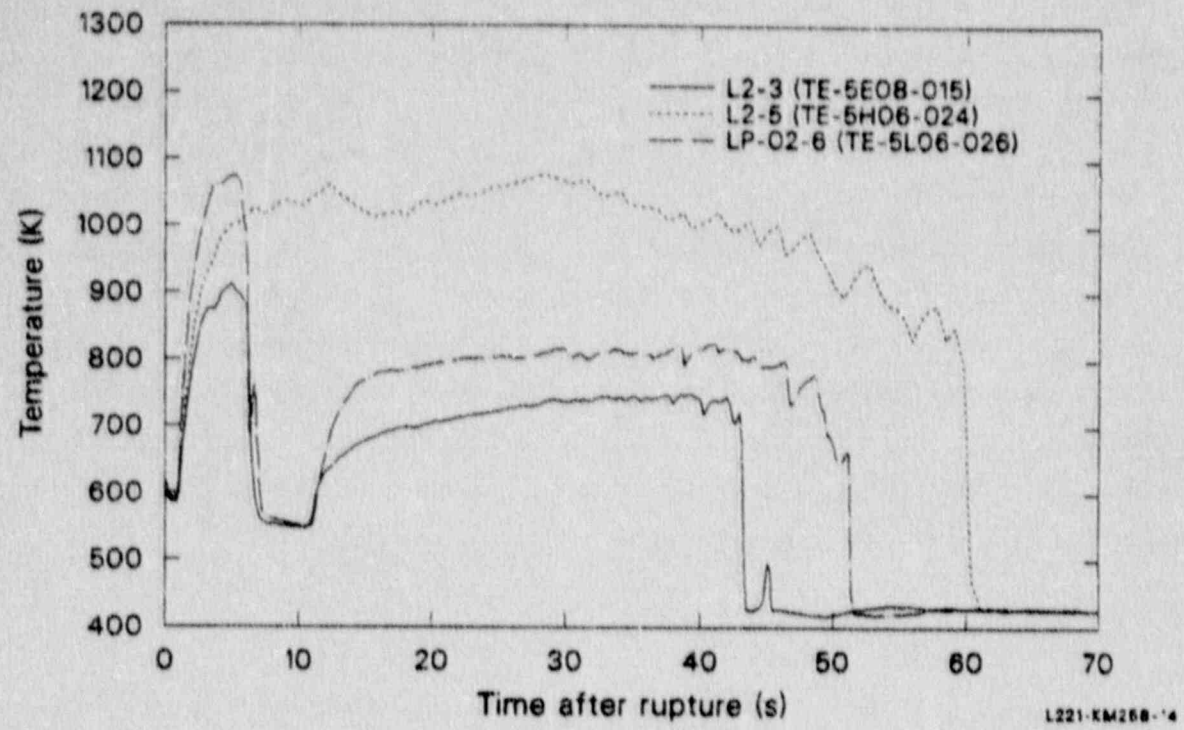

Figure 14. Peak fuel rod cladding temperatures during experiments L2-3, L2-5, and LP-02-6.

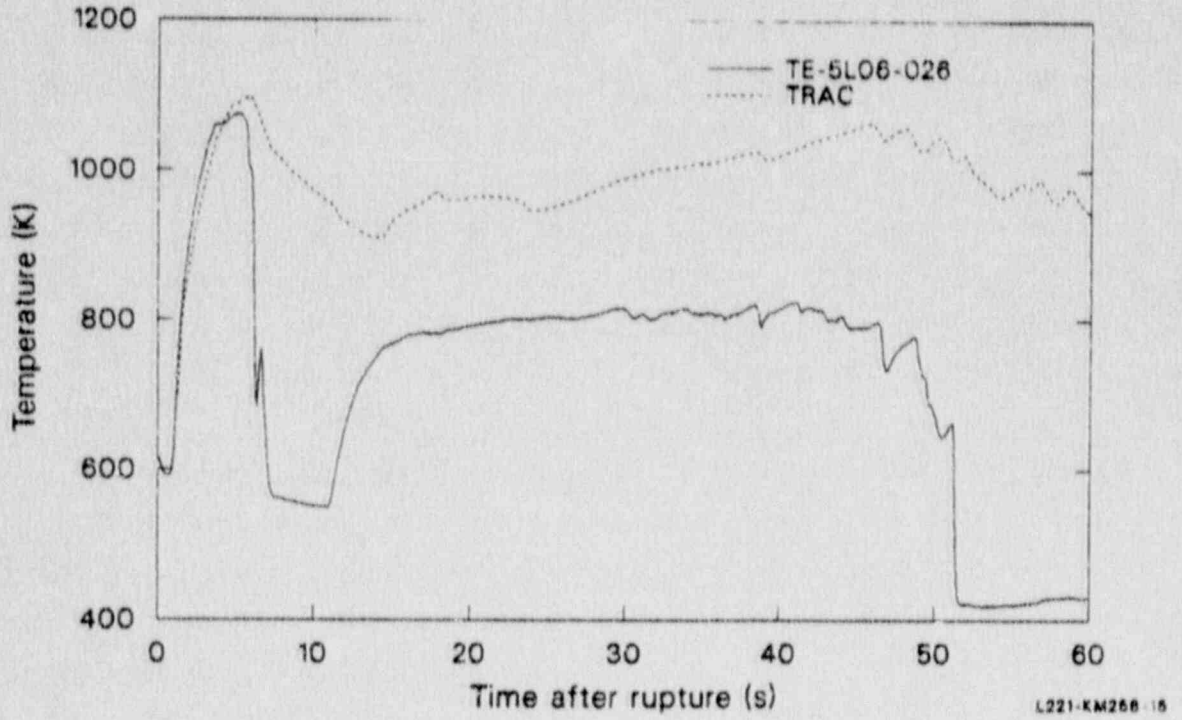

Figure 15. Measured and predicted peak fuel cladding temperatures for Experiment LP-02-6.

also partially for delayed final quench. The time to core quench was also affected by the low minimum film boiling temperature calculated by TRAC. The comparison of measured and calculated reactor vessel cold leg flow balance (Figure 16) also shows some deficiencies in the calculations. The initial coolant depletion from the reactor vessel is calculated to be smaller than measured and reestablishment of coolant addition to the reactor vessel occurs later and is smaller in magnitude than measured. The core thermal behavior is very sensitive to small differences in hydraulic phenomena as the vessel mass balance data indicate. The accuracy in prediction of the hydraulic conditions in the core must be increased for appropriate assessment of low-flow film boiling models that are used for calculation of thermal core behavior during the early quench time.

3.5 Experiment LP-LB-1

Experiment LP-LB-1, the fifth large break experiment in LOFT was designed to reproduce conditions representative to United Kingdom licensing limits [15]. This experiment simulated a double-ended offset shear of one inlet pipe in a four loop PWR. The experiment was initiated from conditions representative of a PWR operating near its licensing limits. The boundary conditions for this experiment were set to simulate loss of offsite power coincident with LOCA initiation and United Kingdom minimum safeguard emergency core coolant injection. These assumptions resulted in utilization of 70% of the accumulator volume and 50% of the pumped ECC injection of that used in the LP-02-6 experiment which represented the U.S. licensing limits. An early rapid primary coolant pump coastdown was included to attain maximum cladding temperatures by suppression of the early rewet phenomena.

The experiment was initiated by opening the blowdown valves from a core power level of 49.3 MW (51.7 kW/m maximum linear heat generation rate)[16]. The reactor was scrammed on a low pressure signal at 0.13 s and the primary pumps were tripped slightly later and disconnected from the flywheels at 0.63 s. The fuel cladding went into DNB in less that 1 s in the high power region. The early decoupling of the primary pumps from their flywheels resulted in insufficient flow into the vessel from the intact cold leg to produce a bottom up flow into the core and an early fuel cladding quench that

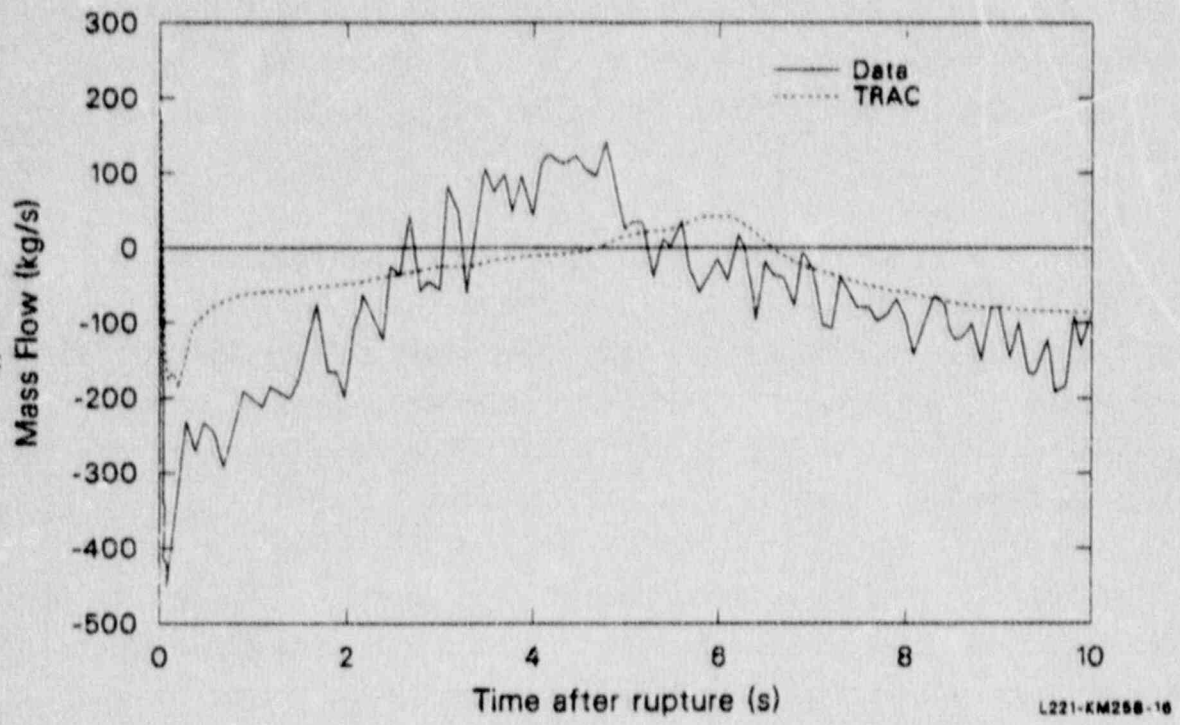

Figure 16. Measured and predicted differences between intact and broken cold leg mass flows for Experiment L2-6.

occurred in experiments L2-2, L2-3, and LP-02-6. The rapid cladding temperature rise had stopped at about 13 s because of liquid fallback from the upper plenum. This top-down liquid flow resulted in quench of the upper part of central fuel assembly (Figure 17) and more extensive cooling in the peripheral fuel bundles. The maximum cladding temperature during the blowdown phase was reached shortly before the top-down cooling trend started and reached 1261K (Figure 18). The top-down cooling lasted until about 25 s when fuel cladding heatup started again. ECC injection from the accumulators began at 17 s and from the LPIS at 32 s and resulted in a core quench at about 34 s. The core quench started at both bottom and top of the core and progressed toward the peak power elevation and was completed at 72 s. The maximum cladding temperature recorded during the ECC injection phase was 1257K.

One of the concerns was whether cladding damage or deformation would occur on the unpressurized fuel rods used in the LP-LB-1 experiment. The very high temperatures reached in this experiment would cause cladding structural weakening and possible cladding collapse onto the fuel pellets. Analysis [16] and coolant samples indicated that cladding was not ruptured but possibly deformed.

The TRAC-PD2/MOD1 code was used to predict this experiment. The version of the code which was used contained an error in the gap conductance model which was believed would affect significantly the calculated cladding temperatures. Immediately after the experiment posttest calculations were performed using a corrected version of the code and measured initial and boundary conditions. Figure 19 shows the pre- and posttest calculation results for peak cladding temperature compared with the measured peak cladding temperature. The predictions show the initial heatup rate in agreement with experiment data but after 4 s the calculated temperatures deviate significantly from the data. These deviations are a direct result of the code error. There are also significant differences between the calculated and measured cooling in the reflood phase. In the experiment the cooling rate increased as the reflood progressed. In the calculations the cooling rate was reduced as the temperature difference between cladding and fluid was reduced.

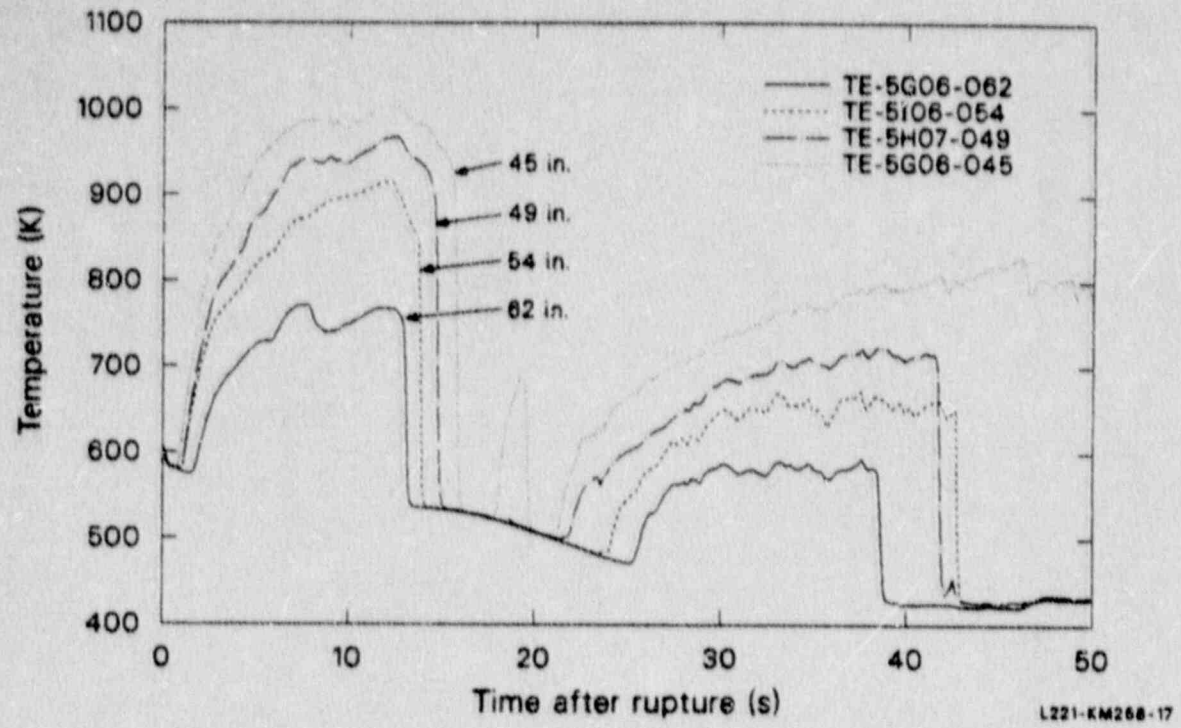

Figure 17. Upper central fuel assembly cladding temperatures during Experiment LP-LB-1 showing top down quench.

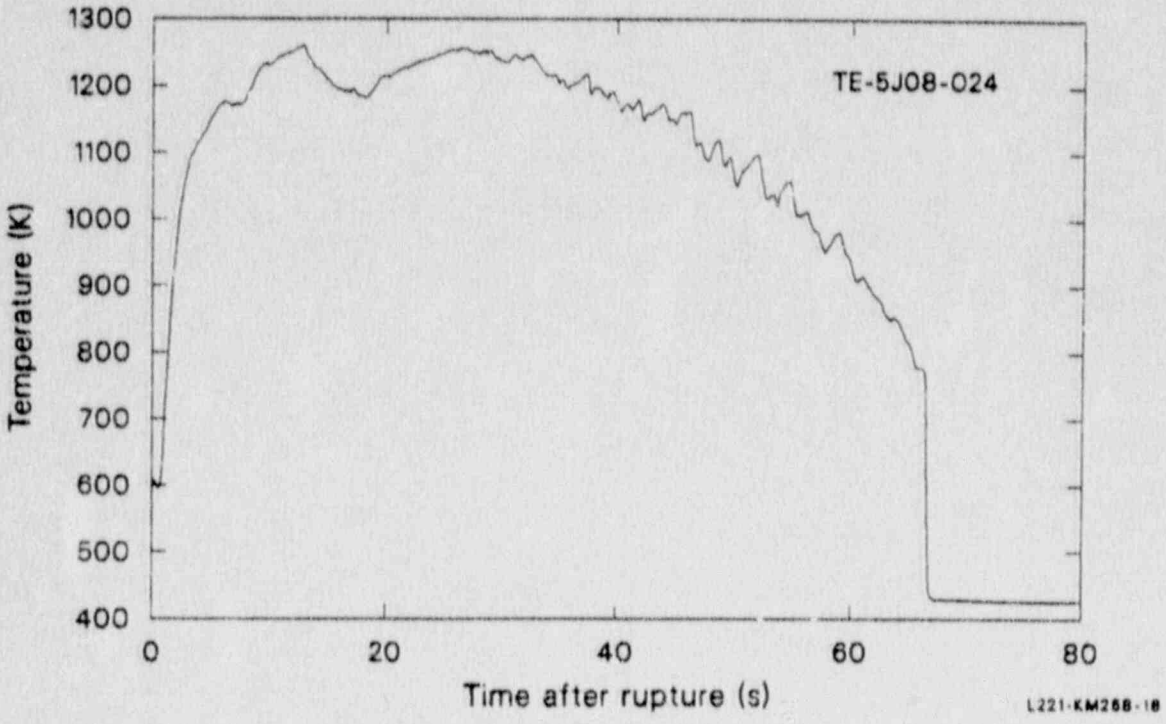

Figure 18. Peak cladding temperature during Experiment LP-LB-1.

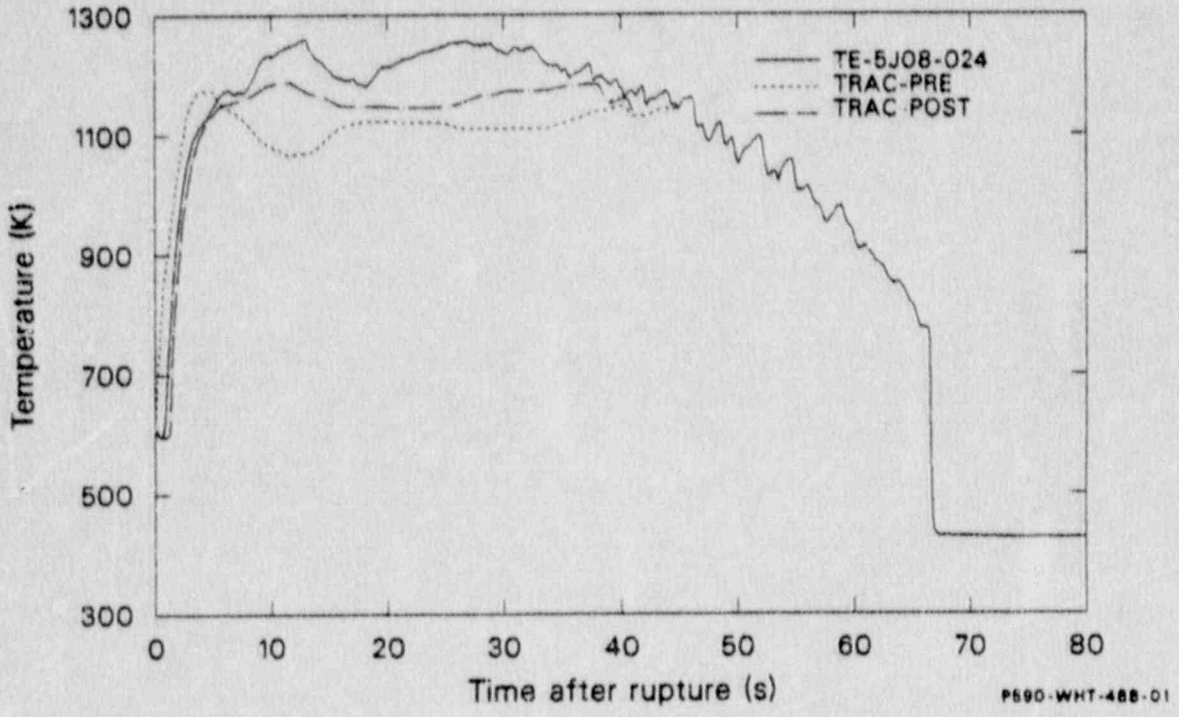

Figure 19. Measured and calculated peak cladding temperature for Experiment LP-LB-1.

The initial heatup was calculated correctly in the post-experiment calculations. The reduction of the heatup after 6 s was also calculated but was slightly more extensive than in the experiment. The time of the peak cladding temperature was calculated correctly though the calculated temperature was approximately 60 K lower than the measured temperature (1261 K). The posttest calculated thermal response during reflood was also less than measured but was in better agreement with measured data than was the pretest calculation.

In general, the code calculated the hydraulic conditions quite well with the exception of the underpredicted depressurization rate during accumulator injection. The code calculated the top-down quench during the blowdown, but underpredicted the extent. The code also calculated properly the simultaneous bottom-up and top-down quench during reflood. The strong, hydraulically controlled azimuthal asymmetry measured in the thermal response of the peripheral bundles was also partially calculated. The major differences between the experiment and the calculations were in the temperatures at the peak power location. The code did not calculate correctly the initial cooling during blowdown, the peak cladding temperature, and the cooling during reflood. These deficiencies in the calculations indicate or reveal limitations of the post-critical heat flux models used in the TRAC code.

3.6 Experiment LP-FP-1

Experiment LP-FP-1 was conducted in December 1984 and was programmatically a fission product release and transport experiment [17]. However, the thermal-hydraulic boundary condition for this experiment was based on a design basis large break LOCA in a FRG PWR. In LP-FP-1, the ECCS was intentionally delayed until cladding rupture had occurred on fuel rods of a CFM specifically designed for this purpose. The ECCS was designed to simulate the FRG PWR ECCS with both hot and cold leg injection.

For this experiment the reactor core was equipped with a 15X15 center fuel assembly with a thin zircaloy shroud which enclosed the inner 11x11 fuel rod array in which 24 of the fuel rods were enriched to 6-wt%. Twenty two of

these fuel rods were also prepressurized (2.41 MPa). The experiment was designed to cause cladding ballooning and rupture to occur 60-90 s after initiation. In order to accomplish this, experiment initiation began with a reactor scram which was followed 1 s later by opening of the quick-opening blowdown valves. This sequence removed sufficient stored heat to cause a delay in reaching high temperatures. This delay was necessary to provide a well-defined set of boundary conditions for fission product release and transport. The primary coolant pumps were tripped and disconnected from their flywheels 1 s after QOBV opening. This provided conditions similar to experiment L2-5.

Figure 20 shows that the core thermal behavior was quite different from the behavior observed in the previous large break experiments. The major characteristic of the core temperature transient is that the expected early cladding temperature rise was prevented by several quenches and the actual core heatup started very late in the transient.

The first core heatup began at about 3 s and continued to about 6 s when the first quench occurred (Figure 20). This was a bottom-up quench which influenced only the lower half of the core. This quench was quite similar to the early quenches observed in the experiments L2-2, L2-3 and LP-02-6. The attempt to eliminate this early quench by tripping the pumps and disconnecting the flywheels failed in this experiment. There are two reasons for this. First, the primary coolant pumps were operated initially at higher speeds than in experiments L2-5 and LP-LB-1 which resulted in higher initial mass flow rate and fluid inertia. This resulted in more delivery of coolant from the intact loop to the downcomer than in the other experiments. Second, the reactor was scrammed before blowdown (intentionally) which removed some of the initial stored heat.

At about 9 s a second quench started, this time a top-down quench. The top-down quench was not uniform across the core as was the bottom-up quench. It started near the intact loop hot leg in peripheral bundle No. 4 as a result of liquid falling back from the hot leg intact loop. At about 10 s a second heatup in the CFM started and was followed again by a quench at 12 s. This quench was a top-down quench and propagated through the entire central

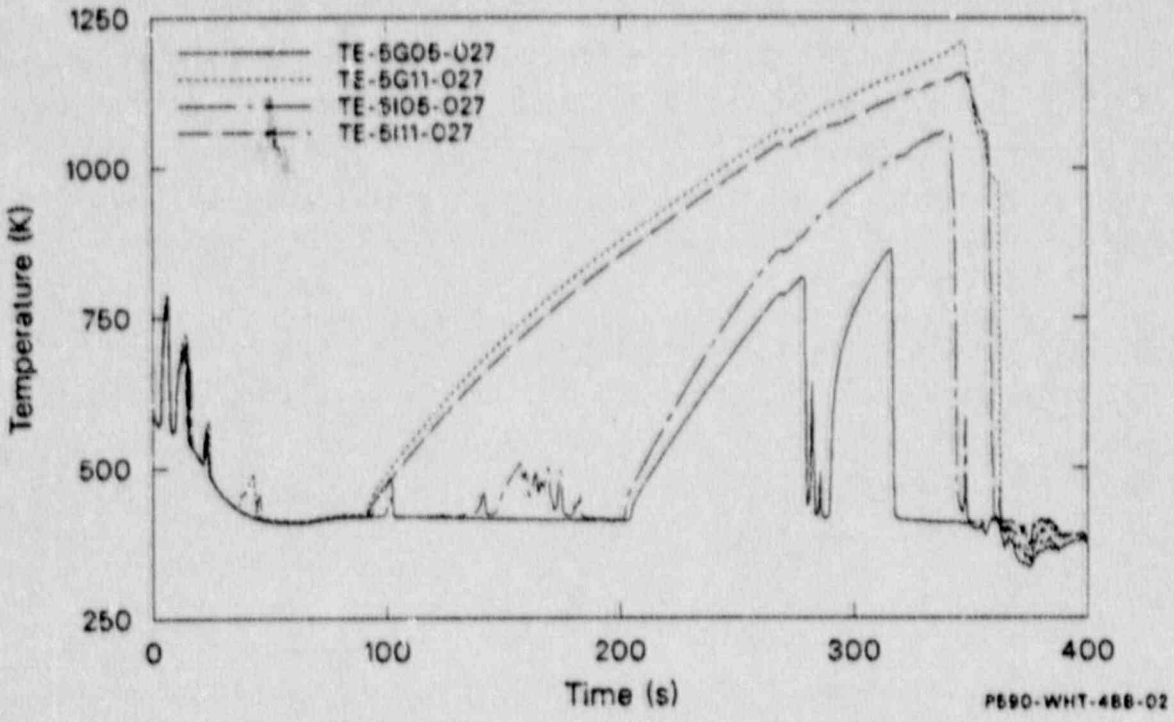

Figure 20. Fuel rod cladding temperatures measured at the peak power elevation during Experiment LP-FP-1.

bundle reaching the bottom at approximately 18 s. The cause of this quench was premature injection of the ECC water initially stored in the ECCS injection line routed to the upper plenum. Detailed analysis of this injection and effects on core behavior are presented in Reference 18.

A third heatup of the core began at about 21 s. It was also not a uniform core heatup. The top of the center fuel module remained at saturation temperature. Also, in the peripheral assemblies most of the thermocouples in the upper parts of the modules indicated saturation temperature. The reason of this extended cooling of the upper parts of the core was the unintentional injection of cold water from the upper plenum ECC injection line. This cold water from the injection line resulted in complete quench of the CFM between 23 and 26 s and also caused cooling to some parts of the peripheral assemblies. Most of this unintentionally injected water was evaporated before reaching the lower regions of the peripheral fuel bundles.

The main cladding heatup in the central fuel assembly started at about 80 s and progressed from the bottom up. The heatup was not uniform radially; fuel rods closer to the broken loop heated up later and quenched earlier. This nonuniform thermal behavior of the center assembly was due to the effects of the unintentional ECC injection.

There was a second unintentional injection at about 266 s which resulted in additional cooling that effected the peripheral fuel assemblies more than the center fuel assembly. Some of this water was able to penetrate to the lower part of the core and cause cladding quenches.

At 344 s the experiment was terminated on a high temperature limit for the peripheral bundles by ECC injection into the upper plenum and the intact loop cold leg. The quench began at the top of the core followed by the core bottom and then the high power region. The quench was not uniform through the core. The CFM was quenched at 370 s. Fuel assemblies 2 and 6 did not quench until 380 s. The maximum cladding temperature recorded in the CFM was 1210K and occurred at 347 s. This temperature is above the temperature required for cladding ballooning and rupture. Posttest analysis revealed that 8 fuel rods had ruptured cladding.

Predictions for this experiment were performed using TRAC-PD2/MOD1, RELAP5/MOD2 and DRUFAN codes. Detailed description of these calculations is given in [19] for TRAC calculations and in [20] for RELAP and DRUFAN predictions. Since an unexpected subcooled liquid injection occurred during this experiment which significantly affected the reactor thermal response, a full comparison of the measured data with the predictions is not meaningful. Discussion of the predictions and of the experimental data is included in Reference 20.

3.7 Experiment LP-FP-1A

The first trial to conduct the experiment LP-FP-1 was carried out on December 12, 1984. The Quick Opening Blowdown Valve (QOBV) in the cold leg opened immediately but that in the hot leg did not open. At about 10 s the Plant Protection Systems (PPS) was actuated with following ECCS realignment: HPIS pump A, accumulator A and LPIS pump A were aligned to inject in the lower plenum, while HPIS pump B, Accumulator B and LPIS pump B were aligned to inject into the downcomer. HPIS flow started at 15 s and achieved full capacity of 1.95 l/s at about 17 s. Accumulators began to inject at about 19 s. At about 30 s the LPIS pump started to inject and the core was completely quenched at about 35 s. Most of the fluid thermocouples just below the core have shown superheating starting at 23 s with a subsequent quench at 31 s. This indicates that the refill phase was completed at 31 s. Post-test analysis and comparison with earlier double ended break tests have shown that the hot leg QOBV opened sufficiently at time zero to allow maximum flow. Only the position indicator of the QOBV did not operate properly. All quench phenomena observed during the blowdown phase in LP-FP-1 and discussed in detail in [18] were also present in LP-FP-1A. The bottom-up quench started at about 6 s in the lower core region and the top-down quench reached the lower core region at about 16 s as shown in Figure 21. The complete quench of this part of the core was reached at about 32 s.

Bottom-up quench occurred in the peripheral bundles simultaneously with the central bundle, while the subsequent top-down quench was heterogeneous specially in the lower core region as shown in Figure 22. Bundle 4 did not

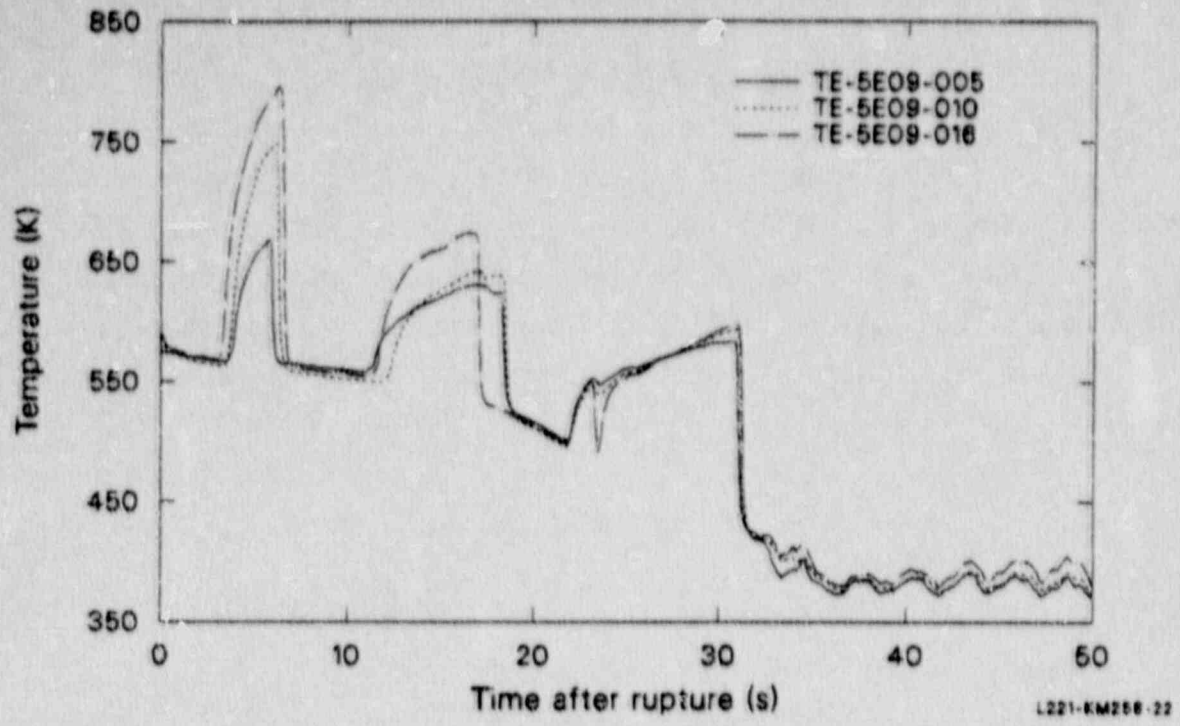

Figure 21. Fuel rod cladding temperatures measured at different elevations in the center fuel module during Experiment LP-FP-1A.

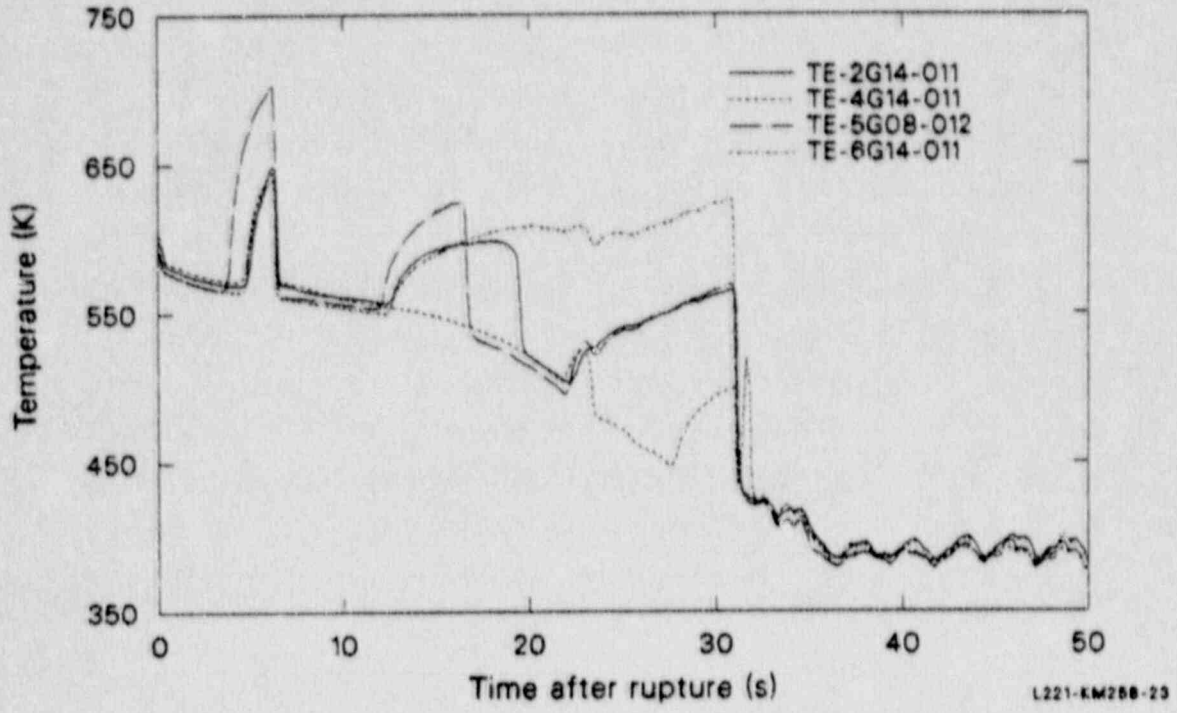

Figure 22. Fuel rod cladding temperatures measured in a peripheral bundle during Experiment LP-FP-1A.

show dryout until 22 s and bundle 6 did not quench during the top-down quench at 16 s. Only bundle 2 was analogous to the central bundle in the quench behavior.

Comparison of LP-FP-1A with LP-FP-1 and a discussion how this experiment was used to explain some phenomena in LP-FP-1 is given in [18].

4. SIGNIFICANT LB LOCA PHENOMENA

Before March 1979 the small break LOCA was of little concern by regulatory bodies and the entire research was concentrated on the large break LOCA. The TMI-2 accident shifted the research efforts towards small break LOCA, anticipated transients, and severe accidents. Since then, with the exception of LOFT experiments L2-5 through LP-FP-1, little was done in the area of large break LOCA research. Today, the nuclear industry appears to have a conviction that the phenomena associated with the large break LOCA are well understood and well-defined by models in codes such as TRAC. In this section we will reassess our understanding of the large break LOCA to confirm this position by reviewing the phenomena observed during the LOFT large break experiments. These experiments up to now are the most important because of the facility scale, the nuclear core of the facility and the experimental results which provided some insight into what may happen in large PWRs during a LOCA.

The first and most important phenomenon is the core-wide fuel cladding cooling and quench during blowdown. This phenomenon, observed for the first time in the LOFT experiments, changed the perspective of large break accidents and also led to a reevaluation of critical and post-critical heat transfer models used in the systems codes. We will discuss the reactor coolant pump operation mode and coolant flow distribution during the early blowdown phase which contribute to this phenomenon. We will also review some experimental aspects related to this phenomenon, specifically the fin-cooling problem of external cladding thermocouples and nuclear fuel rods versus nonnuclear heating elements.

The blowdown cooling in LOFT LBLOCA experiments is not unique to that facility. This phenomena is calculated to occur in 4-loop plants with nominal pump operation and trip criteria. Only under a typical pump operating conditions, such as impeller seizure in one pump, can the cooling phenomena be suppressed. Also, because the cooling phenomena is strongly dependent on the mass inflow/outflow hydraulic balance in the reactor vessel, the cooling phenomena is likely never to occur in PWR configurations with two inlet pipes (cold legs). The cooling phenomena may or may not occur in PWR

designs with three inlet pipes depending on pump trip criteria and coastdown characteristics. As previous stated, the cooling phenomena is considered highly likely in PWR configurations with four inlet pipes.

We will also discuss the effects of top-down quench phenomena, break flow phenomena and finally ECC injection including the effect of accumulator nitrogen injection. The reproducibility and dependence of all of the above identified phenomena on initial and operating conditions imply that the phenomena are real and are associated with this type of transient. Consequently these phenomena can be expected to occur during large break accidents in large power reactors and should be appropriately modeled in systems codes to quantify the magnitudes in the several vendor plant geometries.

4.1 The blowdown bottom-up core quench

The early fuel cladding cooling during blowdown was observed during Experiment L2-2, the first LOFT nuclear experiment. This behavior was different from the expected (and predicted) core thermal behavior. At that time according to the understanding of reactor system behavior during a large break LOCA, the cladding temperature should increase rapidly after LOCA initiation due to equilibration of stored heat and then continue to increase slowly from decay heat to a maximum during the reflood phase. A precusory cooling due to droplet entrainment from the lower plenum after ECCS initiation would reverse the core heatup and begin a slow cooling trend. Finally the cladding temperature would be quenched to the saturation temperature as a result of core reflood with ECC water. This classic large break LOCA scenario was supported with experimental evidence from facilities such as Semiscale and with code analysis.

In experiment L2-2 (and in other LOFT experiments with similar boundary conditions) the cladding temperature increases as expected; however, the temperature increase is stopped in a few seconds and is followed by a core wide bottom-up cladding quench. The cladding temperature enters CHF approximately 5 s later and reaches a second maximum during the reflood phase; however, the highest peak cladding temperatures occur during the first

heatup. This unexpected core thermal behavior is in response to hydraulic phenomena within the primary system during blowdown which cause an upward coolant mass flow through the core. The hydraulic phenomena and effects on core thermal behavior provide a difficult challenge to best estimate systems codes.

After the opening of the blowdown valves in the broken loop the reactor vessel voids rapidly. The flow direction in the core reverses in response to the larger liquid flow out of the broken loop cold leg as shown in Figures 23 and 24 for experiments L2-5 and LP-02-6. Fuel rod cladding DNB occurs at approximately 1 s in the high power region. The reverse flow through the core lasts only a short time (i.e., in experiment L2-2 the flow becomes positive after 2.5 s). During the initial blowdown the flow out of the vessel through the cold leg break greatly exceeds the coolant flow into the downcomer from the intact loop cold leg as it was shown in Figure 4. However, the break flow transitions from subcooled critical flow to saturated critical flow which reduces the magnitude of the break flow below the inflow from the intact loop cold leg. More liquid is being delivered to the downcomer than is being expelled out of the downcomer. The additional liquid penetrates down to the lower plenum and up to the core resulting in a core bottom-up quench of the cladding as measured by thermocouples on the cladding exterior surface. The evidence for core flow reversal, and a coolant density increase within the core is provided by momentum flux transducers at the core exit, a densitometer in the hot leg of the broken loop and in-core self-powered neutron detectors (SPND). The SPNDs contain cobalt emitters which are sensitive to neutron and gamma radiation. In the reactor shutdown state the SPNDs are sensitive to variations in local fluid density through the gamma flux sensitivity and therefore provide good indication of the additional liquid, or sometimes referred to as a density wave travelling through the core [21], [22]. The positive mass flow and density increase causes the bottom-up cladding quench which is relatively uniform radially. The quench lasts for about 5 s at which time the continued mass depletion causes CHF to occur. Also, the coolant flow from the intact loop cold leg decreases below the cold leg break flow at about this time which contributes to reactor vessel coolant depletion.

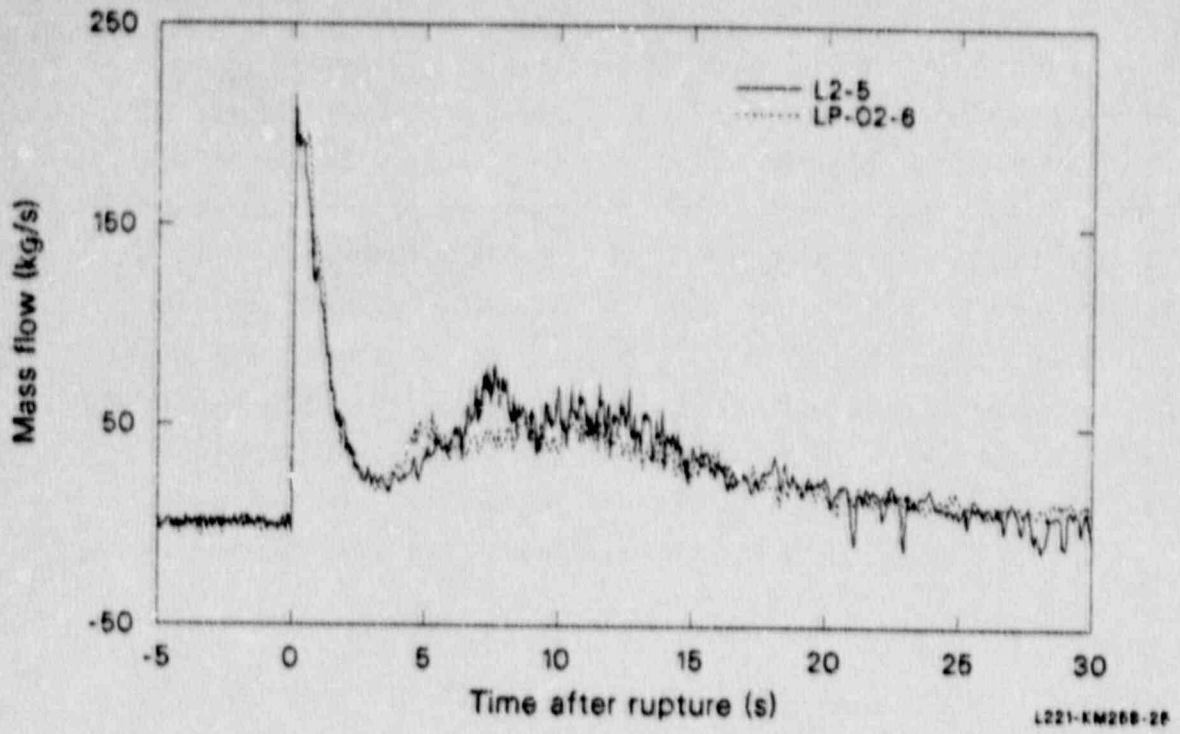

Figure 23. Broken loop hot leg mass flow rates during Experiments L2-5 and LP-02-6.

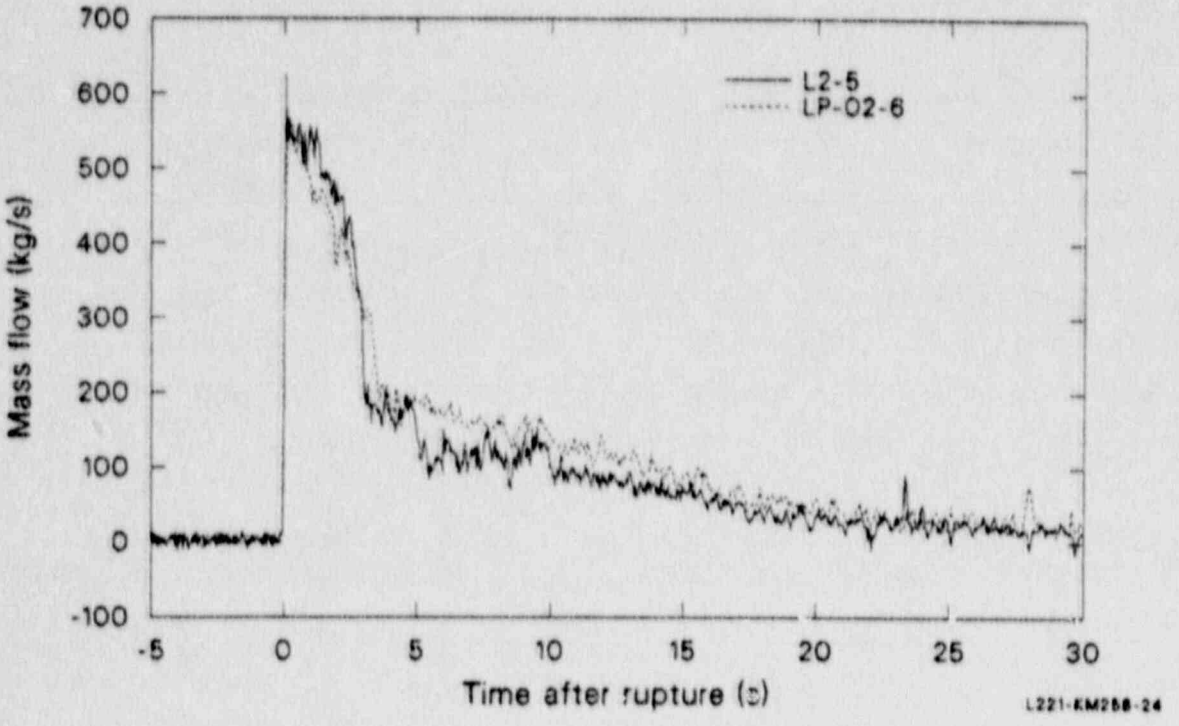

Figure 24. Broken loop cold leg mass flow rates during Experiments L2-5 and LP-02-6.

An estimate of the initial quench wave density is possible from the response of the SPND's located at the axial peak power zone of the LOFT core, as the SPND output signals changed rapidly coincident with the initiation of the cladding temperature quench. The SPND response is shown in Figure 25 for the L2-3 experiment and is compared to the cladding thermocouple response at the same elevation. This change in the SPND output has been correlated to coolant density change through reactor physics calculations. Aksan [23] estimated the value of the quench front coolant density in the center fuel assembly to be 615 ± 80 kg/m3. The calculated densities from the SPND indicate that even at the hot spot region the quality was about 1 to 3%. Therefore, the core inlet flow had to have been at saturation conditions.

Another indication of low-quality flow upwards through the core was obtained from the upper plenum thermocouples, which measure coolant temperatures directly above the core. Figure 26 shows the measured coolant temperature and indicates that from approximately 3 to 6 s, the coolant in the upper plenum nearest the core was superheated vapor. However, at approximately 6 s, the upper plenum coolant temperature was rapidly reduced to saturation temperature.

The cladding thermocouple data are also useful in establishing the general behavior of the quench as it progressed from the bottom to top of the reactor core. Figure 27 shows the measured cladding temperature at the 38 cm (15 in.) axial location (measured from the bottom of the fuel rods). Notice the well-defined time at which the coolant flow initiated the rapid cooling. This behavior was consistent at all axial levels and is summarized in Figure 28 showing the initial quench cooling time versus axial position for each of the 20 axial cladding thermocouple locations. The velocity of the coolant wave as measured from the initial, rapid cladding cooling time versus axial position is estimated from Figure 28 to be approximately 1.00 to 1.00 m/s. (The upper plenum coolant thermocouple quench occurred just after highest elevation fuel cladding thermocouples began to quench). The core inlet mass flux was estimated to be approximately 515 to 1050 kg/m^3s from the coolant velocity and density estimates.

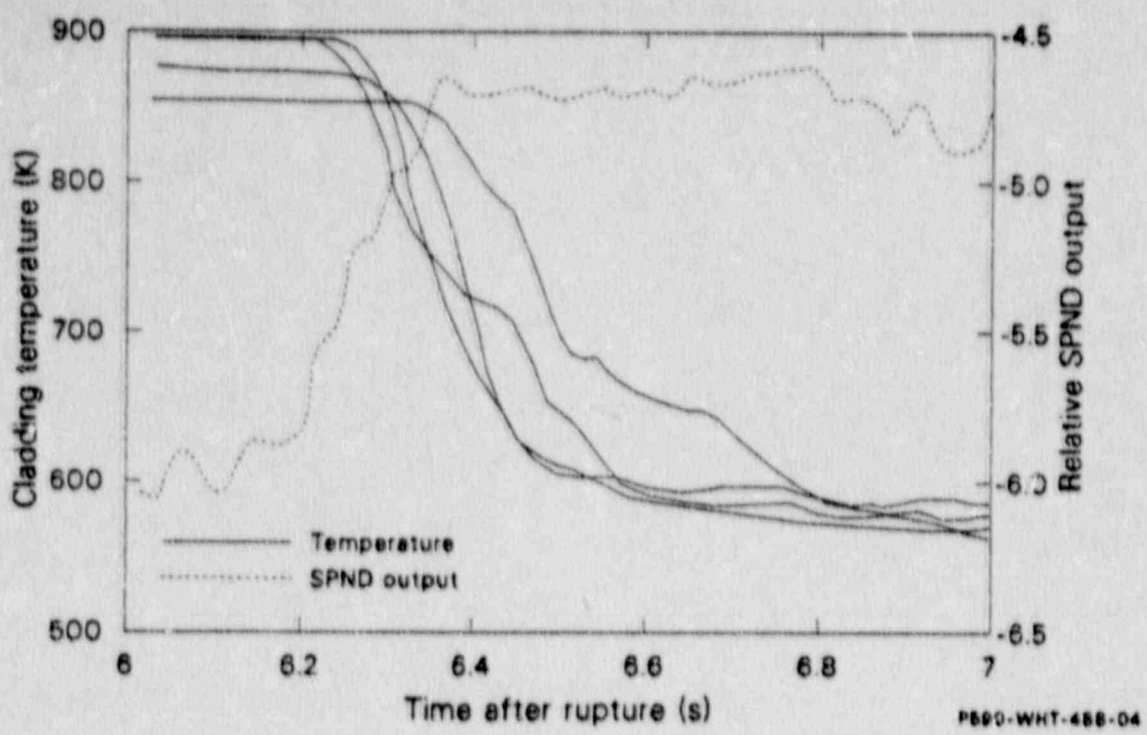

Figure 25. Relative SPND output and cladding temperatures for Experiment L2-3.

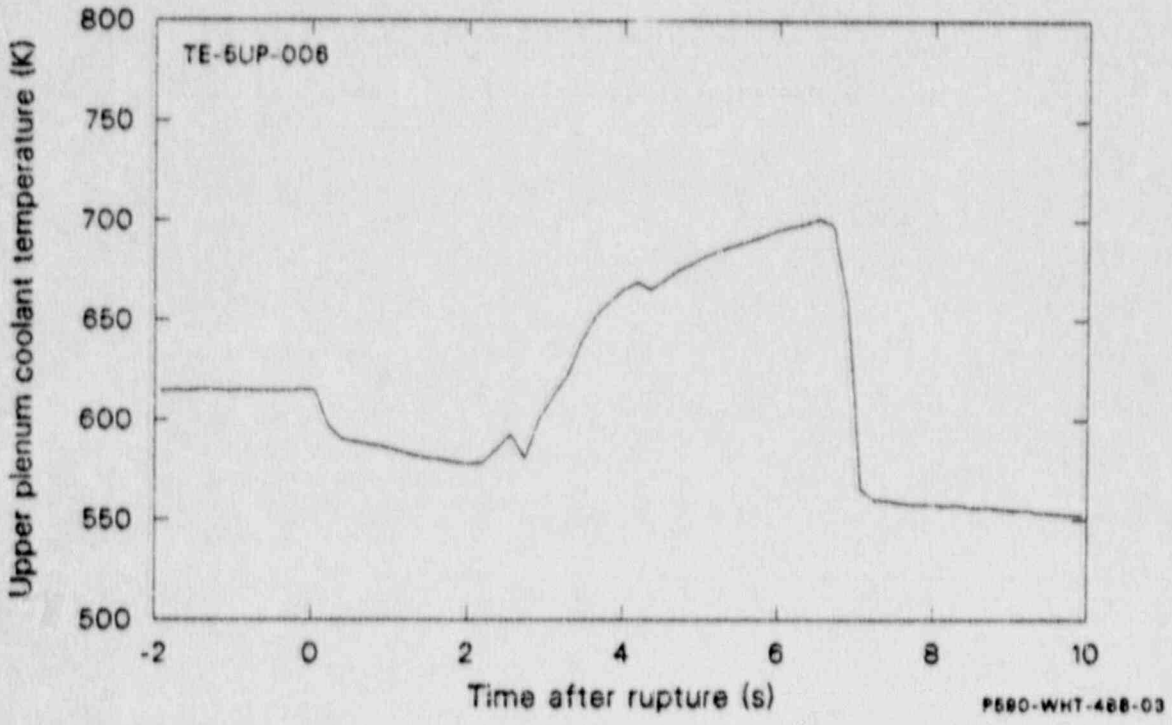

Figure 26. Upper plenum temperature during Experiment L2-3.

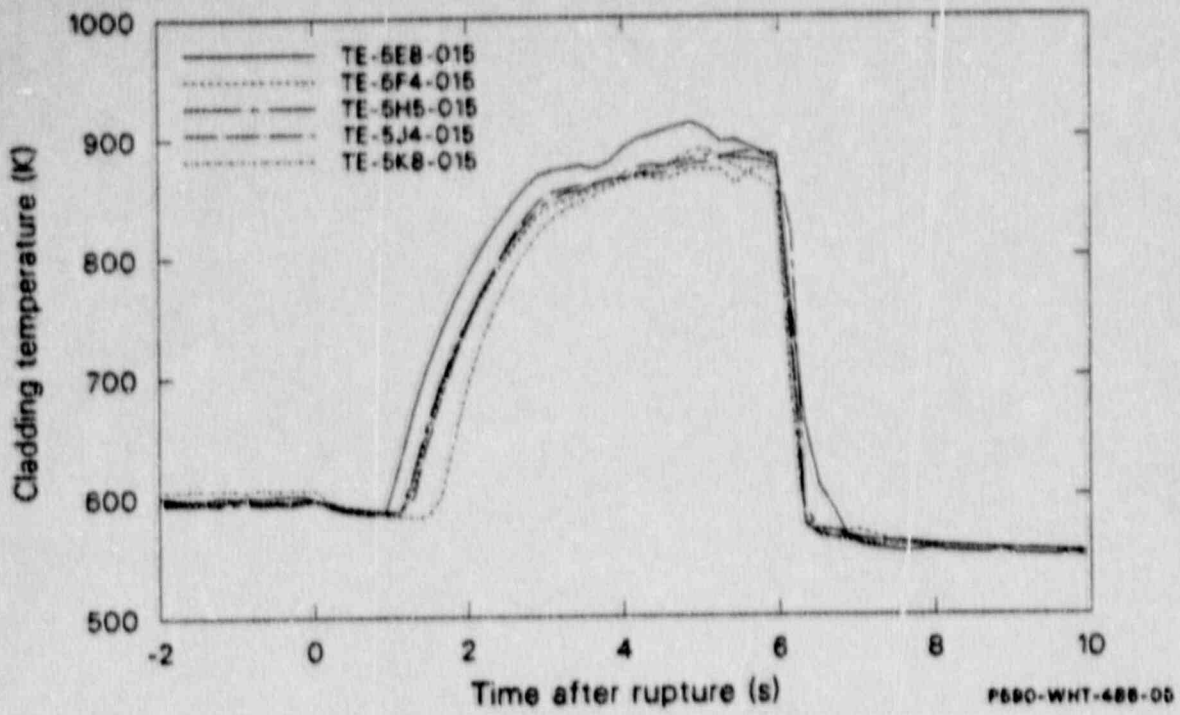

Figure 27. Cladding thermocouple response during Experiment L2-3 at 38 cm (15 in) elevation.

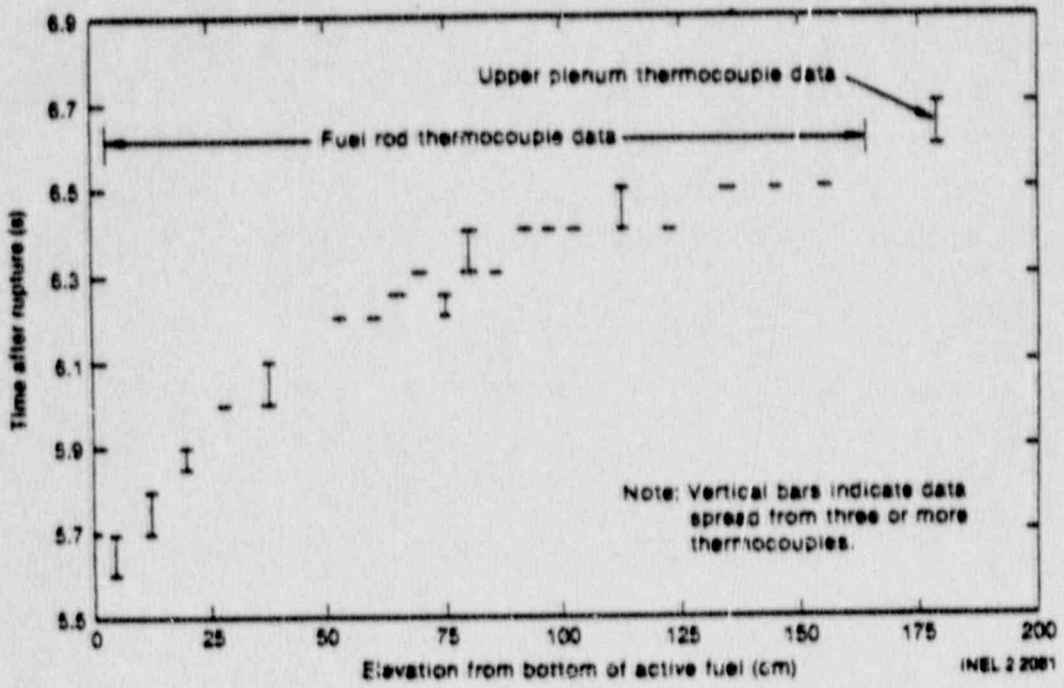

Figure 28. Initial cladding cooling versus axial elevation for center fuel assembly during Experiment L2-3.

In summary, the rapid cladding cooling was primarily a result of low quality, high upward core flow at a time when the system pressure was still relatively high (7 MPa). References 6, 9, 23, and 24 discuss the thermal hydraulic conditions leading to the early quenches during experiments L2-2 and L2-3, in more detail.

4.2 Effects of primary coolant pump operation

The LOFT experiments have shown that the early bottom-up quench is a result of the fine balance of coolant inflow and outflow from the downcomer and flow reversal in the core. Review of the break flow (more discussion of the break flow is included in the Section 4.4) in all of the large break experiments shows that the break flow and cold leg broken loop flow are dependent on primary system pressure and coolant temperature upstream of the break. These parameters were nearly the same for all the experiments. Therefore, the early bottom-up fuel cladding quench depends on hydraulic parameters within the reactor vessel and intact loop.

Three operational modes of the reactor coolant pumps were used in the LOFT large break experiments:

- continuous pump operation
- early pump trip with typical pump coastdown
- early pump trip with fast pump coastdown (decoupled flywheels)

The early quench did not occur only in the experiments in which the pumps were tripped within 1 s of transient initiation and disengaged from the flywheels (L2-5 and LP-LB-1). The experiment results show that the early quench is a function of the pump operation mode, pump characteristics, and initial flow conditions in the intact loop.

The first two large break experiments, L2-2 and L2-3, were conducted with reactor coolant pumps running. The coolant mass flow rate in the cold leg remained almost constant until 6 s during both experiments. Due to this and the decreasing mass flow rate in the broken loop cold leg, the intact loop cold leg mass flow rate exceeded the broken loop cold leg mass flow rate. At

5 s this difference was about 60 kg/s. The difference in the flow rates resulted in an excess of 700 kg of water being delivered to the downcomer between 4 an 6 s. The excess mass of water resulted in the propagation of a density wave upward through the core during this time. In these experiments the early quench was also the most complete, extending through the entire core radially and axially.

In experiment LP-02-6 the pumps were tripped at the beginning of the transient and allowed to coast down under the influences of the flywheels. Figure 29 shows the mass flow rate in the intact loop cold leg. Despite pump trip at about 1 s the mass flow rate in the intact loop cold leg remained almost constant until 5 s (similar to experiments L2-2 and L2-3 where the pumps were not tripped). The amount of the additional coolant entering the downcomer in this early portion of blowdown was initially calculated for LP-02-6 to be 135kg [13], about 5 times less than during the L2-3 Experiment. This mode of pump operation provided enough coolant and head to initiate the bottom-up quench, but the quench front did not propagate through the entire core. This is illustrated by the behavior of thermocouples mounted on fuel rod 5G06 in the center fuel module at four different axial positions shown in Figure 30. The thermocouple at the lowest position TE-5G06-11 (11 inches above the bottom of the core) quenched at about 6 s, while the thermocouple at 45 inch elevation was rewetted at 9 s. The upper thermocouple at 62 inch showed only some cooling effects but not quench.

In experiment L2-5 the reactor coolant pumps were tripped also at about 1 s but the flywheels were disconnected from the pumps resulting in a very fast pump coastdown. The effect of fast coastdown is illustrated in Figure 29 which compares the mass flow rate in the intact loop cold leg for experiments L2-5 and LP-02-6. The coolant mass flow rate decreases rapidly at 2 s in experiment L2-5 compared to 5 s in experiment LP-02-6 with typical pump coast down. This early mass flow rate decrease in the intact loop cold leg happened about 1.5 s before saturation in the broken loop cold leg. Consequently, only about 9 kg of additional coolant [13] could be delivered to the downcomer which was insufficient to quench the core.

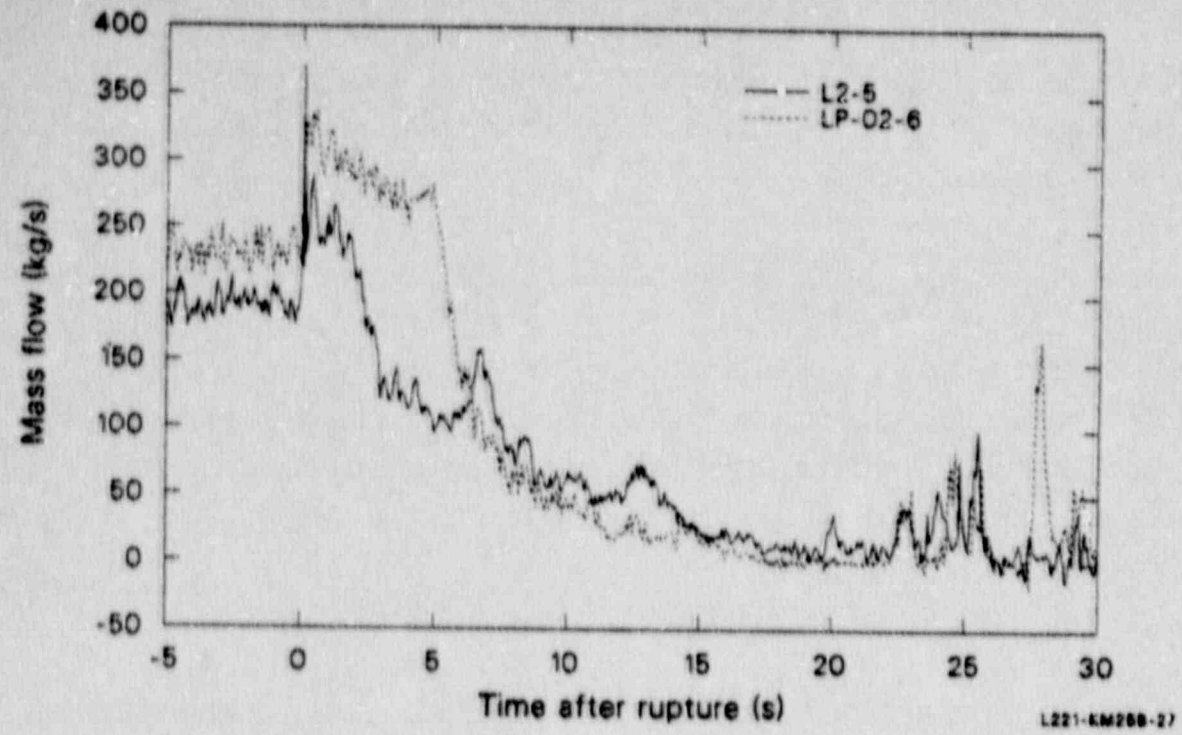

Figure 29. Coolant mas flow rates in the intact loop cold leg during Experiments L2-5 and LP-02-6.

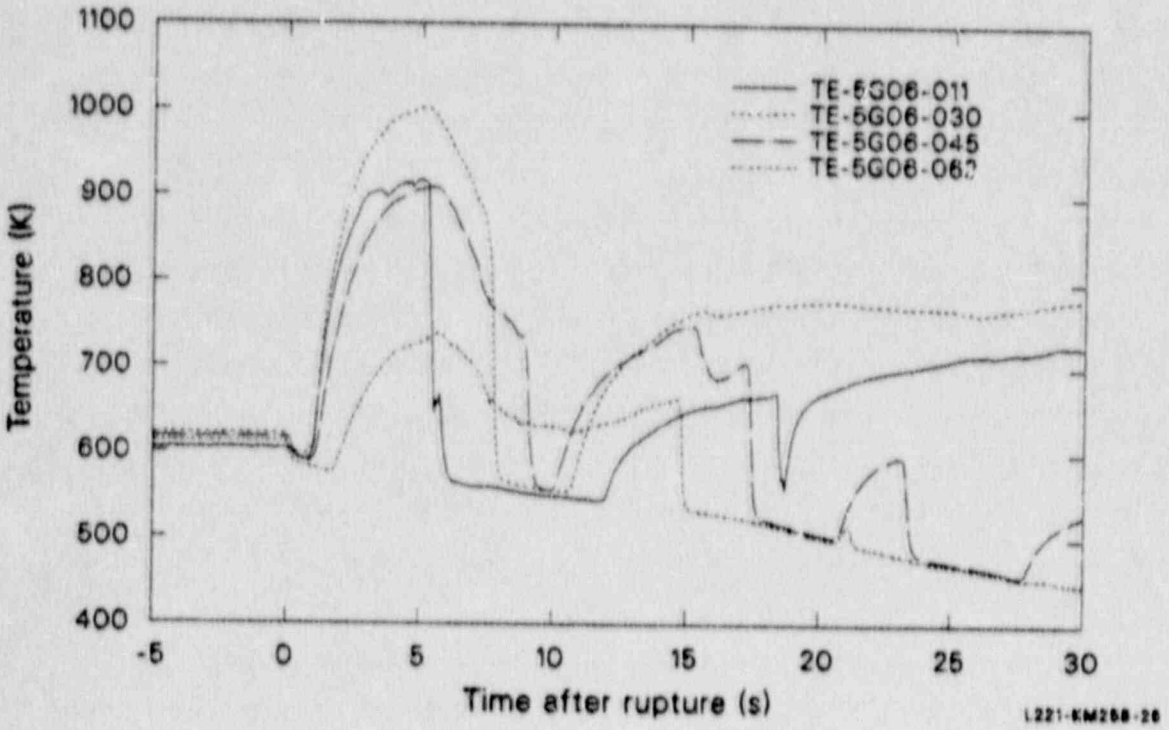

Figure 30. Fuel cladding temperatures measured at rod 5G06 at different elevations during Experiment LP-02-6.

Experiment LP-LB-1 was performed with reactor coolant pumps in the same operation mode as in Experiment L2-5. This experiment also did not contain a bottom up core quench.

Experiment LP-FP-1, in which the reactor coolant pumps were tripped early and disconnected from the flywheels, contained an early quench. The quench occurred in this case because of the higher initial, or steady state, mass flow in the intact loop. The additional mass flow caused the magnitude of the intact loop cold leg flow to be larger than the broken loop cold leg flow at the time of transition to saturated critical flow at the break.

4.3 The blowdown top-down quench

The core cooling during blowdown contains two phenomena: the bottom-up cooling, discussed in the previous sections, and the top-down cooling. Again, LOFT experiments were the first to show the top-down cooling phenomenon. Cladding temperatures measured during the LP-02-6 experiment, as shown in Figure 30, indicate a second quench in the upper part of the core which moved downwards and rewetted the cladding at the 45 inch elevation at 17.5 s. The thermocouple measuring the highest temperature at the 30 inch elevation did not indicate the top-down quench.

This top-down quench affected fuel module 2 as shown in Figure 31. The top-down quench was not uniform across the core as shown in Figure 32. The quench reached the lower half of bundle 4 (Figure 32) earlier than bundle 2. Bundle 6 was not affected in the lower half at all by this quench. Bundle 4 was closer than the other fuel elements to the intact loop hot leg which is a source of water which drains into the reactor vessel. As shown, the top-down quench is multidimensional in contrast to the bottom-up quench which can be treated as one-dimensional as it rewets the center fuel module and the peripheral modules at the same time. Analogous top-down quench phenomena were detected in other LOFT large break experiments. Experiment L2-5 was performed with a rapid RCP coastdown to prevent the bottom-up quench, however this operation did not prevent the top-down quench. In Figure 8, which compares the L2-3 and L2-5 experiments, only the

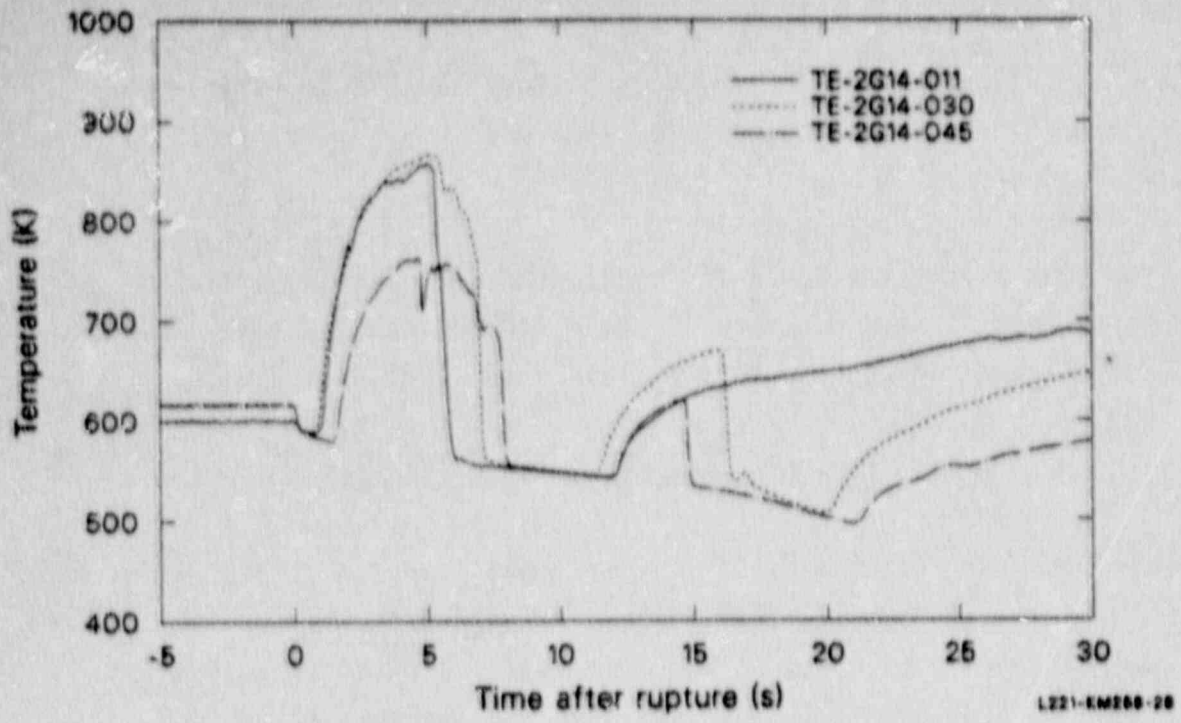

Figure 31. Fuel cladding temperatures in the peripheral bundle 2 during Experiment LP-02-6.

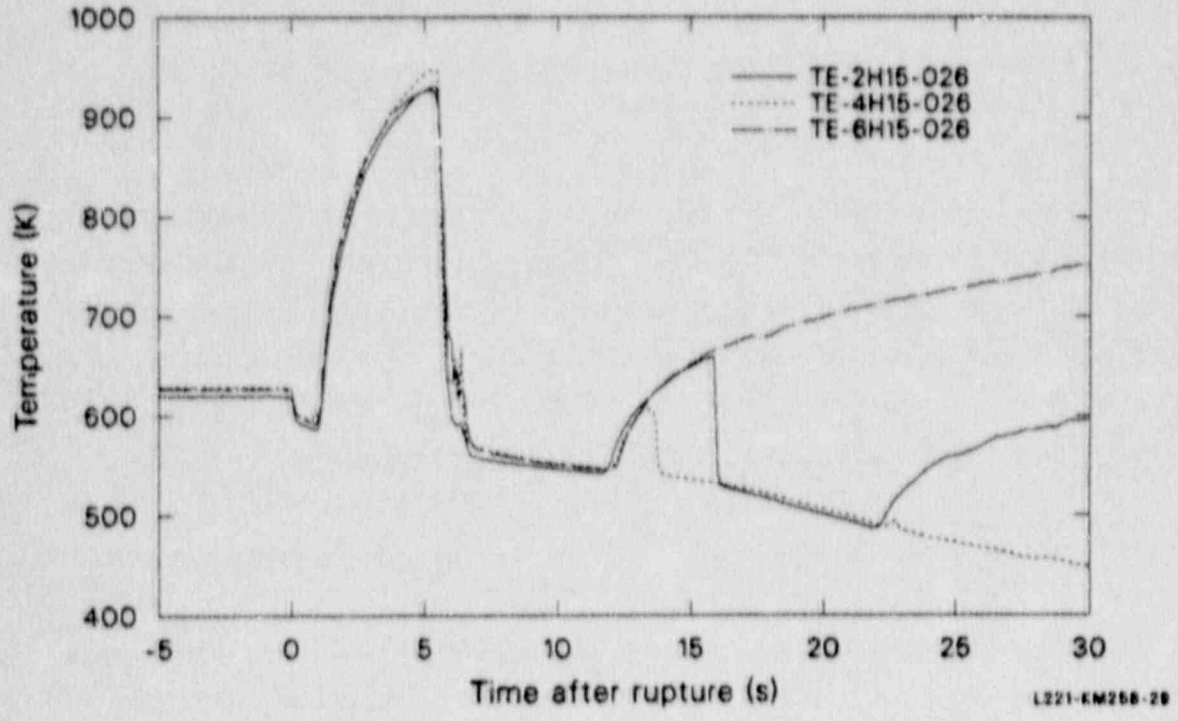

Figure 32. Fuel cladding temperatures in the peripheral bundles 2, 4, and 6 during Experiment LP-02-6.

top-down quench is indicated in the upper part of the CFM in experiment L2-5. Figure 33 shows that only the top-down quench was present in the peripheral fuel modules.

The top-down quench phenomenon is concluded to be very significant because it decreases cladding temperatures which reduces the time needed to quench the fuel cladding during core reflood with the ECCS.

4.4 Blowdown and Reflood Heat Transfer

The LOFT nuclear core had special experimental instrumentation which included 186 thermocouples [2] that were laser welded to the external surface of 76 fuel rods as shown in Figure 34. The fuel rod cladding external thermocouples indicated that the reactor core was quenched early in the blowdown transient as explained in the previous sections. Since the phenomenon of the early quench is very important with regard to removal of a substantial amount of stored energy from the fuel and with regard to the ability of computer codes to predict large break LOCA peak cladding temperature cooling and quench phenomena have been extensively studied. However, the true nature of this early cooling and quench phenomenon remains in question.

The postulation has been made that the LOFT external fuel thermocouples indicate only local quenches of the thermocouple itself or of small cladding area around it. Our position is that there is enough evidence that the LOFT cladding surface thermocouples were indicating a true complete quench during blowdown. However we recognize that the external thermocouples do not measure the cladding surface temperature accurately because of the fin-cooling effect. In the following sections we will discuss in detail the problems associated with the external cladding thermocouples with regard to the blowdown quench and the reflood quench. We will review separate effect experiments conducted to study the thermocouple effects and we will discuss the evidence from the LOFT experiments indicating complete fuel rod quenches during blowdown.

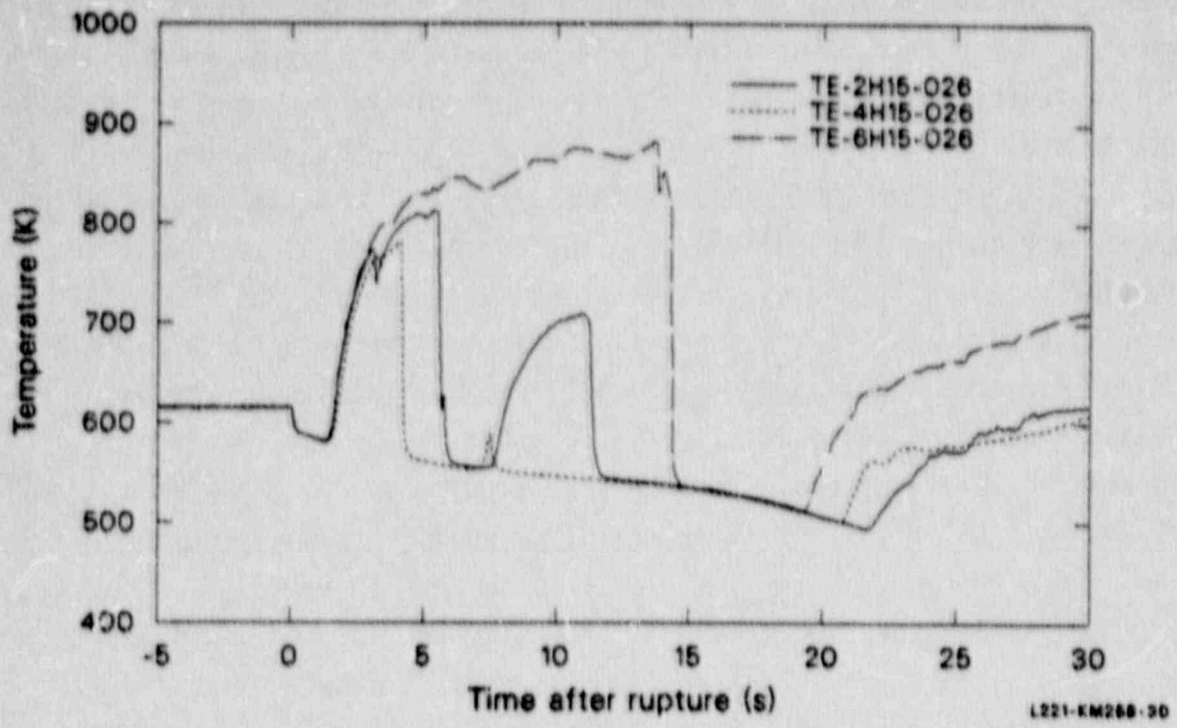

Figure 33. Fuel cladding temperatures in the peripheral bundles 2, 4, and 6 during Experiment L2-5.

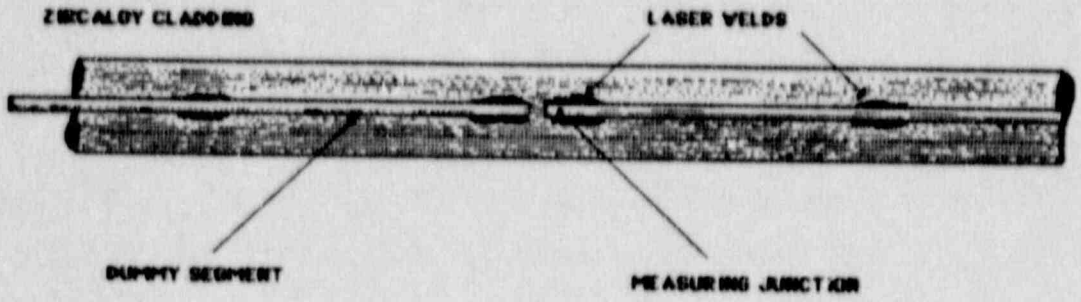

Figure 34. LOFT fuel rod external thermocouple.

We will also address the differences in behavior of nuclear and electrically heated rods since these differences influence the understanding of the surface thermocouple effect. It can be concluded from the review of the work on nuclear rod versus electrical heater rod behavior under rapid flooding conditions that solid-internal heater rods of the Semiscale design cannot simulate the rapid quenching of a nuclear rod, due to the relative high thermal diffusivity of the electrical heaters. Because the UO_2 conductivity and the fuel-to-cladding gap limit the energy delivery rate to the nuclear fuel rod cladding during a rapid cooling transient, the nuclear rod cladding can be quenched by removing only the energy in the cladding. For the solid-type heater rod, not only the cladding energy but also a significant portion of the rod internal energy must be transferred before cladding quench can occur. In other words, a nuclear fuel rod is conduction limited and a solid-type electrical rod is convection limited. Consequently, a large amount of energy must be removed from the solid-type electrical rod before it can quench. The calculated nuclear rod cooling rates can be from 4 to 5 times greater than for Semiscale electrical rods, depending on the inlet coolant flooding velocity.

4.4.1 Effect of Cladding Surface Thermocouples on Blowdown Heat Transfer

The effects of cladding external thermocouples on the early quench phenomena were analytically and experimentally investigated at the INEL. Two different sets of experiments were conducted in the LOFT Test Support Facility (LTSF). These tests were performed in a single rod geometry and in a nine rod bundle geometry and involved solid heater rods and rods with simulated pellet-to-cladding gap. Another set of experiments with nuclear fuel was conducted in the Power Burst Facility (PBF). This section includes the results of these experiments and also analyses of LOFT data, specifically the comparison of fuel centerline temperature measurements with cladding surface temperature measurements.

4.4.1.1 LTSF Experiments

The LTSF quench experiments provide a simple geometrical configuration with well-quantified inlet hydraulics and the capability to maintain system pressure as high as 7 MPa. The detailed description of the test facility is given in References 25 and 26. The first series of tests in LTSF were performed using a single Semiscale rod which is a typical "solid" internally heated fuel rod simulator used in many light water reactor research projects. Four external thermocouples had been laser welded to the outer surface of this heater rod similar to LOFT cladding thermocouples. The heater rod also had four internal cladding thermocouples to measure the rod temperature response. A second rod was built without the external thermocouples. Identical experiments were conducted with both rods. The results of one of the 20 quench tests, conducted in LTSF are shown in Figure 35, for the boundary conditions given in the Figure. The data presented were taken from cladding internal and external thermocouples located at the heater rod hot spot. The time of coolant arrival at the thermocouple location is indicated by the rapid change in the test section gamma densitometer response. Thus, the quench times can be estimated with respect to coolant arrival. During the high-pressure (7 MPa) tests the heater rod with external thermocouples consistently quenched in about half the time required by the heater rod without surface thermocouples. It can also be seen from the data that the surface thermocouple is preferentially cooled and quenches much sooner than the cladding, as indicated by the internal thermocouple data. However, further analyses [23,28] indicated that solid heater rods of Semiscale design cannot simulate the rapid quenching of a nuclear rod, due to the relative high thermal diffusivity of the electric heater rods. The differences between nuclear fuel and solid heater rods will be discussed in more detail in Section 4.4.2. Details of these LTSF experimental results can be found in References 25 and 27.

The second series of LTSF tests investigating quench behavior of a different fuel rod simulator design was conducted with a nine-rod (3x3) bundle. The tested rod was always in the center of the nine-rod configuration (Figure 36). The eight surrounding rods were solid-type FEBA heater rods (similar to Semiscale heater rods).

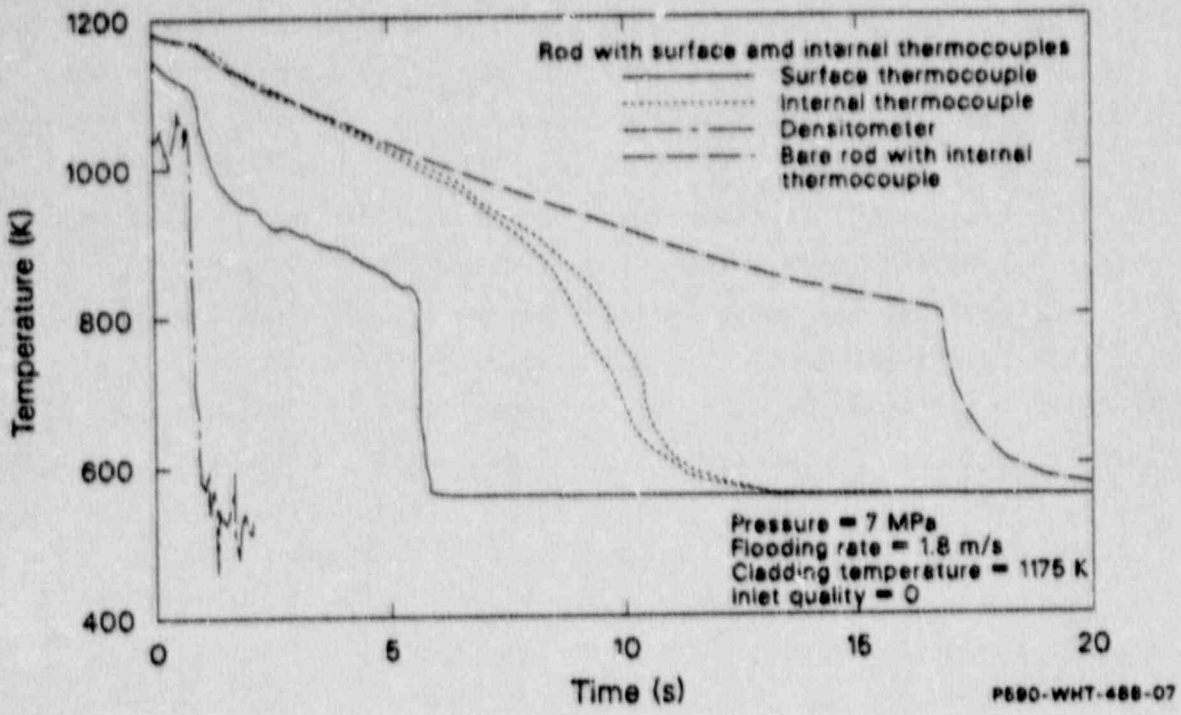

Figure 35. LTSF single rod quench test thermocouple response for initial cladding.

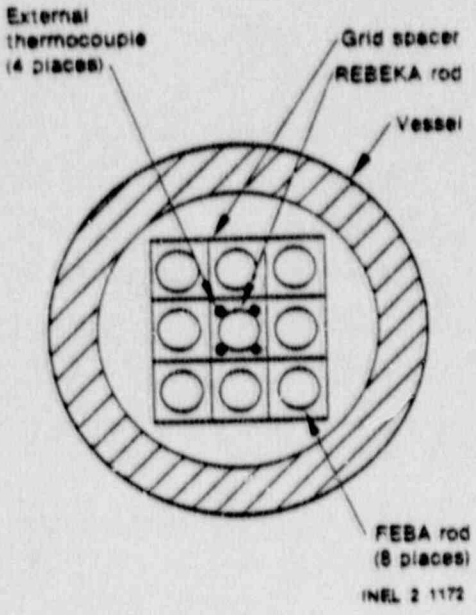

Figure 36. LTSF test nine-rod bundle configuration

A REBEKA cartridge-type heater rod and a FEBA solid-type heater rod (Figure 37) were each tested in the center position in the nine-rod bundle, which provided a geometry and thermal-hydraulic environment typical of a nuclear fuel rod cluster. The REBEKA heater rod has Zircaloy cladding and aluminum oxide pellet construction with a pellet-cladding gap to simulate the thermal characteristics of a nuclear fuel rod. This heater rod was tested with and without cladding external thermocouples. The main objectives of this experimental program were to evaluate the effect of cladding external thermocouples on the early blowdown phase quench behavior of a cartridge-type nuclear fuel rod simulator, to determine how accurately cladding external thermocouples measure cladding temperature during a blowdown phase quench, and to compare the high-pressure quench behavior of a cartridge-type heater with that of a solid-type heater rod under thermal-hydraulic conditions that occurred during the blowdown phase (0 to 10 s) of LOFT experiments. The experimental program and the results of the tests are given in detail in Reference 26.

This research program showed that the REBEKA rod satisfactorily simulates the thermal response of a nuclear rod. It was shown also that the quench behavior of FEBA rods is significantly different than that of REBEKA and nuclear fuel rods. Due to the higher thermal diffusivity of solid-type heater rod and lack of pellet-cladding gap, the rod undergoes a lengthy period of precursory cooling before quenching; whereas a cartridge type heater rod and nuclear fuel rod quench very rapidly from high temperatures when subjected to rapid flooding conditions. The REBEKA rod quenched in less than 3 s from about 900 K, whereas, the FEBA heater rods experienced an extended period (10 s) of precursory cooling before quenching at about 700 K (Figure 38).

The results of the experimental program indicate that cladding external thermocouples had a negligible effect on the cooldown rate and quench behavior of a REBEKA cartridge-type heater rod under rapid (1 to 2 m/s) flooding conditions at high pressure (Figure 39). Rods with or without external thermocouples undergo the same quenching under the same hydraulic conditions. However the cladding external thermocouples are preferentially cooled during the quenching process and do not accurately measure cladding

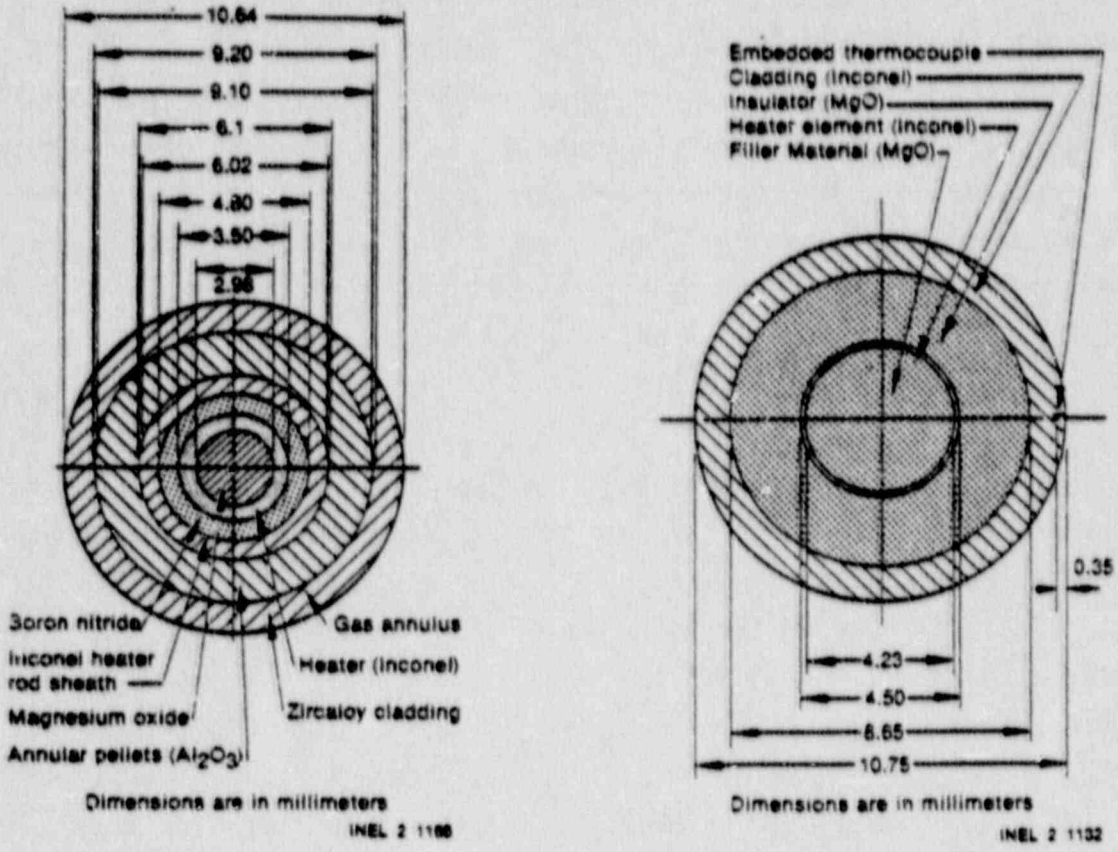

REBEKA FEBA

Figure 37. Cross section of FEBA and REBEKA fuel rod simulators

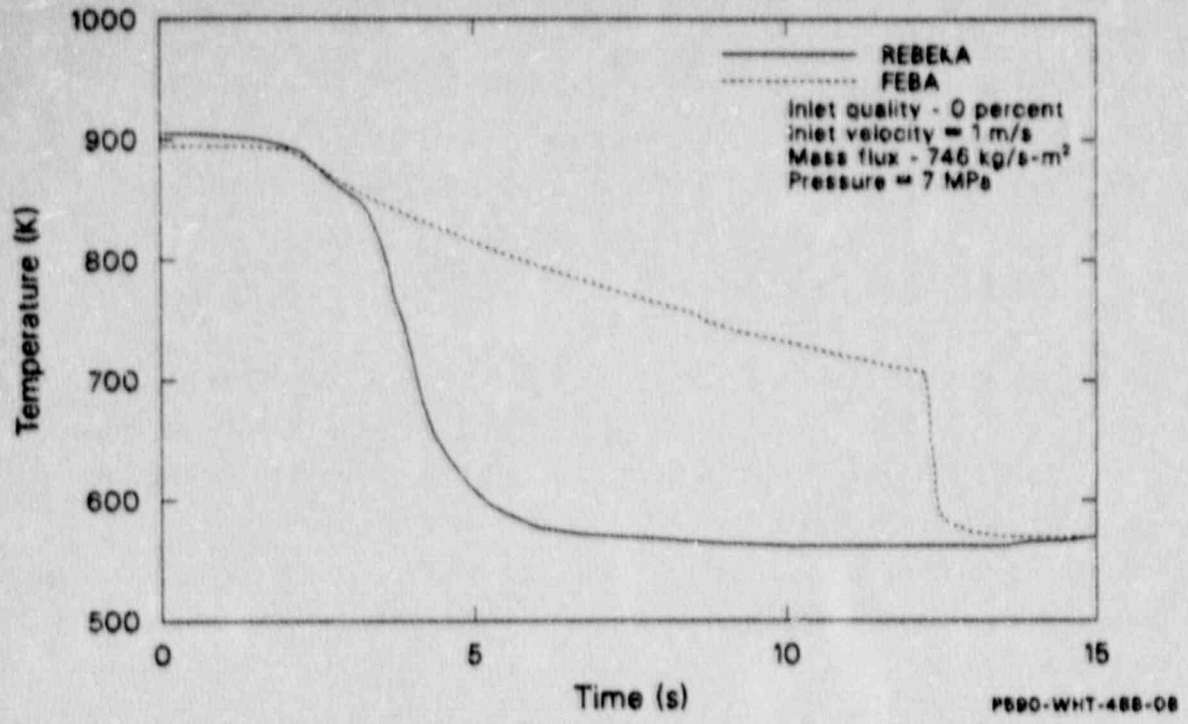

Figure 38. REBEKA and FEBA heater rod 7 temperature responses for runs 1A (REBEKA) and 1F (FEBA).

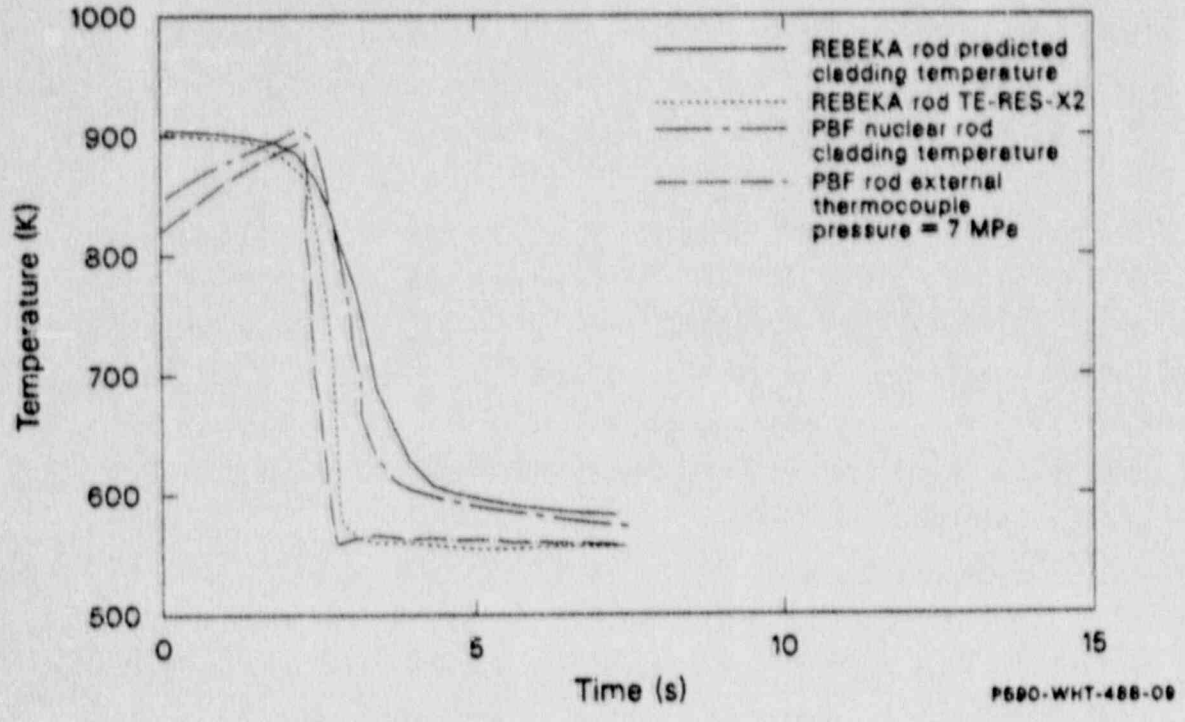

Figure 39. Blowdown quench beahvior of a REBEKA heater rod (from LTSF bundle test) and a nuclear fuel rod (from PBF-TC tests) with external cladding thermocouples.

temperature during reflood. Since the REBEKA rod has been shown to satisfactorily simulate the thermal response of a nuclear rod, [28], the REBEKA rod results are considered applicable to LOFT nuclear fuel rods.

4.4.1.2 PBF Experiments

Three series of light water reactor fuel behavior experiments (Thermocouple Effects Experiment series TC-1, TC-3 and TC-4) were performed in the Power Burst Facility (PBF) at the INEL to specifically evaluate the influence of cladding surface thermocouples on the thermal behavior of nuclear fuel rods under LOCA conditions. A total of twelve experiments were conducted. Each experiment was performed with four LOFT-type fuel rods contained in individual flow shrouds. Two of the rods were instrumented with four LOFT cladding external thermocouples located near the high power region of the fuel rods. All four rods were also instrumented with internal thermocouples at the same axial level as the external thermocouples. Details of the experiment design, conduct and results are presented in References 29, 30, and 31. The analysis of the PBF data contains larger uncertainties than the analyses of other facility experiment data because the hydraulics were not exactly the same among all four separately shrouded rods. However, the following is considered to be qualitatively accurate.

Evaluation of the measured temperature difference across the cladding indicated that the cladding surface thermocouples measured cladding surface peak temperatures during blowdown that were only slightly lower (20 to 30 K) than the actual cladding temperatures. However, comparison of externally instrumented rods with bare rods showed that the surface thermocouples influenced the cladding temperatures during the blowdown phase of the TC tests in two respects:

1. The cladding surface thermocouples increase the surface heat transfer area of the fuel rods and enhance the heat transfer during the initial few seconds of blowdown. As a consequence, CHF is delayed on the externally instrumented rods which results in a reduction of stored energy in the fuel rods at the time-of-CHF.

2. The presence of external thermocouples influences the fuel rod thermal response through a "fin cooling" effect during cladding heat-up.

These two effects resulted in a reduction of blowdown peak cladding temperature ranging from 101 to 115 K (Figure 40). Garner [30] estimated that 35-58% of this reduction is related to delay in time-to-CHF with peak cladding temperatures reduced 74 K for each second of delay, and 42 to 65% of peak cladding temperature reduction is due to fin cooling.

The PBF-TC experiment results showed that fuel rods with and without external surface thermocouples were quenched. The effect of surface thermocouples on rod thermal response during this blowdown quench (Figure 40) appears to be relatively small. If the quality of the flow is very low and the rods are quenched extremely fast, the surface thermocouple effect is negligible. In addition, the effect of surface thermocouples on nuclear fuel rod thermal response during the blowdown quench decreases as the rod initial power decreases, and at low power the effect disappears.

4.4.1.3 Analysis of LOFT Data

In December 1981, analysis of fuel rod perturbations was begun for several geometries of internally located thermocouples. The purpose of this work was to determine the thermal perturbations of placing thermocouples inside the fuel rod pellets. Fuel centerline thermocouples were being designed for placement in LOFT CFMs as a further study of the thermal response during blowdown. This analysis [32] used the COUPLE/MOD5 heat conduction code [33] in both steady state and transient modes. Transient boundary conditions of (1) power generation in the fuel as a function of time, (2) heat transfer coefficient at the fuel rod surface, (3) coolant temperature, and (4) the fuel to cladding gap conductance were obtained from FRAP-T5 prediction calculations of the then designated NRC LOFT Experiment L2-6, which subsequently became OECD LOFT Experiment LP-02-6. The COUPLE/MOD5 calculations of fuel and cladding temperatures are typically as

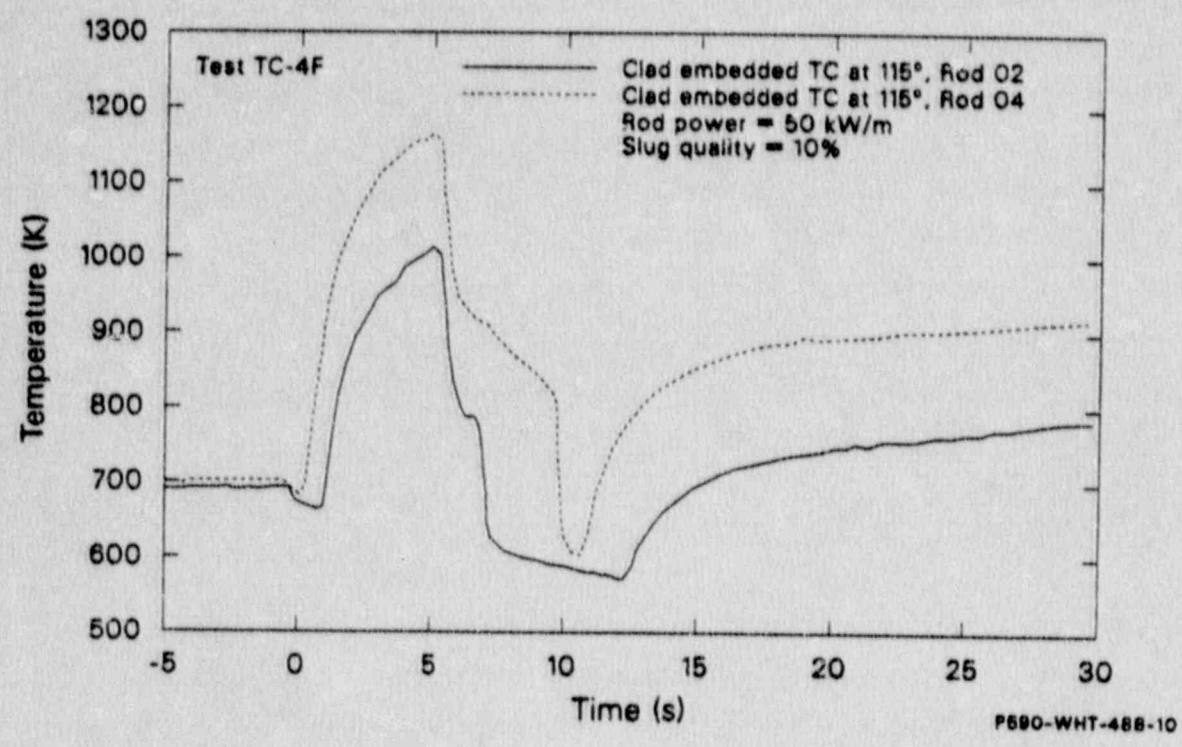

Figure 40. Embeded and internal cladding thermocouple response in rod 04 (bare) and rod 02 (externally instrumented) during blowdown of PBF test TC-4F.

shown in Figure 41 (taken from Reference 32). The results indicate that the fuel centerline temperature is sensitive to the occurrence of a short duration quench of the cladding.

FRAP-T5 calculations were based on the thermal-hydraulic behavior calculated by the RELAP series of codes. The thermal-hydraulics of L2-6 were calculated to be similar to the thermal-hydraulics in Experiments L2-2 and L2-3 [7]. Post-experiment calculations with appropriate revisions to the existing models resulted in good agreement with the measured quench phenomena [7]. Quench phenomena also was calculated to occur in Experiment L2-6 because of the similar thermal-hydraulics. However, the formal prediction of the approved OECD LOFT Experiment LP-02-6 was done with the TRAC-PD2/MOD1 code [14]. The following conclusion is taken from Reference 14:

> An early rewet was not calculated to occur during Experiment LP-02-6. However TRAC-PD2/MOD1 calculated core hydraulic conditions for Experiment LP-02-6 which were similar to the hydraulic conditions which were responsible for the early rewets in previous LOFT large break experiments. Since the early rewets in the previous experiments were also not calculated by TRAC there is a definite possibility that an early rewet could occur in Experiment LP-02-6.

The preceding information provides two principal conclusions which sets the basis for the succeeding discussion. These conclusions are:

1. Fuel rod heat transfer is strongly dependent on fuel cladding-to-coolant heat transfer and cladding temperature. The dependency extends to and includes the fuel center.

2. Systems codes have difficulty calculating quench behavior during the blowdown phase. However, specific use of correlations such as the Biasi correlation can lead to calculated quench behavior very similar to that indicated by cladding thermocouples.

The OECD LOFT Experiment LP-02-6 did include early quench phenomena [13] similar to that observed in Experiments L2-2 and L2-3 [7] as discussed in detail in Section 3.4. Figure 42 shows the response of the fuel centerline

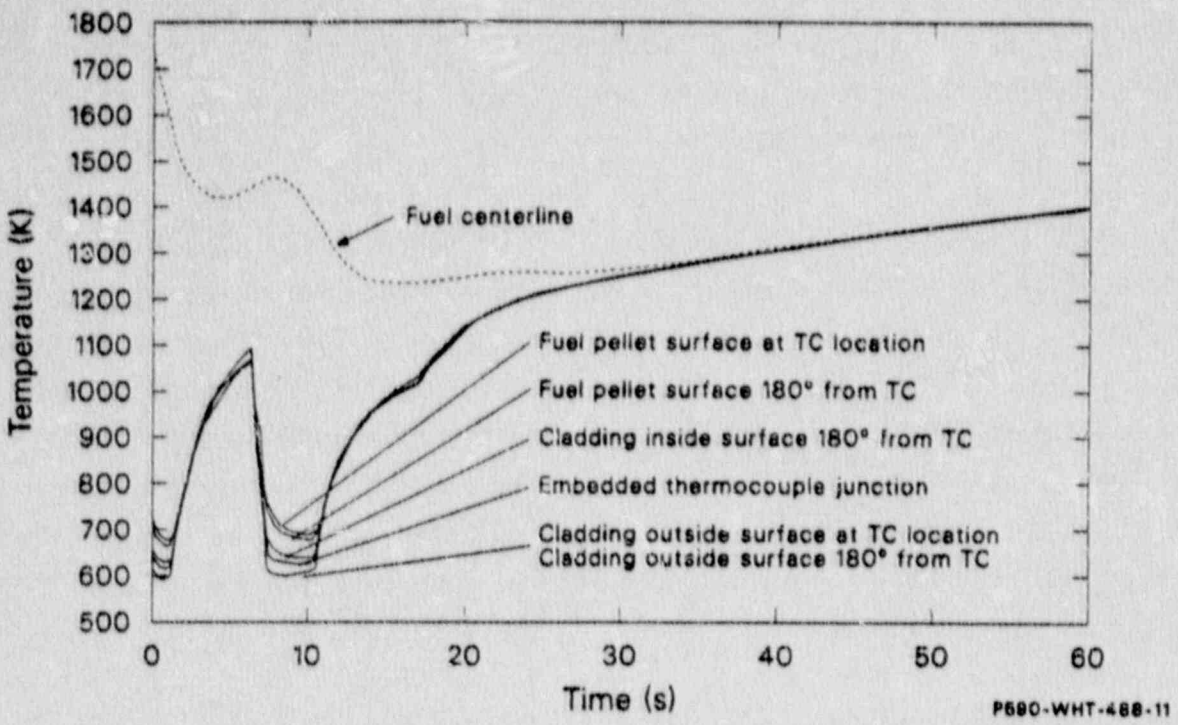

Figure 41. COUPLE/MOD5 calculation of fuel rod temperatures using FRAP-T5 boundary conditions originating from RELAP5 code.

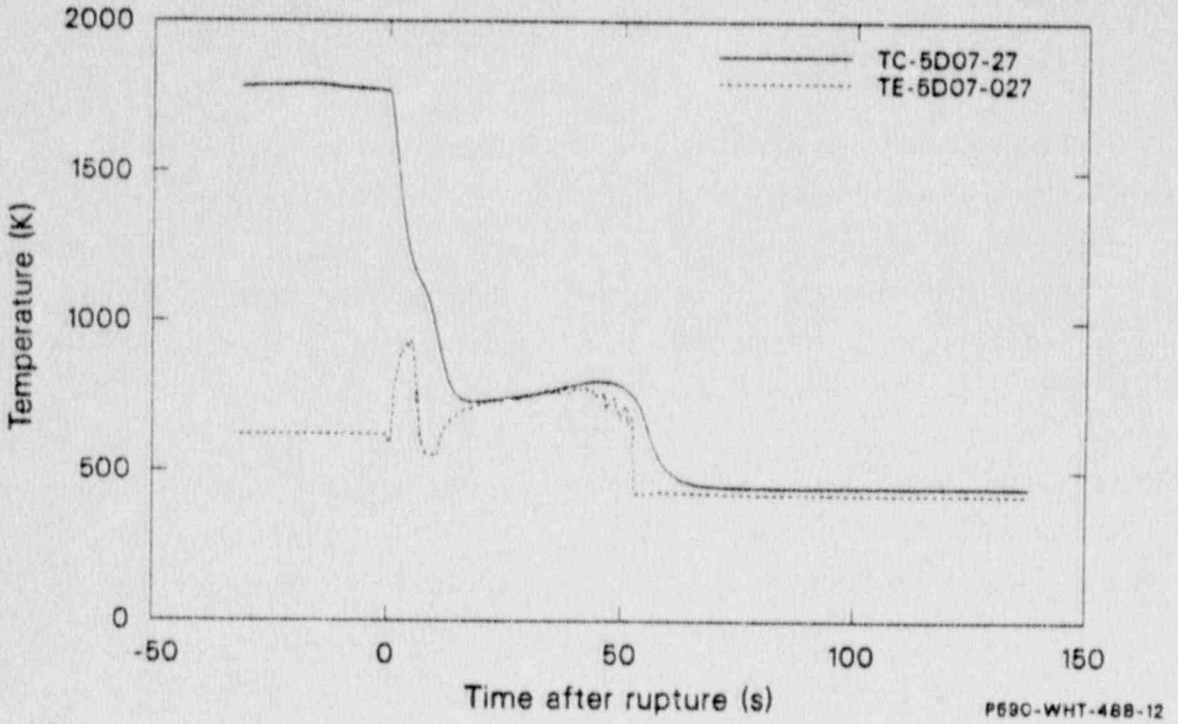

Figure 42. Fuel centerline and cladding temperature at the 27-in elevation on fuel rod 5D07 during experiment LP-02-6.

temperature to the measured cladding temperature at the same elevation. The fuel centerline temperature responds to the change in cladding temperature shortly after the blowdown quench at approximately 8 s and similarly after the reflood quench at approximately 53 s. Figure 43 shows the fuel centerline temperature for two fuel rods which did not have externally mounted cladding thermocouples compared with the fuel centerline temperature shown in Figure 42. The three centerline temperatures are essentially identical in behavior. These data conclusively show that the hydraulics cause complete fuel cladding quench and not just thermocouple quench or localized cladding quench.

Post-transient calculations of LP-02-6 with the RELAP5/MOD2/CYCLE36 code [34] showed cladding quench behavior at all core elevations except at the 26 in elevation which showed significant cooling but no quench. Post-transient calculations with the TRAC-PF1/MOD1 [35] showed only some cooling of the cladding at all elevations. Comparison of calculated and measured fuel centerline and cladding temperatures, shown in Figures 44 and 45, reveals that the calculated cladding temperature must be in error since (1) the fuel centerline temperature comparison is poor, and (2) the fuel centerline temperature is strongly dependent on the cladding temperature (or cladding-to-coolant heat transfer) as has been shown in Reference 32 and actual LP-02-6 data.

The data in LP-02-6 shows that cladding quench occurs at high temperatures, well above the values that have been used in codes such as TRAC-PF1/MOD1 [35]. Nelson [24] describes forced-convective heat transfer mechanisms and explains how minimum wall superheats greater than the homogeneous nucleation temperature result. The conclusion is that quenching can occur at high temperatures in forced-convective water systems. An extensive collaborative effort by Gottula, Condie, and Nelson of EG&G Idaho, Sundaram, Yankee Atomic Electric Company, and Neti and Chen, Lehigh University produced a large experimental data bank from forced-convective, post-CHF heat transfer experiments [36]. To quote from the report, "Quasi-steady state (slow moving quench front) experiments were conducted at pressures of 0.4 to 7 MPA, mass fluxes of 12 to 70 $kg/m^2 \cdot 5$, inlet

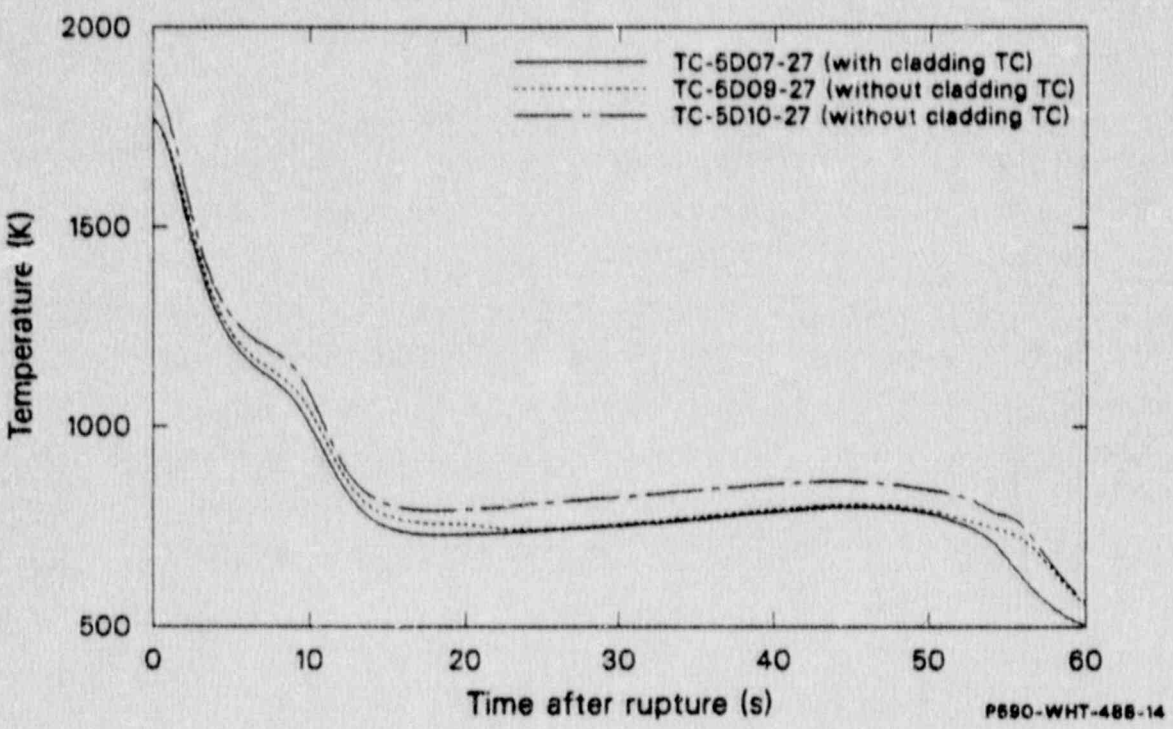

Figure 43. Fuel centerline temperatures at the 27-in. elevation during Experiment LP-02-6.

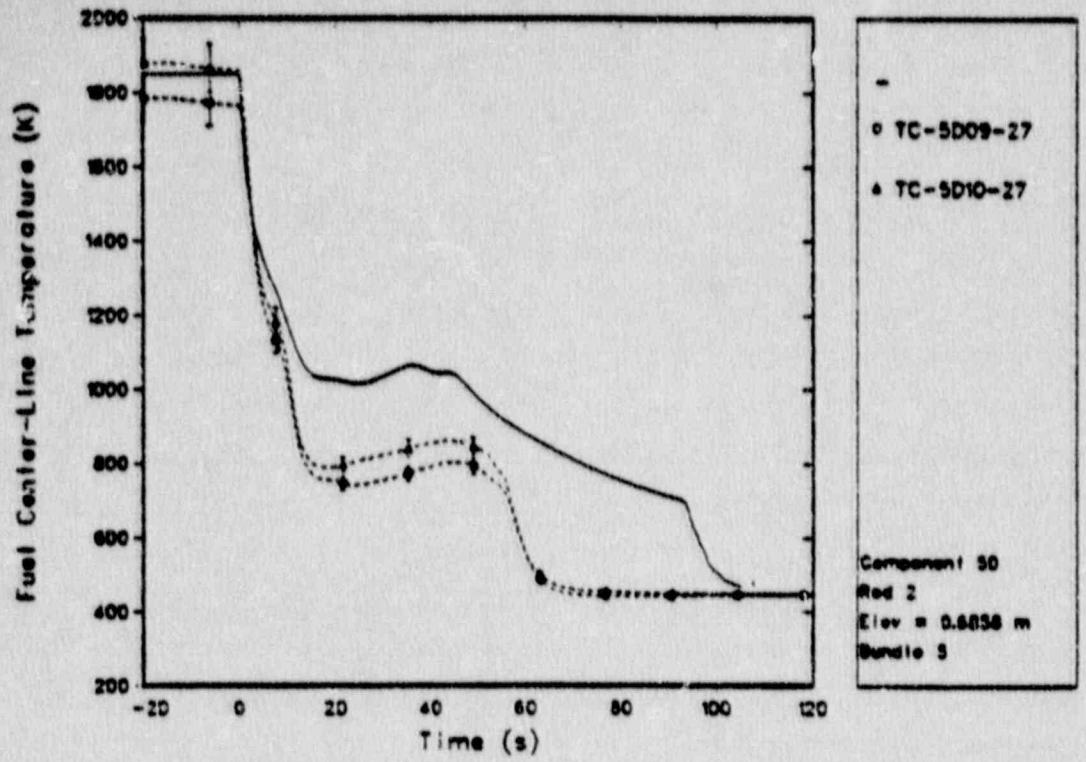

Figure 44 Measured and calculated with TRAC-PF1/MOD1 fuel centerline temperature for experiment LP-02-6 at the 0.6858 m (27-in) core elevation.

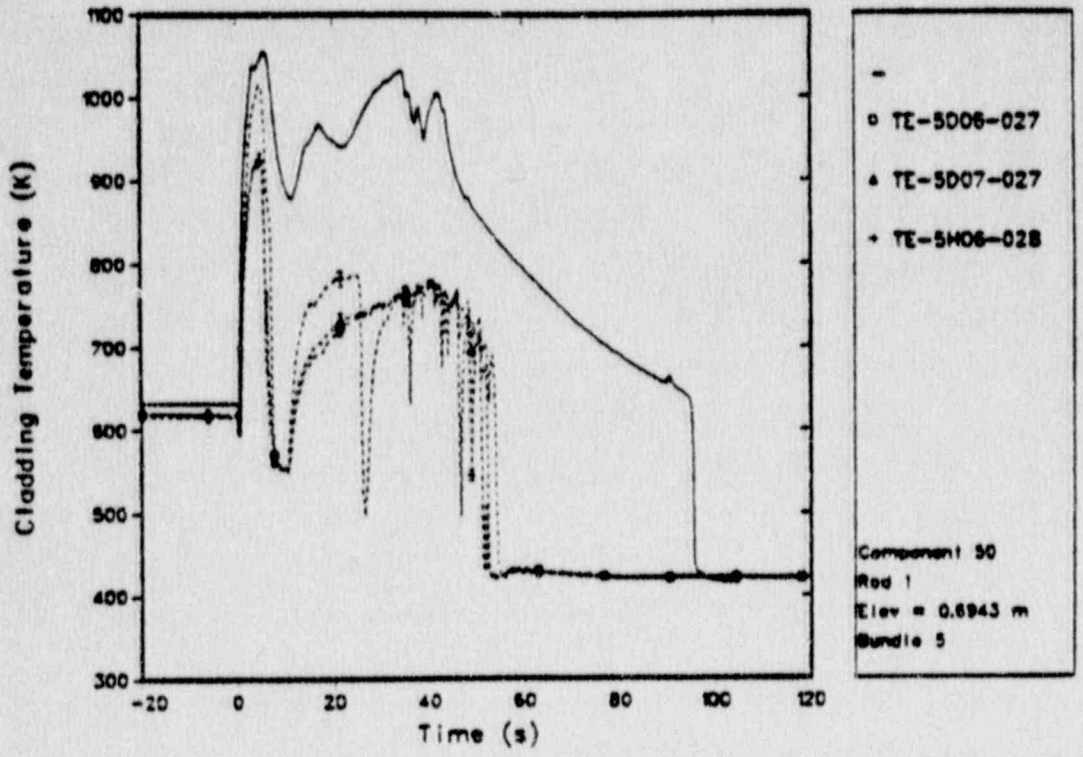

Figure 45. Measured and calculated with TRAC-PF1/MOD1 cladding temperatures for experiment LP-02-6 at the 0.6943 m (27-in) core elevation.

qualities of -7 to 47%, and heat fluxes of 8 to 225 KW/m^2...."The data above 0.4 MPA extend the existing data base. The data was compared with currently used wall heat transfer correlations, and the results were unsatisfactory. A regression analysis of the data showed thermal nonequilibrium, quench front quality, and distance from the quench front to be significant factors in the correlation of the data. These effects are not included in current correlations and are thought to be the major reason for the poor comparisons." The authors further conclude that there is a need for further post-CHF model development that include such factors as quench front conditions and elevation. These are needed for advanced codes to predict the post-CHF heat transfer, thermal nonequilibrium and quenching phenomena. This recent work combined with the experimental results of Experiment LP-02-6 and the results of code calculations such as those in Figures 44 and 45 clearly indicate that the current generation systems codes do not adequate predict post-CHF heat transfer and quenching.

OECD LOFT Experiment LP-LB-1 also contains data showing the strong dependency of the fuel centerline temperature on the cladding temperature and heat transfer. In Experiment LP-LB-1 the early bottom-up quench phenomena was suppressed. However, there was a weak partial top-down quench that occurred in the 10-30 s time interval and extended over approximately the top third of the core [16]. Figure 46 shows fuel centerline temperature at the 27-in. elevation for rods with and without cladding surface thermocouples. The centerline temperature behavior indicates no quench in agreement with the measured cladding temperature. Figure 47 shows similar temperature data at the 43.8 in. elevation. A small early cooling occurs in this region as indicated by the cladding temperature in Figure 47 compared with that in Figure 46. The fuel centerline temperature is sufficiently sensitive to show even this small cooling. The data in Figures 46 and 47 during the final quench does show that the final quench occurs up to approximately 20s earlier on fuel rods with thermocouples. These results are consistent with fuel rod results in PBF [30]. Comparison of several other pairs of fuel rods in Reference 16 all show the same trends. Figures 48, 49, and 50 show fuel centerline and cladding temperature measurements at the 43.8 in. elevation. These fuel rods experienced larger degrees of cooling than those in

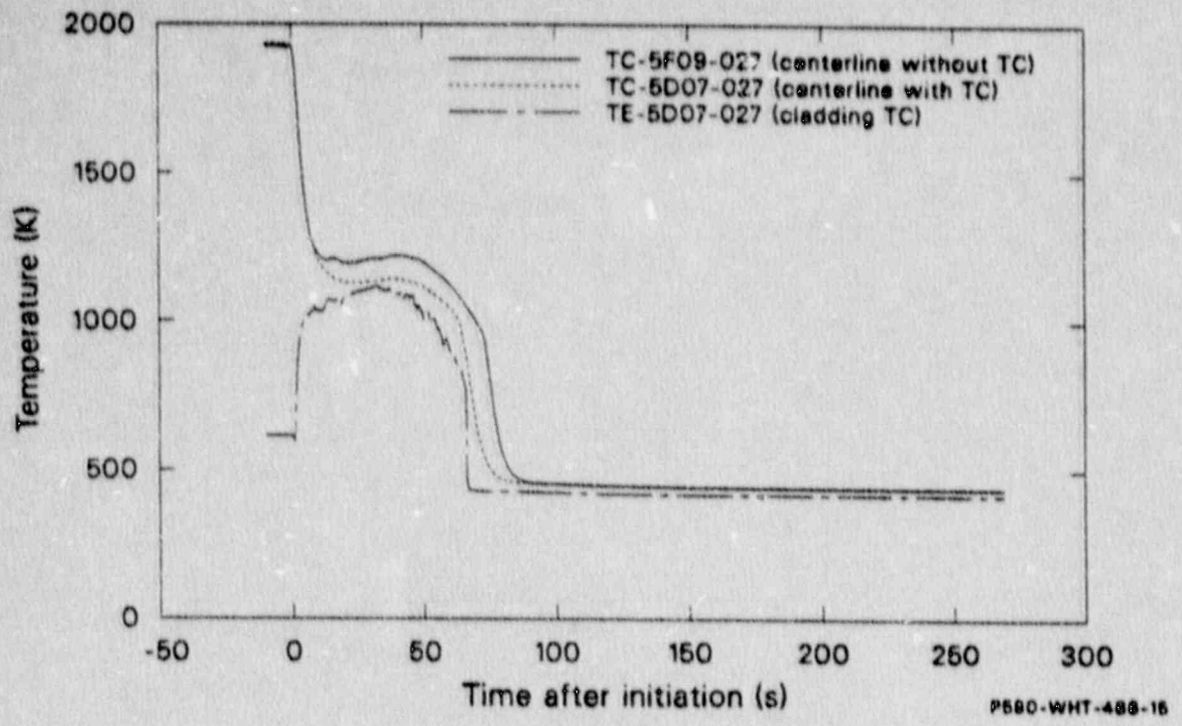

Figure 46. Fuel rod centerline temperature with and without cladding surface thermocouple and cladding temperature measurement during Experiment LP-LB-1 at the 27-in elevation.

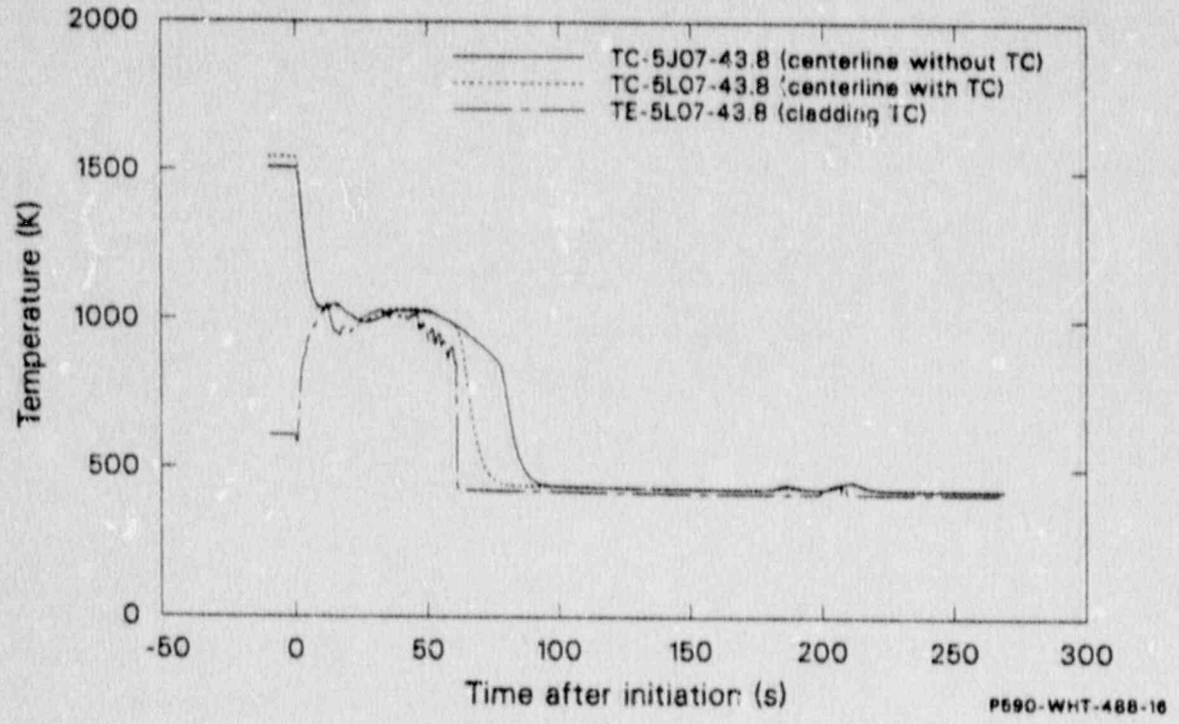

Figure 47. Fuel rod centerline temperature with and without cladding outer surface thermocouple and cladding temperature measurement at the 43.8-in elevation.

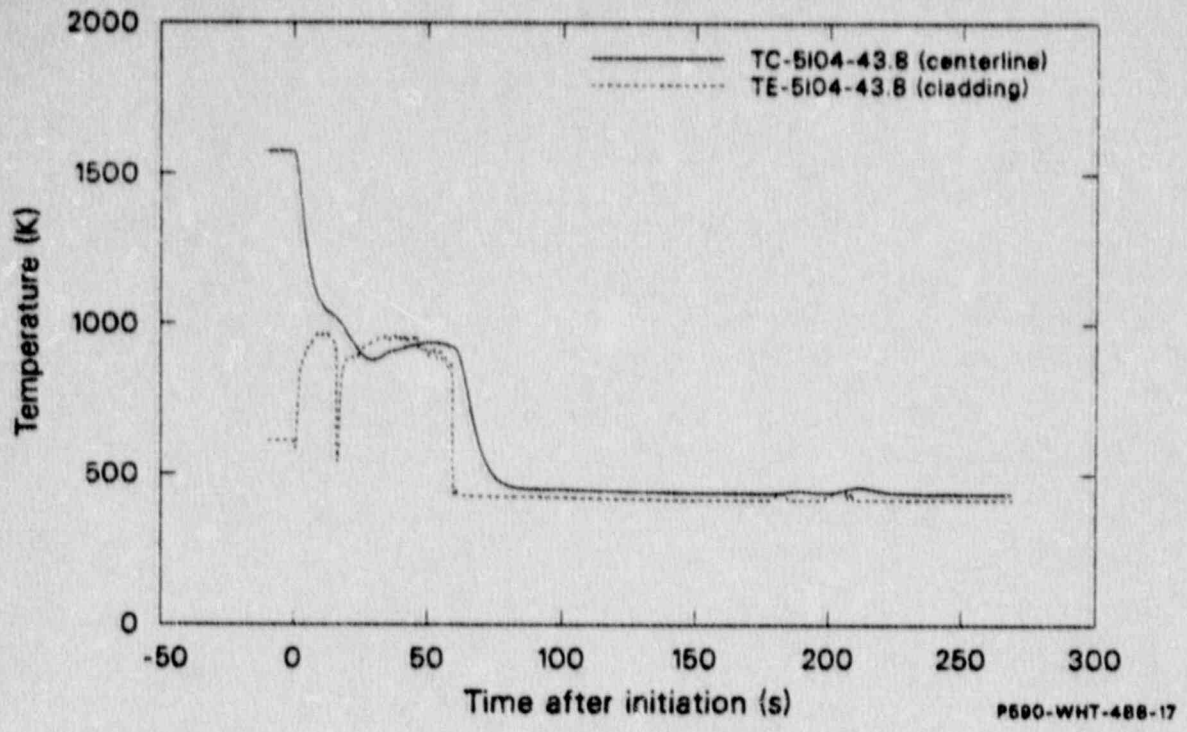

Figure 48. Fuel centerline and cladding temperatures on rod 5I04 at the 43.8 in elevation during Experiment LP-LB-1.

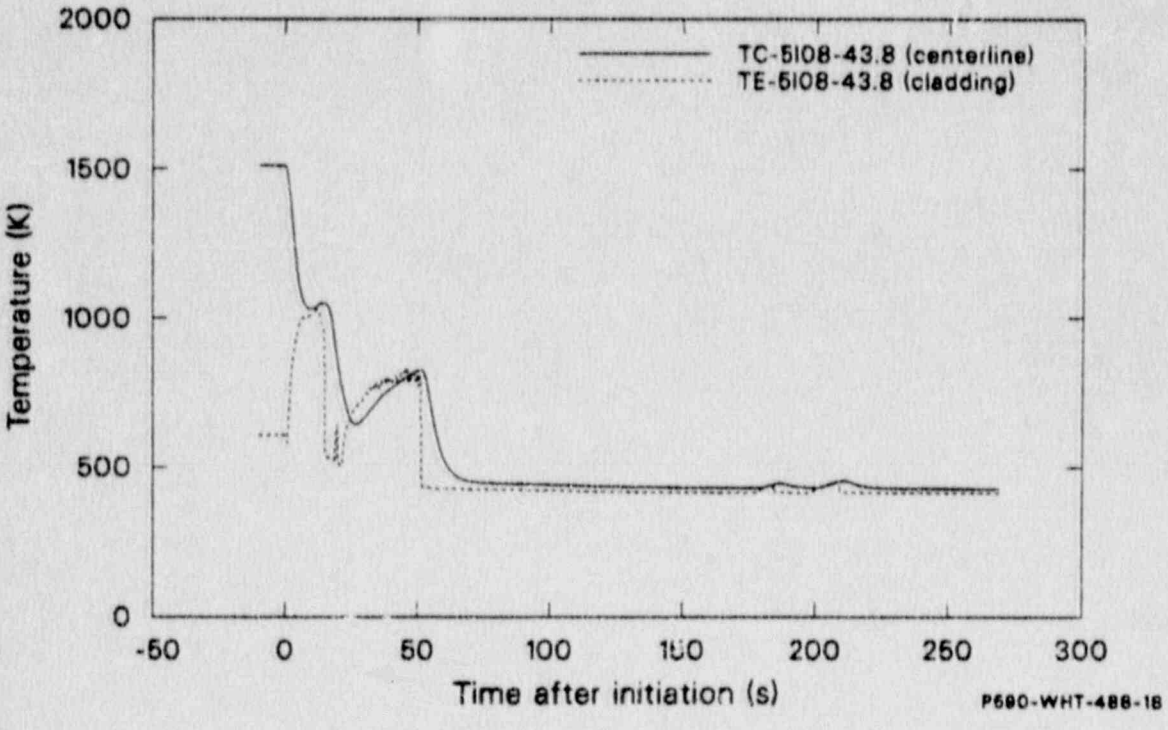

Figure 49. Fuel centerline and cladding temperature on rod 5I08 at the 43.8 in elevation during experiment LP-LB-1.

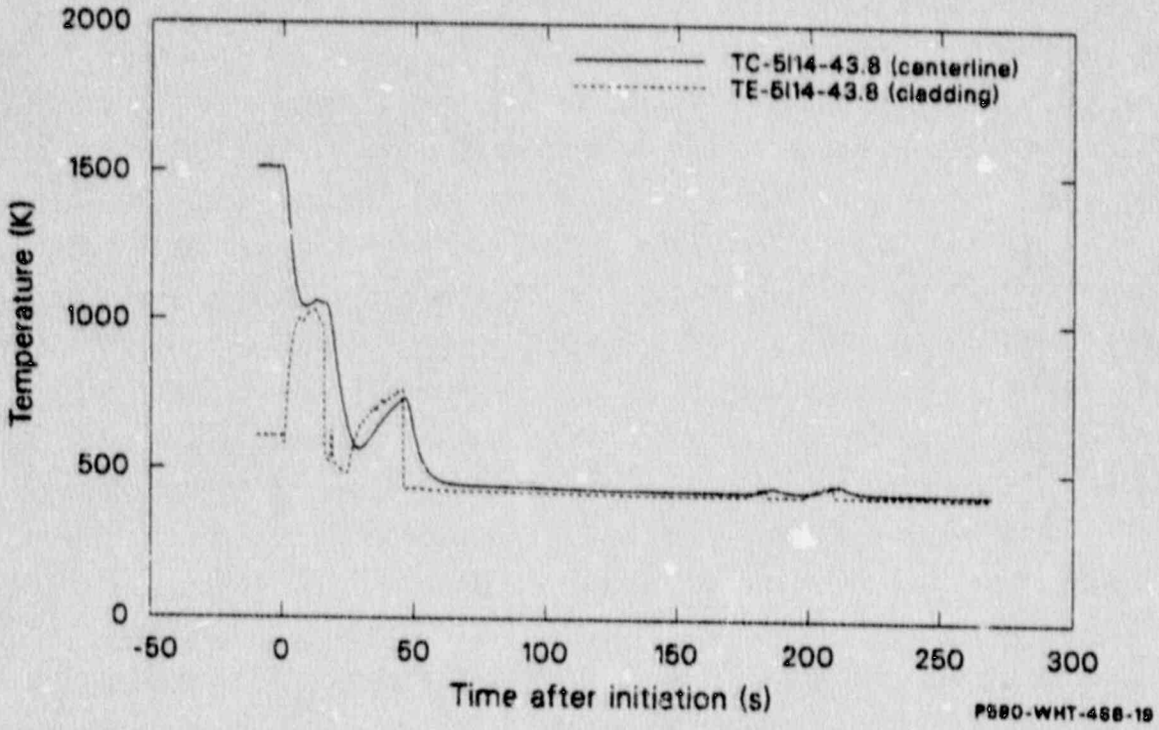

Figure 50. Fuel centerline and cladding temperature on rod 5I14 at the 43.8 in elevation during experiment LP-LB-1.

Figures 46 and 47. The correlation between fuel centerline and cladding temperature is consistent with previous comparisons and indicates that more than just thermocouple cooling is occurring. The data in Figures 48, 49 and 50 also show that at specific times the cladding temperatures exceeds the fuel centerline temperature. The reason is that the surrounding rods were not cooled as much and as a result heat transfer occurs from those rods. The fuel centerline data shows that the heat transfer occurs through the rod at the time constant for the fuel thermal properties.

Experiment LP-FP-1 [20] provided cladding temperature data for the case where the cladding thermocouple is quenched but not the fuel cladding on the same or adjacent fuel rods. Typical data is shown in Figure 51. Rods 5G05 and 5I05 did not show thermocouple dryout until shortly after 200 s whereas thermocouple dryout occurred before 100 s on rods 5G11 and 5I11. The higher rate of temperature increase on 5G05 and 5I05 relative to the other rods indicates that adjacent rods had significant cladding temperature at the time of thermocouple dryout on rods 5G05 and 5I05. The thermocouple on 5G05 was quenched again at approximately 270 s. The more rapid rate of heatup following subsequent dryout indicates that only the thermocouple was affected. The phenomena in Figure 51 has not been observed in any of the cladding thermocouples in Experiments L2-2, L2-3, and LP-02-6 during the quench-dryout period early in the depressurization.

Cladding temperature data in the hot region of the core shown in Figure 52 for LP-02-6 (early quench phenomena) and LP-LB-1 (no early quench), can be used directly to assess the validity of the assumption that only the thermocouple in LP-02-6 was quenched. If the assumption is true then, (1) the rate of temperature increase following subsequent dryout should be greater than that following DNB, and (2) the maximum temperature following dryout should equal or exceed the maximum temperature reached following DNB. Neither result is evidenced in the data in Figure 52. The conclusion is that the assumption is incorrect and that significant cooling occurred on all fuel cladding. The cooling was sufficiently large initiate and precipitate early quench.

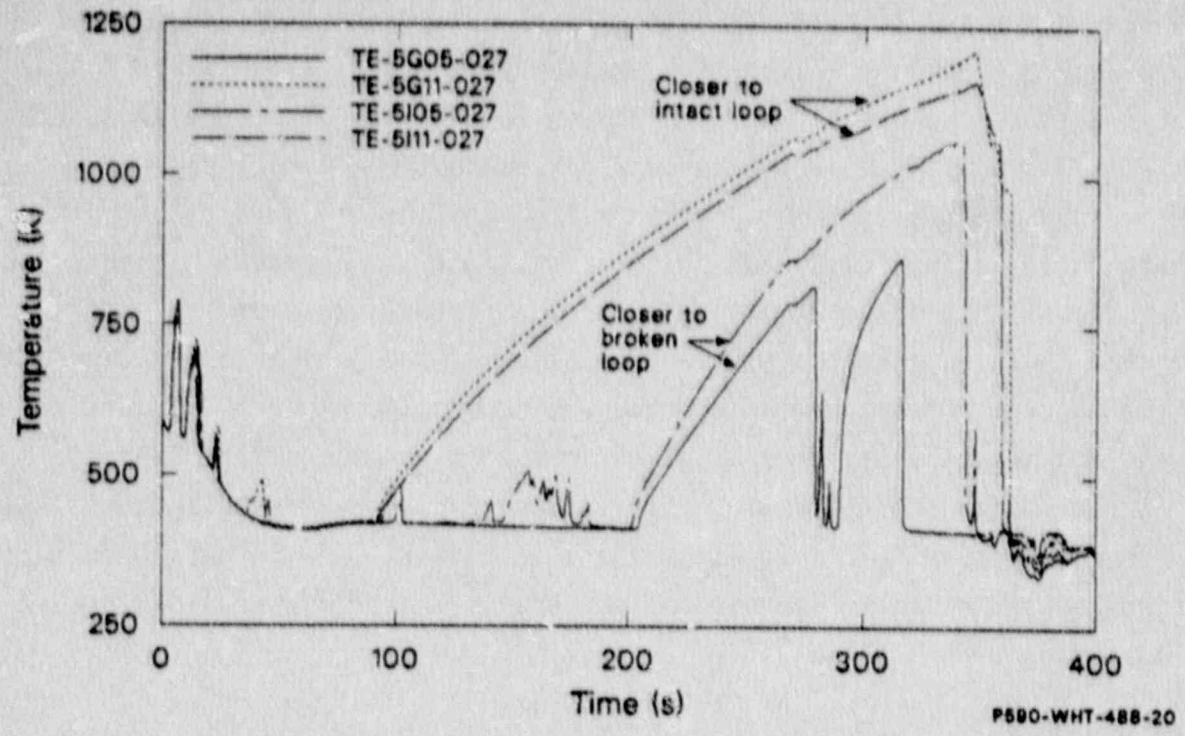

Figure 51. Comparison of cladding temperatures at the 27-in elevation in the central fuel assembly during Experiment LP-FP-1.

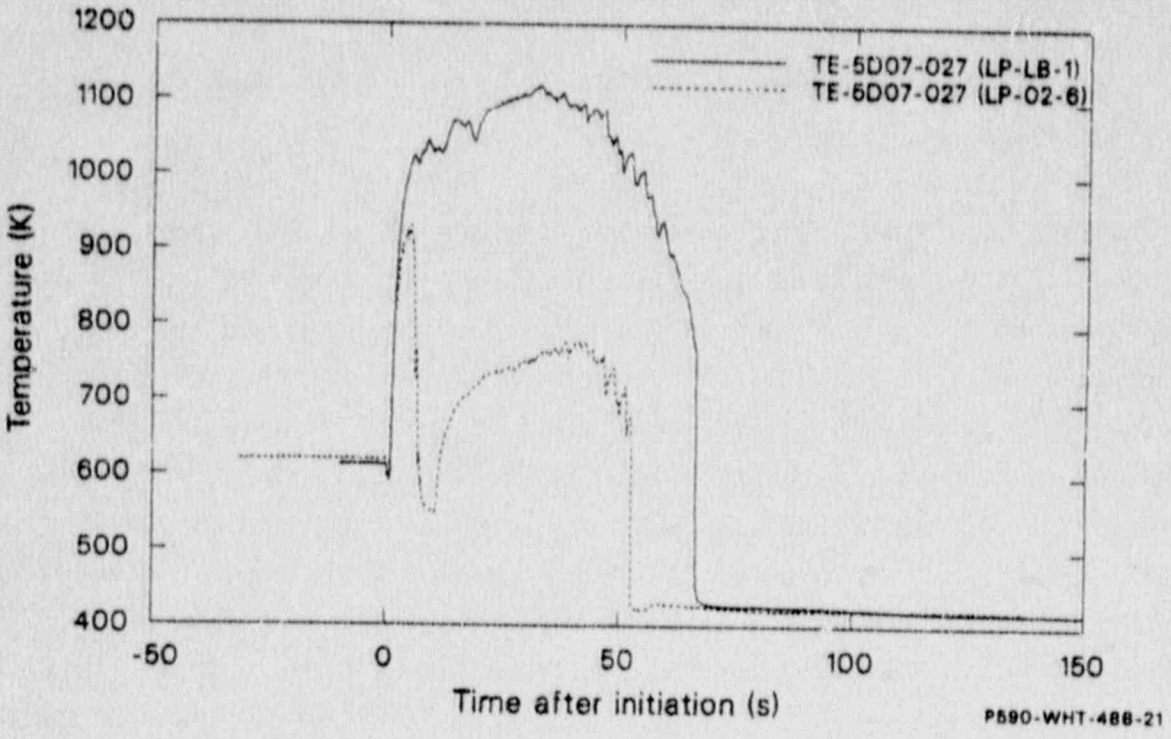

Figure 52. Cladding temperatures at the 27-in. elevation on rod 5D07 during Experiments LP-02-6 and LP-LB-1.

There is one final topic for discussion. As mentioned in Section 4.1 the early quench phenomena involves high pressures (5-8 MPA) and rapidiy moving density waves through the core. The latter is calculated to be approximately 1.8 m/s. This moving density wave causes a quench propagation of approximately 1.5 m/s in the core. Nelson [24] states that for those conditions (1) no applicable data base exists, and (2) conduction-controlled quenching cannot be the controlling factor. He states further that these conditions comprise a second case where downstream quenching is influenced by both the quenching front and convection (the quench front in this case is termed a conduction-convective propagating quench front). It is apparent that currently used heat transfer correlations cannot handle this case. The research reported in Reference 36 provides data to extend the data base into the required range and shows that current heat transfer correlations are in poor agreement with the new data.

In summary, the early blowdown quench phenomena in LOFT is concluded to be real and not an artifact of thermocouple-only or thermocouple induced quenching. Further, current systems codes cannot calculate this phenomena because adequate heat transfer correlations have not been developed.

4.4.2 Nuclear Fuel Versus Electrical Fuel Rod Simulators: Simulation Limitations During Blowdown

The typicality of the blowdown quench behavior of a solid-type electrical heater rod relative to that of a nuclear fuel rod has been questioned because of the different thermal properties and lack of a simulated fuel-pellet cladding gap. In this respect, LTSF experiments, which investigated the blowdown quench behavior of a Semiscale solid-type heater rod with only internal thermocouples, can be used as a basis for evaluation of code model calculations. Details of such calculations using the RELAP4/MOD6 computer code [37] are given in References 23 and 28. Having established the validity of the heat transfer models to calculate the initial cooldown rate of a quench, a series of RELAP4 calculations were performed to compare the initial cooldown rates of the nuclear fuel with gap, REBEKA cartridge-type electrical heater rod with gap, and Semiscale solid-type electrical heater rod for rapid cooling transients. These calculations under typical LTSF single-rod

experiment conditions were performed by substituting the individual rods in the RELAP4/MOD6 LTSF model. The calculated results for LTSF experiment 12 are given in Figure 53. These calculations show that the REBEKA heater rod simulates the nuclear fuel rod cooling very well for the conditions investigated.

The nuclear fuel rod with gap was calculated to cool approximately five times faster than the Semiscale solid-type heater rod. These comparison calculations [28] were carried out over a range of inlet flooding velocities (2 to 6 m/s). The predicted initial cooling rates are summarized in Figure 54. Also indicated in this figure are the initial cladding cooling rates measured on nuclear fuel rods from the PBF Thermocouple Evaluation Experiment Series [30]. The limited number of nuclear fuel rod data suggest that the calculated cooldown rates may be 10 to 20% too high. The results of those PBF experiments also indicate that the thermal decoupling of the cladding and fuel was apparently significant, allowing the cladding to rapidly quench during the blowdown phase. This thermal decoupling of fuel and cladding demonstrates the importance of in-pile experiments or out-of-pile experiments where the fuel-to-cladding gap is properly simulated.

Additional experiments were conducted in LTSF using a REBEKA cartridge-type fuel rod simulator with gap and zircaloy cladding and thermal diffusivity much closer to the nuclear rod diffusivity. The experimental results without external thermocouples show very rapid cooling (150 to 200K/s) and quench times (2 to 3 s) similar to the nuclear fuel rod data at 4 m/s inlet flooding rates (Figure 54). A comparison of the cladding temperature response of the REBEKA rod with external thermocouples and a nuclear fuel rod with external thermocouples, where the initial temperatures of the rods prior to quenching were about the same (900 K) is shown in Figure 39. Similar results exist for rods without external thermocouples as mentioned above. The quench behavior of the REBEKA rod is similar to that of a nuclear fuel rod, which is also consistent with the results of calculations performed by RELAP4/MOD6 code (Figure 53).

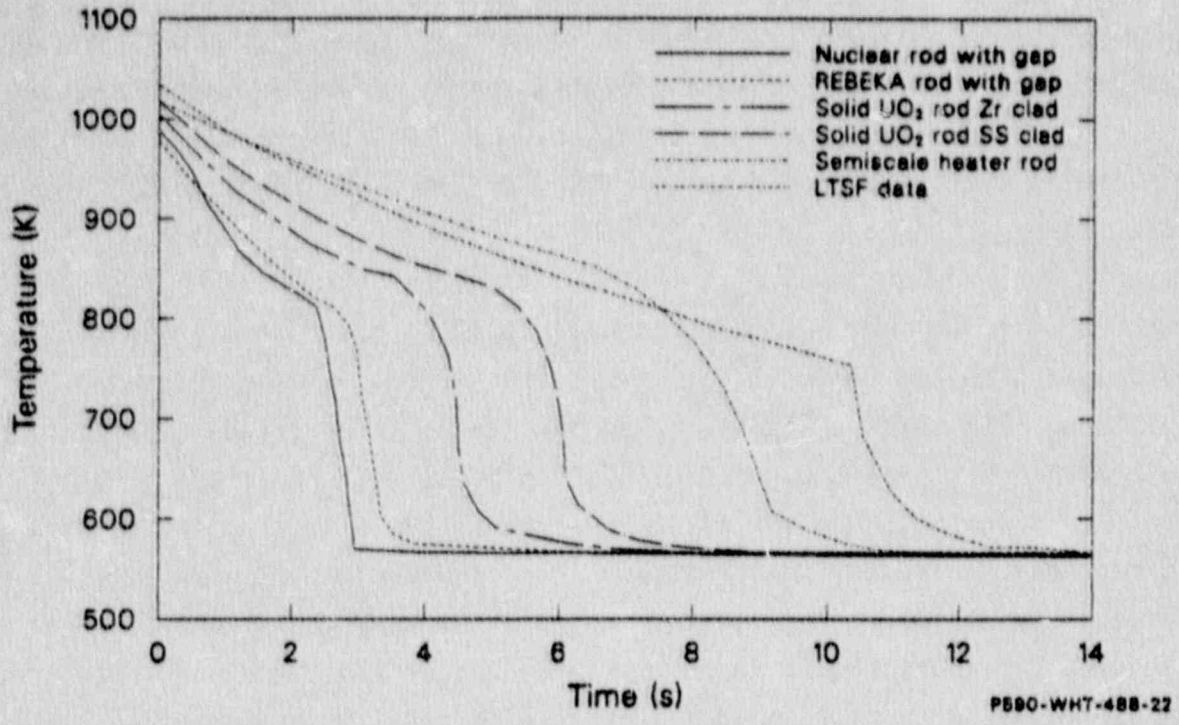

Figure 53. Calculated cladding temperatures for nuclear fuel rod, cartridge-type and solid-type heater rods for LTSF single rod blowdown quench test.

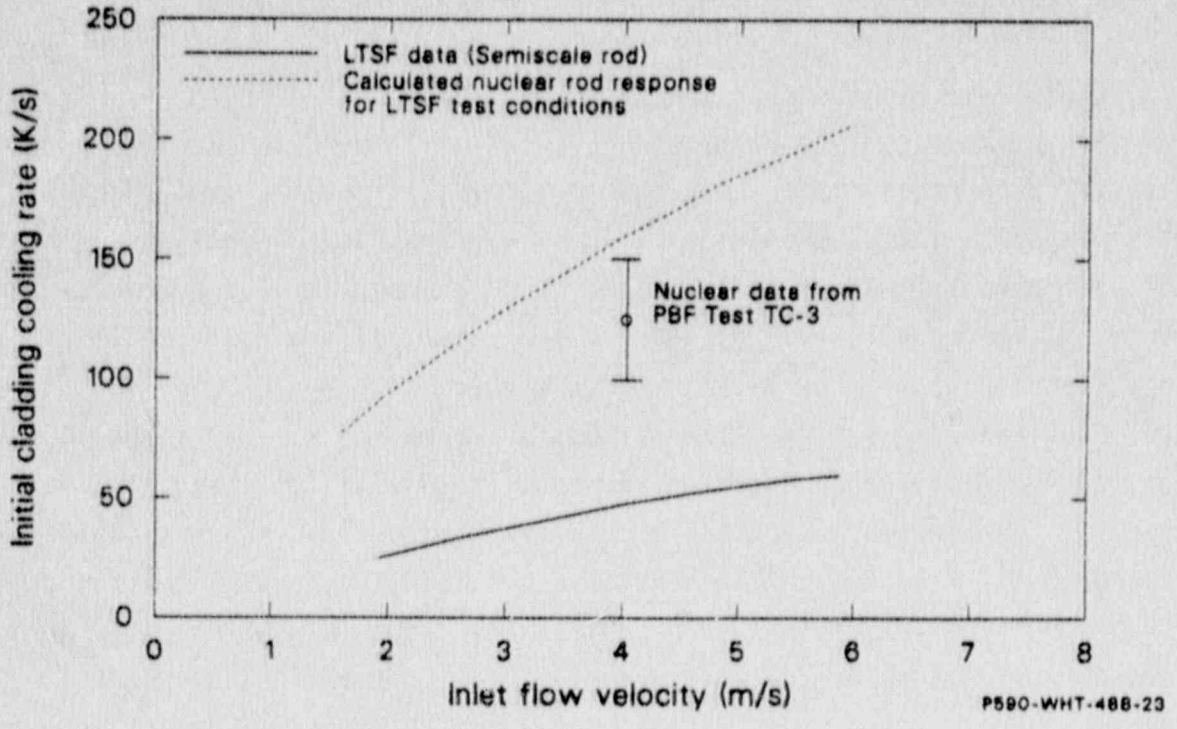

Figure 54. Comparison of measured Semiscale heater rod initial cooling rates from LTSF single rod quench test with calculated nuclear fuel rod initial cooling rates.

Additionally, the bundle experiments performed in the LTSF produced valuable evidence with respect to the behavior of cartridge-type REBEKA and the solid type FEBA fuel rod simulators (Figure 38). The analysis indicates that the solid-type heater rod temperatures are controlled by convective heat transfer at the cladding surface. This is due to the high thermal diffusivity of the rod allowing rod internal energy to be transferred rapidly to the cladding. As the rod begins to cool down in film boiling, internal rod energy is conducted to the cladding about as fast as the surface convective heat transfer removes the energy; thus, the cladding cools slowly since the rod energy must be transferred before the cladding temperature is low enough to allow surface quenching. This is clearly seen in Figure 53, where the film boiling cooldown lasts for 8 s. The nuclear rod, by contrast is internally conduction limited by the greater thermal resistance of the UO_2 fuel and the fuel-cladding gap thermal resistance. The inability of the nuclear rod to rapidly transfer internal energy to the cladding, together with a much smaller zircaloy cladding heat capacity, significantly changes the energy balance at the cladding surface, causing a more rapid cooldown during the film boiling (see Figure 53). In comparison, at these high flow rates the nuclear rod cooling is controlled more by the cladding stored energy, while the cooling of the solid-type heater rod is controlled more by total rod internal energy.

The detailed investigations performed on the effect of changing power history for both nuclear fuel and solid-type heater rods [23] indicated that an attempt to simulate nuclear fuel rod behavior with solid-type of high thermal diffusivity heater rods would require unrealistic changes in electrical heater rod input power, even including applying negative power. Figure 55 indicates the required heater rod power necessary to simultaneously duplicate the nuclear rod surface temperature from Figure 53 and corresponding heat flux obtained from RELAP4/MOD6 calculations. A large amount of negative power is needed to force the solid-type heater rod to duplicate nuclear rod response. The unrealistic amount of negative power needed to simulate nuclear fuel rod response indicates that observed differences in electrical and nuclear fuel rod response result from inherent limitations in any solid heater rod design.

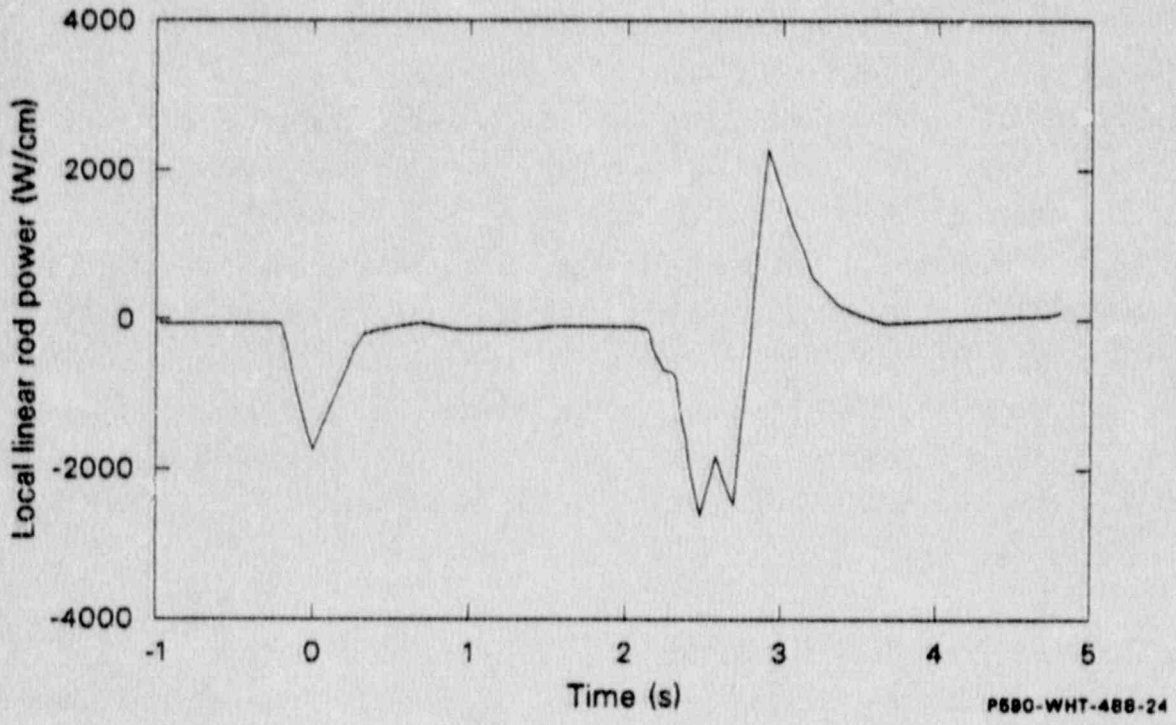

Figure 55. Calculated peak linear Semiscale heater rod power needed to duplicate nuclear rod temperature response shown in Figure 53.

Similar types of analysis were performed for the Semiscale counterpart experiments to the LOFT experiments. The experimentally used power history for the Semiscale large break LOCA experiment was obtained from predicted LOFT nuclear fuel rod cladding temperatures. But the cladding temperature response during the LOFT nuclear experiments was very different from the predicted values used to specify the electrical power for the Semiscale experiments. As stated previously, during the first 10 s of the LOFT L2-3 experiment, more than 60% of the stored energy in the core was transferred from the fuel rods due to the high core inlet flow, causing a cladding rewet. This early cooling was not predicted by the code calculations to occur in the LOFT experiments and therefore was not included in the calculation to specify cladding temperatures for the Semiscale solid-type heater rods. Thus, the Semiscale electrical rods were overpowered compared to the LOFT measured data. Tolman and Carboneau [38], shows that to duplicate the LOFT cladding temperatures, negative rod powers are required for substantial periods of the transient (Figure 56). This is a condition that can not be achieved and it also indicates that the solid-type heater rod can not exactly simulate the nuclear rod thermal response under the same hydraulic conditions.

4.4.3 Reflooding and Boil-off: External Cladding Thermocouple Effect, and Nuclear Fuel Rod and Electrical Heater Rod Behavior

Large break experiments in LOFT were intended to validate the performance of the emergency core cooling systems for the design basis loss-of-coolant accident. As discussed in previous sections the L2-2, L2-3 and LP-02-6 experiments showed that about 60% of the initial steady state stored energy is transferred to the primary coolant prior to emergency core coolant delivery to the core. The final core quenches are primarily due to accumulator fluid delivery. The characteristics of the relatively rapid (10 to 15 cm/s) core quenching for the L2-3 and L2-5 experiments are compared in Figure 57. The core reflood behavior was very similar during both experiments even though significant difference is initial stored energy and cladding temperatures existed. All of the other LOFT large break loss-of-coolant experiments (L2-2, LP-LB-1, LP-02-6), showed similar type of behavior during rapid core reflooding. A significant observation is that the reflooding rates always exceeded the 2.5 cm/s licensing regulation

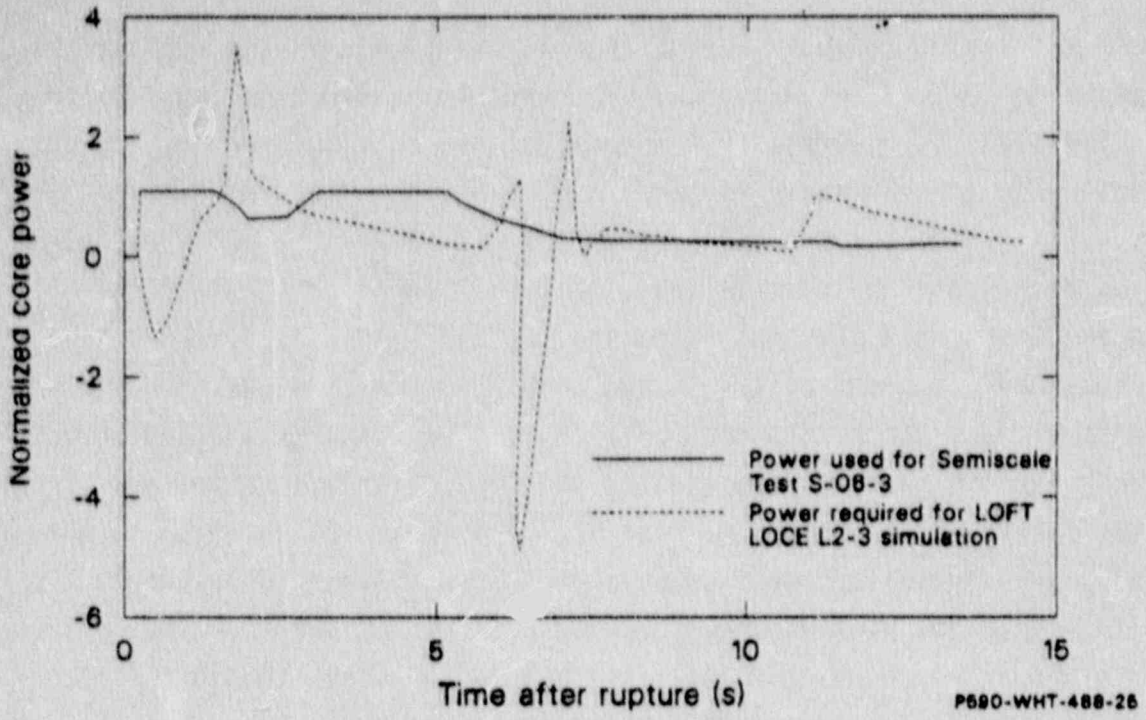

Figure 56. Comparison of Semiscale core power used for Experiment S-06-3 with that required to simulate LOFT Experiment L2-3.

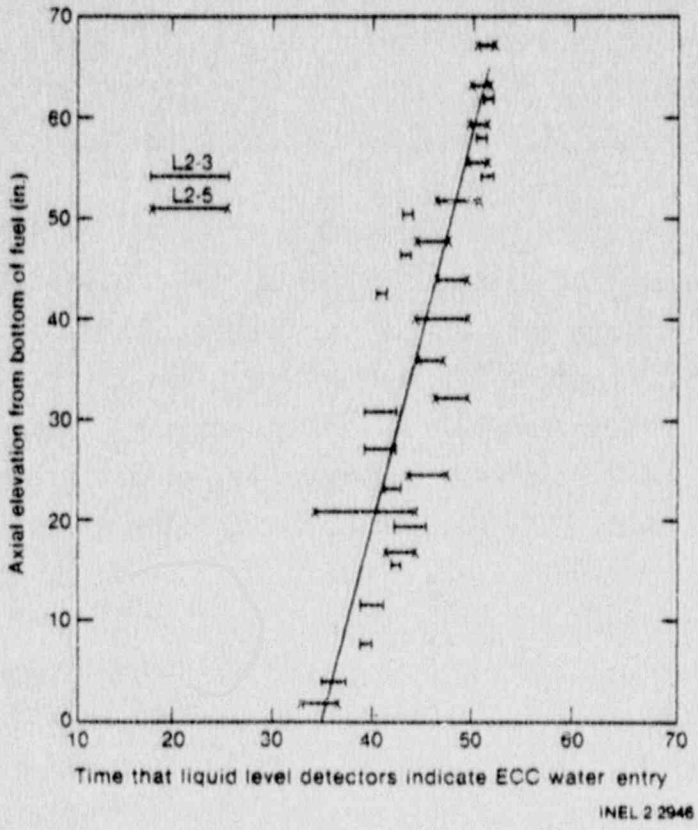

Figure 57. Reactor liquid level during final reflood for Experiments L2-3 and L2-5.

limitation. Additionally the LOFT large break loss-of-coolant experiments showed that the blowdown hydraulics and heat transfer (early blowdown quench) is more important in removing the initial fuel rod stored energy than reflood heat transfer.

The relatively rapid reflooding observed during the LOFT large break loss-of-coolant experiments was questioned because of the fin effect of external thermocouples. As a consequence, separate effect bundle reflooding experiments using electrical heater rods instrumented with both external and internal cladding thermocouples were conducted in the NEPTUN test facility [39] in Switzerland at the Paul Scherrer Institute (formally EIR). The NEPTUN-I series of experiments were performed with five central heater rods instrumented with both external and internal cladding thermocouples and the NEPTUN-II series of experiments were performed only with internal cladding thermocouples. The results and comparison of experimental data from these two experiment series [40, 41], indicated that electrical heater rods instrumented with LOFT external thermocouples experience preferential cooling during reflooding compared to heater rods with internal embedded cladding thermocouples (Figure 58). The effect is reduced with higher reflooding rates (e.g., 15 cm/s). During the precursory cooling until the quench, the rods with external thermocouples show comparable temperature histories as the rods with internal thermocouples but heater rods with external thermocouples quench at higher temperatures and earlier than the other heater rods. An overall comparison between repeat experiments NEPTUN-I (five central rods equipped with external thermocouples) and NEPTUN-II (all thermocouples embedded on the cladding of the heater rods) is shown in Figure 59. Differences between similar experiments are small especially during precursory cooling.

The ability of electric heater rods to duplicate nuclear fuel rod thermal response during reflooding was also questioned because of the large differences in electric and nuclear fuel rod thermal properties. In this respect, the Halden Project Test Program Instrumented Fuel Assembly 511 (IFA 511) in Norway, in Holden Research Reactor was designed to systematically evaluate the ability of electric heater rods (Semiscale

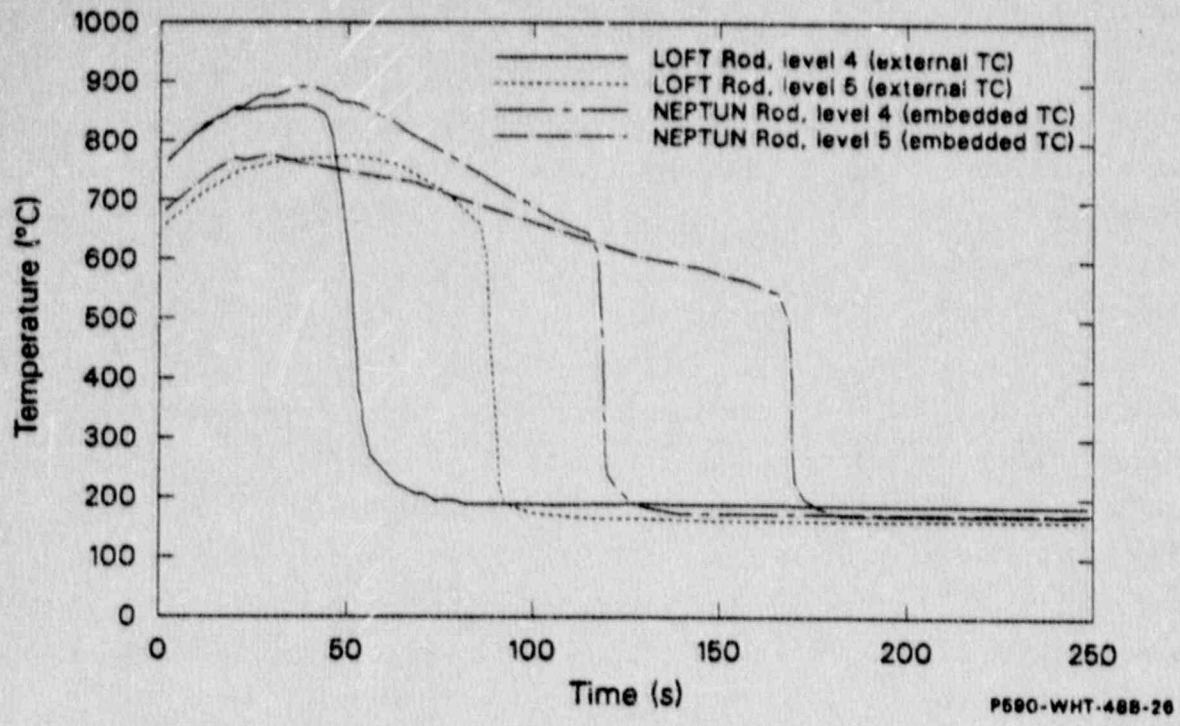

Figure 58. Cladding temperatures during NEPTUN-I and NEPTUN-II experiments, with and without external cladding surface thermocouples.

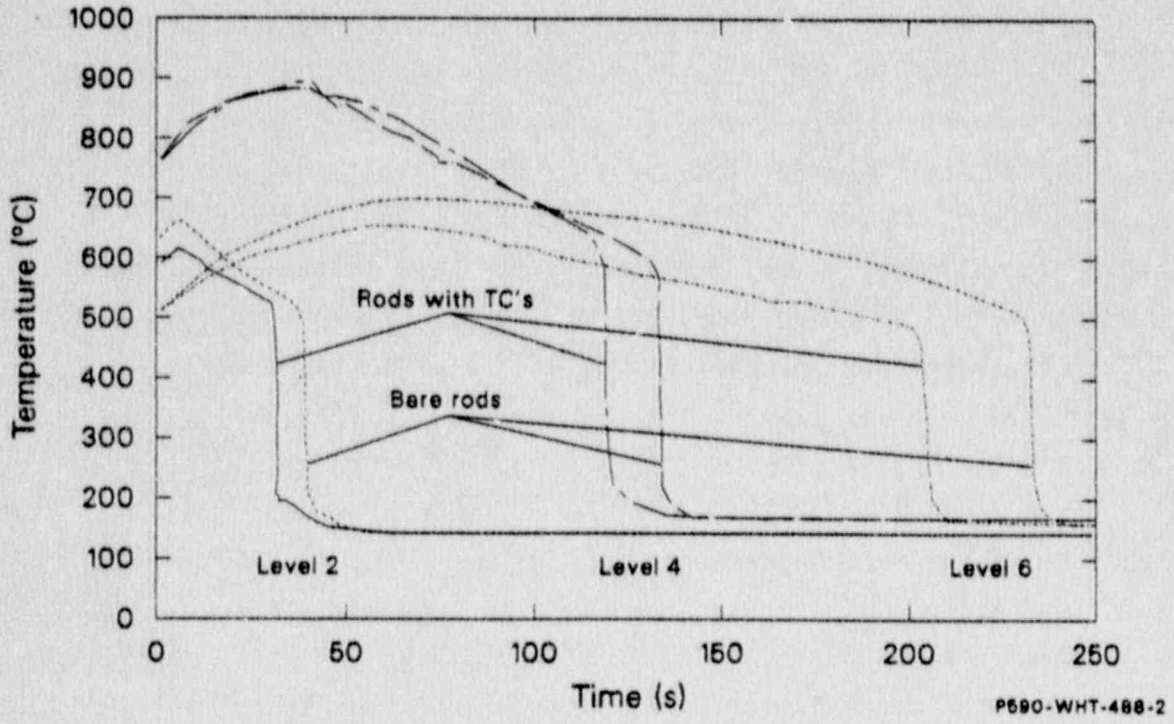

Figure 59. Cladding temperatures during NEPTUN-I and NEPTUN-II experiments, with and without external cladding surface thermocouples.

solid-type) to simulate the response of nuclear fuel rods during the heatup and reflood phases of a large break loss-of-coolant accident. The experiment rods were also instrumented with both external and internal cladding thermocouples to determine if external thermocouples provide an accurate measurement of cladding temperature. The experiments consisted of one series with nuclear fuel rods [42] and two other series with electric heater rods, semiscale solid-type rods [43, 44] and REBEKA heater rods with cladding gap [45]. In these experiments the nuclear fuel rods were quenched substantially earlier (four times faster) than solid-type electrical heater rods (Figure 60). REBEKA heater rods closely simulated the actual nuclear fuel rod behavior under reflooding conditions. Also, the electric rod, unlike the nuclear fuel rod, is characterized by a well defined quench. Experimental data also shows that the response of the external thermocouples was significantly different than the comparative internal cladding thermocouples during reflooding at about 7 cm/s flooding rates. The indicated temperature of the external thermocouple was at least 50 K less than that indicated by the internal thermocouples throughout reflood and the external thermocouples indicated quench 20 s earlier. The different thermal behavior indicated by the external thermocouples was primarily caused by fin cooling effects.

Additional experiments were performed in the FEBA test facility (at KFK Karlsruhe, Federal Republic of Germany) within the SEFLEX test program in order to quantify the influence of the design of different fuel rod simulators on the cladding temperature transients under reflood conditions. These experiments were done by employing a solid-type FEBA heater rod bundle and a corresponding bundle of REBEKA fuel rod simulators with gap (for rod cross-sections see Figure 37). The experimental data [46], indicates that the reflooding behavior between the two bundles consisting of 5x5 FEBA and 5x5 REBEKA rods is significantly different (Figure 61). At an inlet flooding velocity of 3.8 cm/s, the influence of the rod design on the peak cladding temperature is around 100 K lower for REBEKA rods. The reasons for the lower cladding temperatures and the faster quench front progression for the REBEKA rod bundles are the lower heat capacity of the zircaloy cladding and the pronounced decoupling of the cladding from the heat source due to the cladding gap.

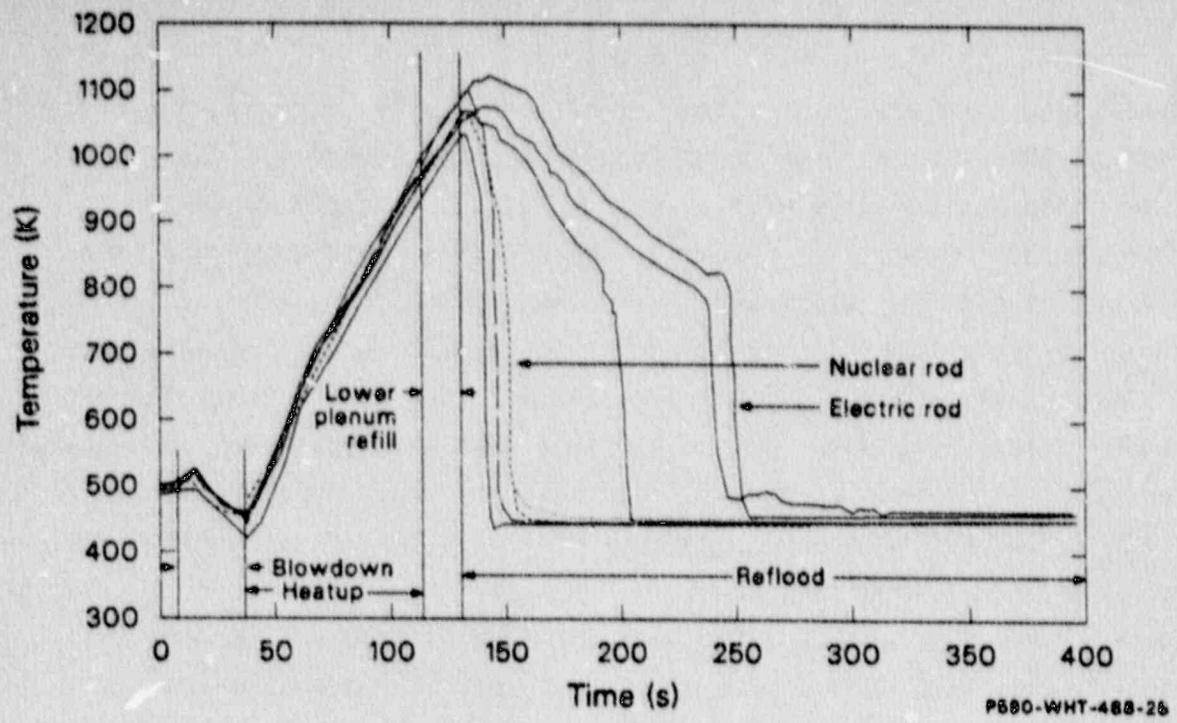

Figure 60. Cladding temperatures of electric heater rods and nuclear fuel rods during quench experiments in Halden.

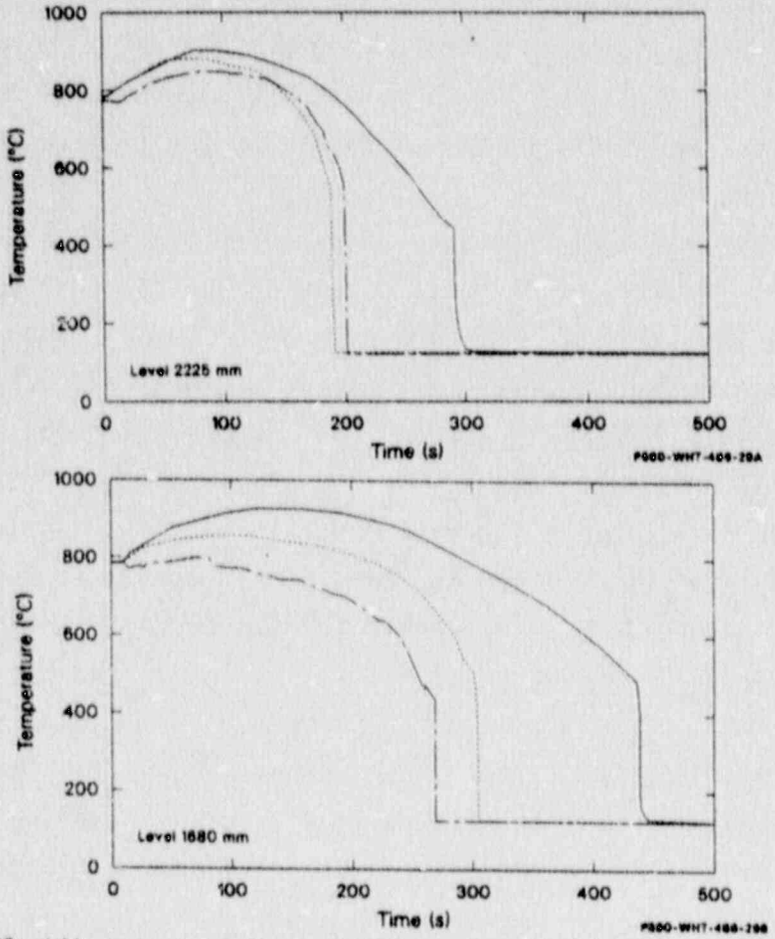

Figure 61. Cladding temperatures measured at two different axial levels in FEBA and REBEKA rod bundles.

Core uncovery (boil-off) experiments were conducted in the NEPTUN experiment facility which has been already mentioned above. The results of NEPTUN boil-off experiments at 5 bar [47] showed that the external cladding thermocouples do not cause a significant cooling influence in the rods to which they are attached. The dry-out times of the internal and external cladding thermocouples were within 10 seconds of each other at any axial elevation for all rods in the bundle. The cladding external thermocouples measure the cladding temperatures that would have been measured in their absence within 0 to -20 K (Figure 62). The experimental data from IFA 511 experiments for the heat-up phase at low pressures showed that the response of the external and internal thermocouples was nearly identical through heat-up until temperatures exceeded 700 K. However, after about 700 K, the cladding surface temperature measured by the external thermocouple was lower than that measured by internal thermocouples and the difference increases thereafter. The measured cladding peak temperature was 25 to 40 K less, for both electrical heater and nuclear fuel rods. These results confirm the findings of the NEPTUN boil-off experiments.

4.5 The Break Flow

The break flow is a principal parameter in the reactor safety research because of its strong influence on primary system coolant inventory and consequently core thermal behavior. The break flow influences almost every feature of a LOCA sequence. The most important factor which was driving the research associated with the break flow and development of special mass flow rate measurement systems was the need to obtain accurate data on break flow for assessment of the computer system codes against experimental data. The LOFT facility was very well instrumented to provide good resolution on the break flow for interpretation of the system behavior during a large break LOCA.

There are generally four phases for the break flow: subcooled flow, saturated water flow, two phase flow and steam flow. Subcooled break flow ended in the hot leg (Figure 23) at about 0.2 s compared with 3.4 s in the cold leg (Figure 24). Saturated water flow out of the cold leg ended at about 5 s followed by two-phase flow which ended at about 20 s. The break

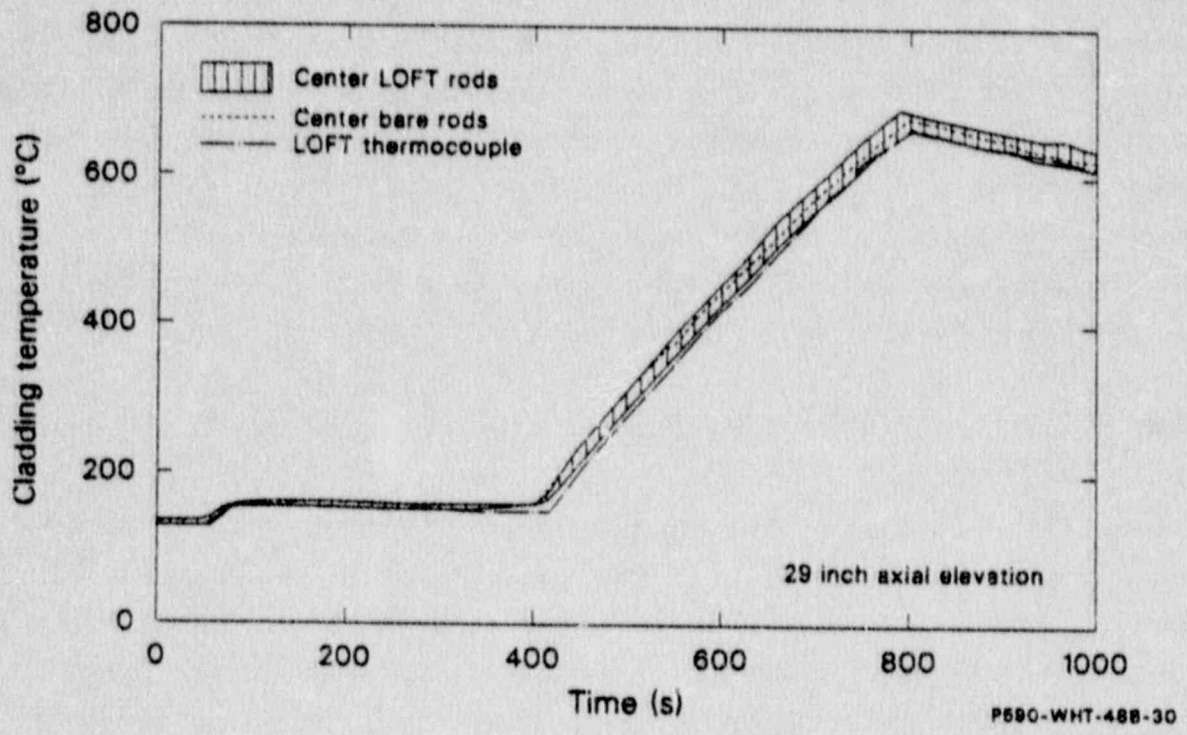

Figure 62. Cladding temperatures measured in NEPTUN experiment with External cladding surface (LOFT) thermocouple and with embeded thermocouples.

flow consisted of steam for the remainder of the transient. Phase changes in the hot leg occurred much faster because the initial temperature was higher and no cooling was present in the steam generator simulator. Break flow of saturated water out of the hot leg ended at 0.6 s. The following two-phase flow decreased rapidly from 190kg/s at 0.6 s to 20 kg/s at 3 s. From the minimum value of 20 kg/s (steam flow) it increased again to a maximum of 80 kg/s at 7 s and then decreased again to steam flow at about 20 s. The mass flow rates were determined from measured densities and measured momentum flux using a procedure given in [9]. The uncertainty of the mass flow rate magnitudes shown in Figure 23 and 24 is approximately $\pm$ 20 kg/s, which is on the order of the differences in mass flow rates between L2-5 and LP-02-6.

The same break size and geometry was used in all LOFT large break experiments which resulted in similar break flow for all experiments as illustrated in Figure 63. Figure 63 shows break mass flow rate measured in the broken loop cold leg for experiments L2-5, LP-02-6, LP-LB-1 and LP-FP-1. The similarity in the initial break flow for experiments L2-5, LP-02-6, LP-LB-1 despite different initial power and/or pump operation mode indicates that during the first few seconds of the blowdown the break flow depends only on break geometry and initial coolant temperature and pressure. A slight influence of pump operation mode is visible for the time period between 4 and 6 s when smaller mass flow rates are measured for experiments L2-5 and LP-LB-1. A rapid coastdown of the pumps in these experiments caused less coolant to flow into the downcomer and to the cold leg break. The initial mass flow rate during the Experiment LP-FP-1 varies from the massflow rate measured in the other experiments because the reactor was scrammed before break initiation in this experiment.

4.6 ECCS Performance

In 1967 evaluation of the ECCS performance became the main objective of the LOFT program. Two equivalent but independent ECC systems were designed for the LOFT facility to satisfy two objectives:

- Plant protection
- Simulation of ECCS variations in large pressurized water reactors (LPWR).

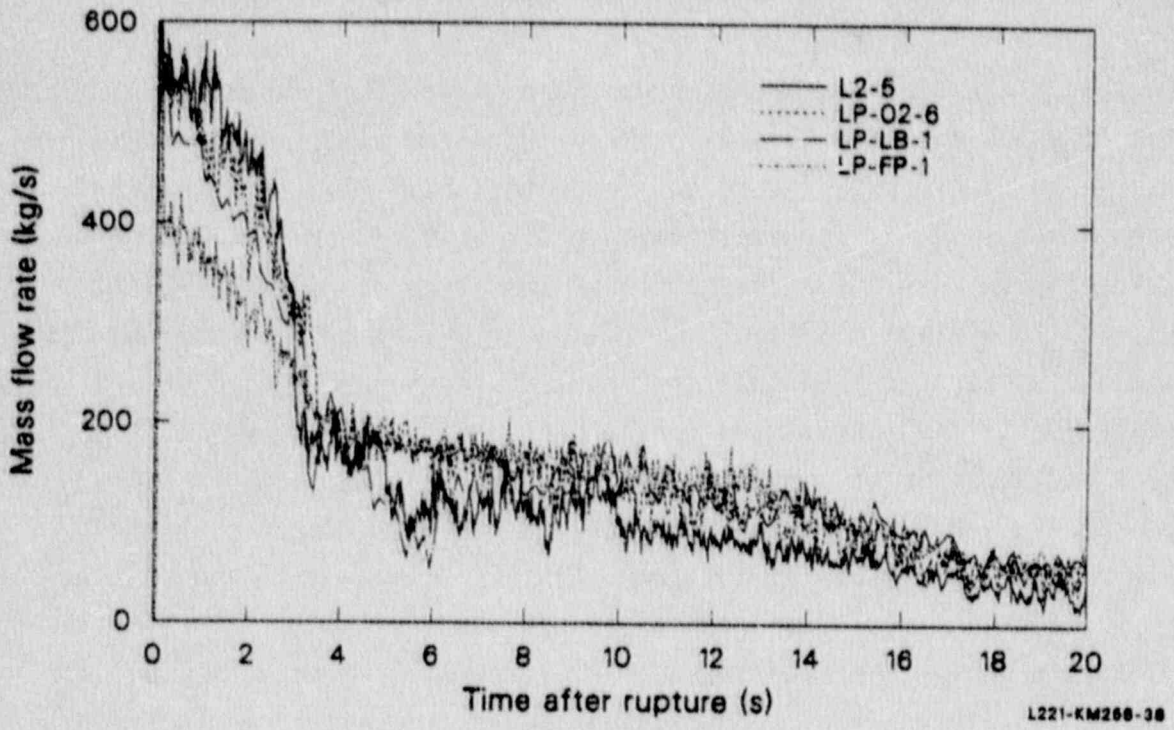

Figure 63. Mass flow rates in the broken loop cold leg during Experiments L2-5, LP-02-6, LP-LB-1, and LP-FP-1.

Each of the ECC systems included an accumulator, High Pressure Injection System (HPIS) and Low Pressure Injection System (LPIS). Figure 64 shows a simplified schematic diagram showing the connections of the different components in system A and system B. This diagram also shows that the water from system A can be injected in the intact loop cold leg or directly into the lower plenum. In case of system B water can be injected in the intact loop hot leg, in the upper plenum or in the downcomer. Most of the experiments were carried out by utilizing system A, while system B was kept as a backup system. If the ECCS is activated for plant protection, system A will inject in the lower plenum and system B in the downcomer. Some details of the accumulator and its instrumentation are shown in Figure 65. The difference between the initial water level in the accumulator tank and the position of the lower edge of the variable standpipe determines the amount of water to be injected. When the water level decreases below the low end of the variable standpipe, N_2 penetrates into the injection line.

The ECCS was used in all LOFT large break experiments. However, in order to determine the influence of the injection mode on the refill and reflood processes, we will discuss here ECCS performance only for the following experiments: L2-5, LP-02-6, LP-LB-1, LP-FP-1 and LP-FP-1A. These experiments were selected because of differences in ECCS operation mode and phenomenological results of these experiments. Tables 4 and 5 show the major characteristics of these experiments with regard to ECCS.

ECCS injection in the first three experiments was in the same location (intact loop cold leg) but different amounts of emergency coolant were injected. During the LP-FP-1 experiment a combined injection into the upper plenum and intact loop cold leg was used. The LP-FP-1A test was aborted at about 10 s into the transient by activation of the Plant Protection System (PPS).

First, the experiments with intact loop cold leg (ILCL) injection will be compared and discussed. Figure 66 shows the liquid level behavior in accumulator A during experiments L2-5, LP-02-6 and LP-LB-1. Similar amounts of water were injected into primary system during experiments L2-5 and LP-02-6. However, despite higher initial water level, much less ECC was

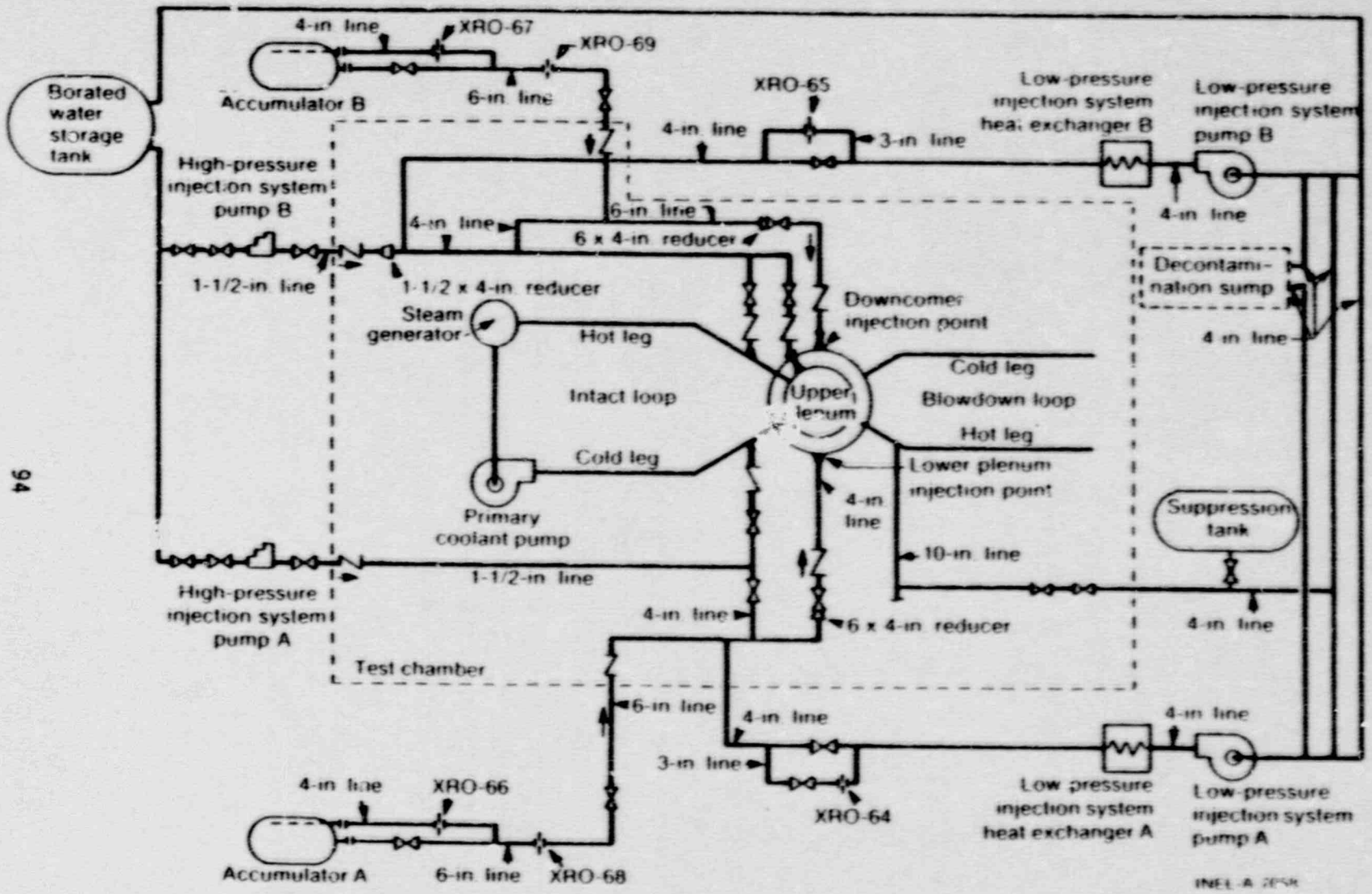

Figure 64. LOFT ECCS simplified schematic diagram.

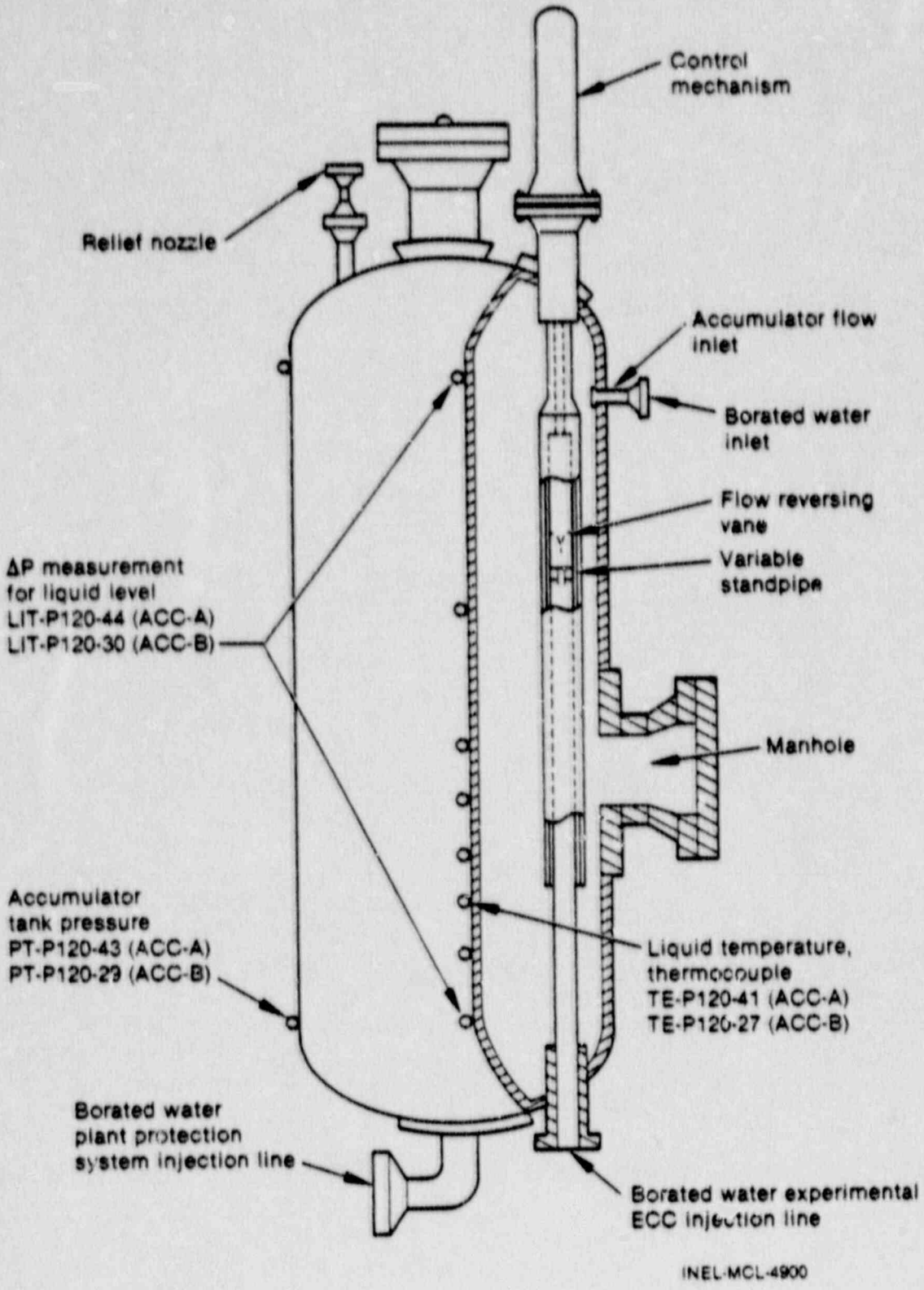

Figure 65. LOFT accumulator and variable standpipe.

TABLE 4. LARGE BREAK EXPERIMENTS INVESTIGATED

Experiment	Reactor Power MW	Pump Coast down	ECC Mode	Injection Acc. s	Initiated HPIS s	Initiated LPIS s	Acc. Empty s	Core Quench s
L2-5	36.0	rapid	ILCL	16.8	23.9	37.3	53.0	65
LP-02-6	46.0	normal	ILCL NRC	17.5	24.1	37.1	50.0	56
LP-LB-1	49.3	rapid	ILCL UK	17.5	--	30.6	40.0	72
LP-FP-1A	37.0	rapid	PPS	19.0	15.0	30.0	A 63.0 B 72.0	33
LP-FP-1	37.0	rapid	U.P. ILC.	344.5	515.8	--	507.0	376[a]

a. Unintentional injection in the U.P. in LP-FP-1 started at about 2 s. Highest injection rate was 25 to 75 s. 80% of the core was completely quenched at 60 s with 200 kg of water.

TABLE 5. ACCUMULATOR CONFIGURATIONS

Experiment	Acc.	Inject pt.	Liquid Level m	Gas Vol. m^3	Liquid Vol. m^3	Liquid Inject. m^3
L2-5	A	ILCL	2.1	0.84	1.52	1.96
LP-02-6	A	ILCL	2.1	0.95	1.236	1.69
LB-LB-1	A	ILCL	2.362	0.66	0.724	1.18
LP-FP-1A	A	L.P.	2.15	1.189	2.93	3.37
	B	D.C.	2.10	1.133	2.81	3.38
LP-FP-1	A	ILCL	2.18	1.189	1.64	2.08
	B	U.P.	2.12	1.133	2.17	2.17

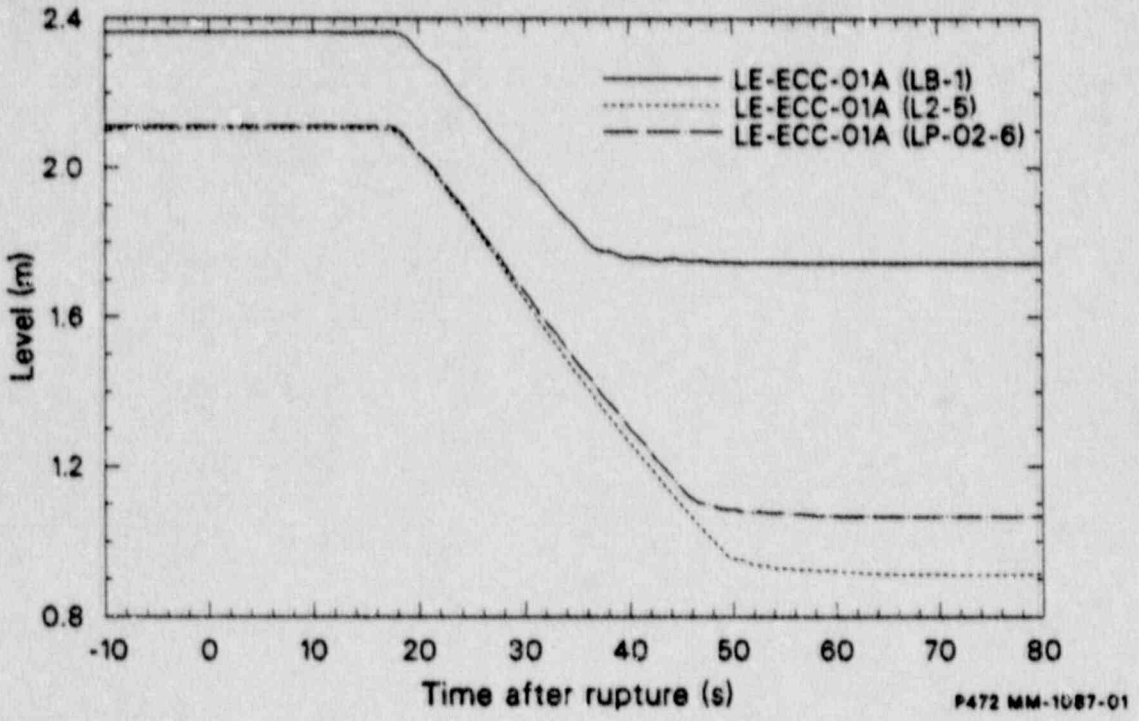

Figure 66. Accumulator A liquid level during Experiments L2-5, LP-02-6, and LP-LB-1.

injected from the accumulator during experiment LP-LB-1. In all three experiments the liquid level in the accumulator started to decrease about 18 s after experiment initiation. HPIS (Figure 67) was activated in L2-5 and LP-02-6 at nearly the same time but different amounts were injected. In LP-LB-1 no HPIS was activated. LPIS injection was activated in L2-5 and LP-02-6 at the same time and the injection rates were very similar as shown in Figure 68. In LP-LB-1 the LPIS was activated earlier, at 31 s but with only about half the capacity of L2-5 or LP-02-6. The general shape of the injection rate curve was analogous to previous experiments L2-2 and L2-3. The differences shown in Figure 68 are mainly due to the earlier activation and lower flow rates.

The ECCS affected the core thermal behavior differently in these three experiments due to differences in operation. The effects of ECCS injection on phenomena in the reactor vessel during these three experiments can be easily understood if we keep in mind the following facts:

- Most of the water injected during the initial 20 s after ECCS initiation originates from the accumulator (HPIS and LPIS amounts to about 0.2%)
- The injection point in all three experiments was the same
- The injected ECC was partly lost through a bypass to the broken loop cold leg
- LP-LB-1 and LP-02-6 are alike with regard to the initial power level but different in pump behavior
- LP-LB-1 and L2-5 are alike in pump behavior but different in initial power
- The least amount of ECC was injected in LP-LB-1.

The completion of the refill phase is indicated by quenching of fluid thermocouples just below the core at the lower end box. Figure 69 shows the behavior of such a thermocouple during the experiments. In L2-5 and LP-02-6 the thermocouple quenches at nearly the same time (31 s) but 2 s later in LP-LB-1. This small delay is attributed to a slightly smaller injection rate

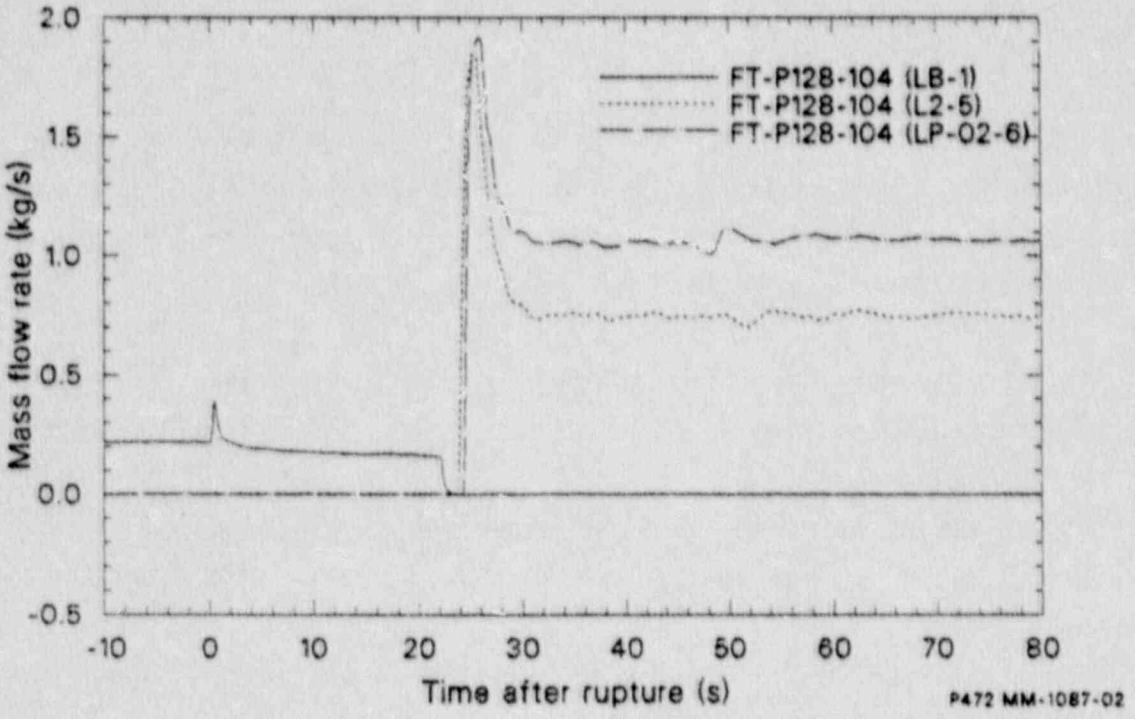

Figure 67. HPIS injection rates during Experiments L2-5, LP-02-6, and LP-LB-1.

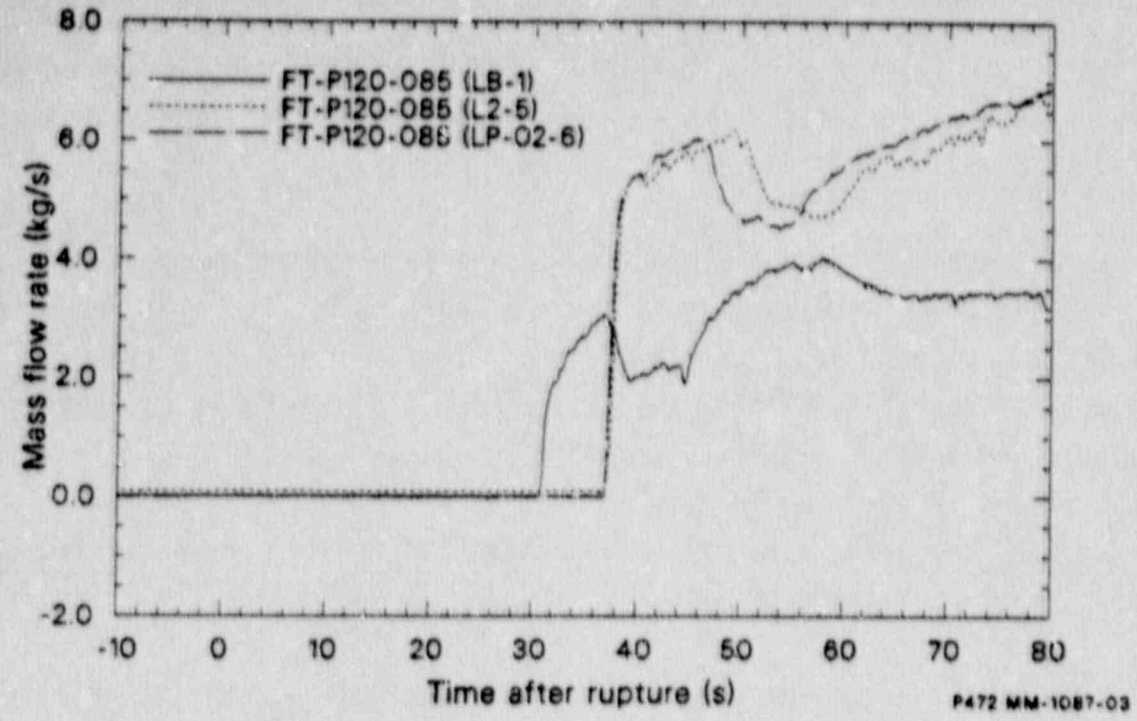

Figure 68. LPIS injection rates during Experiments L2-5, LP-02-6, and LP-LB-1.

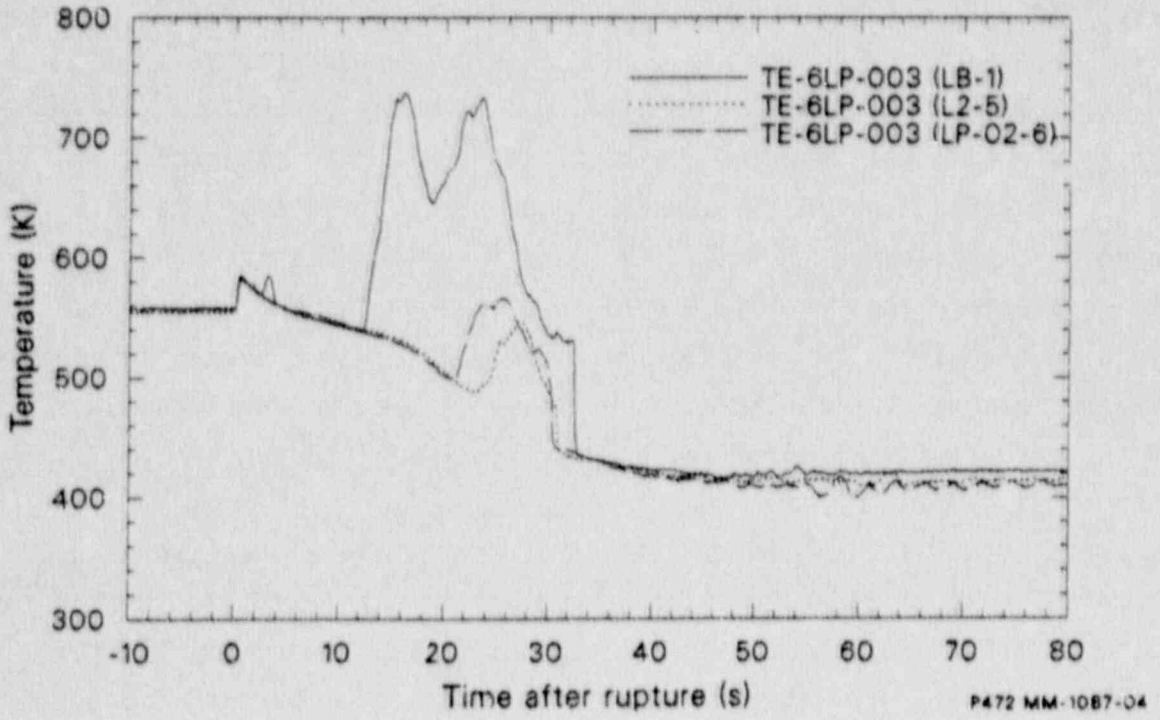

Figure 69. Temperatures measured at the lower end box during Experiments L2-5, LP-02-6, and LP-LB-1.

in LP-LB-1 (Figure 4). Approximately 512 kg of water were delivered from the accumulator between 18 s and 31 s in LP-LB-1 versus 625 kg delivered in the same time in L2-5 and LP-02-6.

Larger differences among the experiments are seen by comparing the behavior of cladding thermocouples in the hot region of the core as shown in Figure 70. For experiment LP-LB-1 the quenching time of the 5H06-027 thermocouple is representative of the entire core (72 s in Table 3). This thermocouple indicated the highest temperature measured in LP-LB-1. The hot spot in L2-5 and LP-02-6 was located at a different position as shown in Figure 71. The quenching time of thermocouple 5I04-27 was representative of the entire core in L2-5 and LP-02-6.

The quenching time of thermocouples in the upper plenum near the top of the core is a good indication of the end of the reflood phase. Figure 72 shows the behavior of one such upper plenum thermocouple. The final quench of this thermocouple, indicating the end of the reflood phase, occurred at nearly the same time in L2-5 and LP-02-6 (57 and 58 s) but occurred about 10 s later (68 s) in LP-LB-1. This delay in quench in LP-LB-1 can be related to the reduced amount of water injected in that experiment (Figures 66 through 68). The end of the reflood phase was coincident with the time of complete core quench only for the LP-02-6 experiment. In L2-5 and LP-LB-1 the end of the reflood phase was about 8 s and 4 s earlier than the total core quench, respectively. This indicates that in the case of higher cladding temperatures the reflood liquid level passes the hot spot without quenching the cladding. During experiment LP-02-6 the clad temperatures were significantly reduced due to the early bottom-up blowdown quench which allowed the core to quench simultaneously with the reflood front.

As mentioned earlier the first fission product release experiment in LOFT was attempted on 12.12.84 and conducted successfully on 19.12.84. During the first attempt (LP-FP-1A) the experiment was terminated during the blowdown phase with PPS (Plant Protection System) initiation. The second attempt on 19.12.84 (LP-FP-1) was successful despite the occurrence of an unintentional ECC injection in the upper plenum which substantially delayed fuel rod rupture. The experiment was terminated as planned through combined ECC

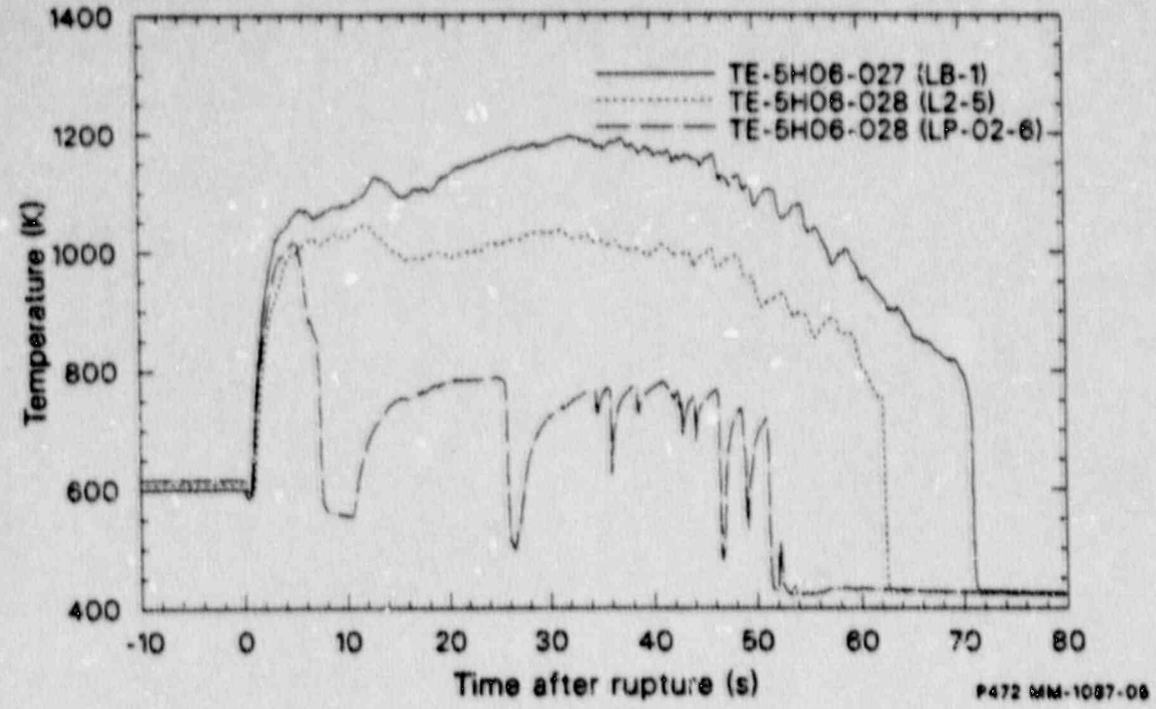

Figure 70. Cladding temperature in the central bundle during Experiments L2-5, LP-02-6, and LP-LB-1.

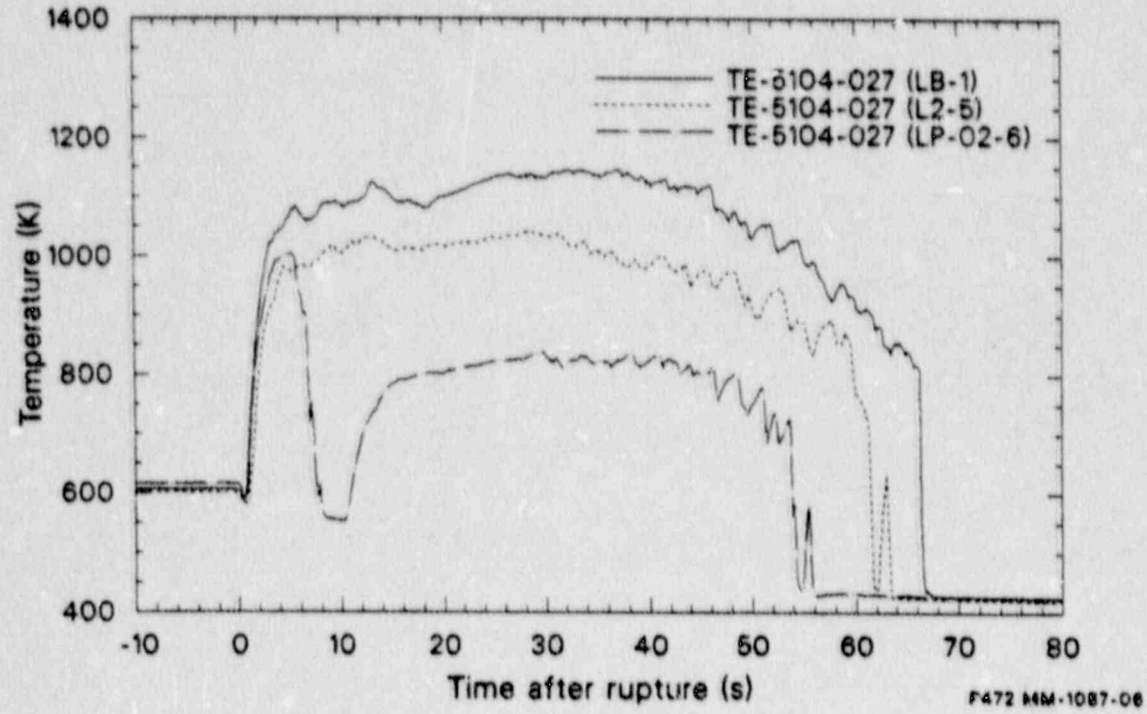

Figure 71. Cladding temperature in the central bundle during Experiments L2-5, LP-02-6, and LP-LB-1.

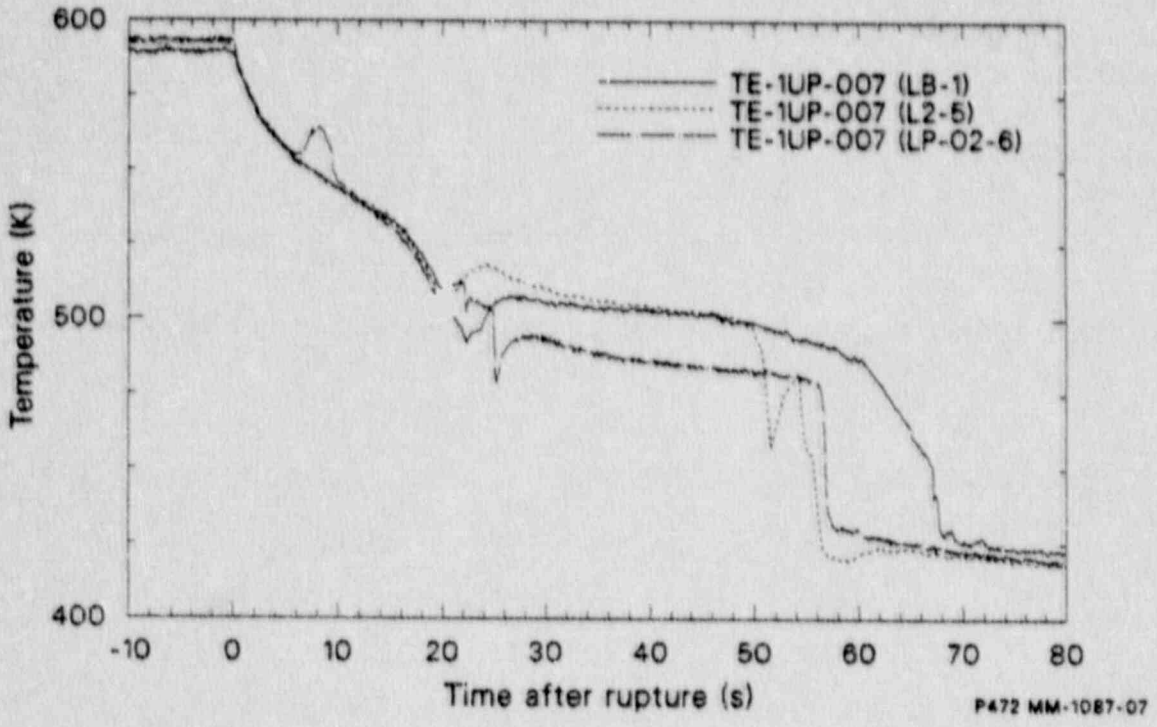

Figure 72. Temperatures measured in the upper plenum during Experiments L2-5, LP-02-6, and LP-LB-1.

injection in the upper plenum and intact loop cold leg. In summary, three ECC injection modes occurred in the first LOFT fission product release experiment:

- Combined lower plenum and downcomer injection (PPS in LP-FP-1A)
- Upper plenum injection (unintentional ECC pipe draining in LP-FP-1)
- Combined upper plenum and intact loop cold leg injection (ECC in LP-FP-1)

The upper plenum ECC injection system in LOFT was specifically designed for LP-FP-1 using accumulator B and the connecting pipes to the Reactor Vessel as shown in Figure 73. The total volume of the 30 m long piping was 0.458 m^3. The volumes of the different parts of the piping are given in Figure 73. The configuration of the injection nozzles in the upper plenum is shown in Figure 74. Eight nozzles arranged to inject towards the peripheral bundles were located about 13 cm above the central bundle and 6 nozzles arranged to inject in the central bundle were located 42 cm above core outlet. During the PPS operation in LP-FP-1A the entire water volume in the accumulator and some N_2 were injected. In the week between 12.12 and 19.12.84 the pipes shown in Figure 73 were not degassed. The unintentional injection during LP-FP-1 was caused by the expansion of the residual N_2 in the ECCS line.

LP-FP-1A results show that the HPIS initiation about 12 s after rupture (Figure 75). Accumulator initiation occurred several seconds later, at nearly the same time as in L2-5, LP-02-6 and LP-LP-1. The end of the refill phase occurred at about 31 s approximately the same time as in the other experiments, as shown in Figure 76. The accumulators inject directly in the downcomer and the lower plenum in the PPS mode to exclude bypass losses to the broken loop cold leg. In view of this and since the end of the refill phase in LP-FP-1A occurred at the same time as in the earlier large break LOCA experiments, the bypass losses during intact loop cold leg injection are concluded to be negligible.

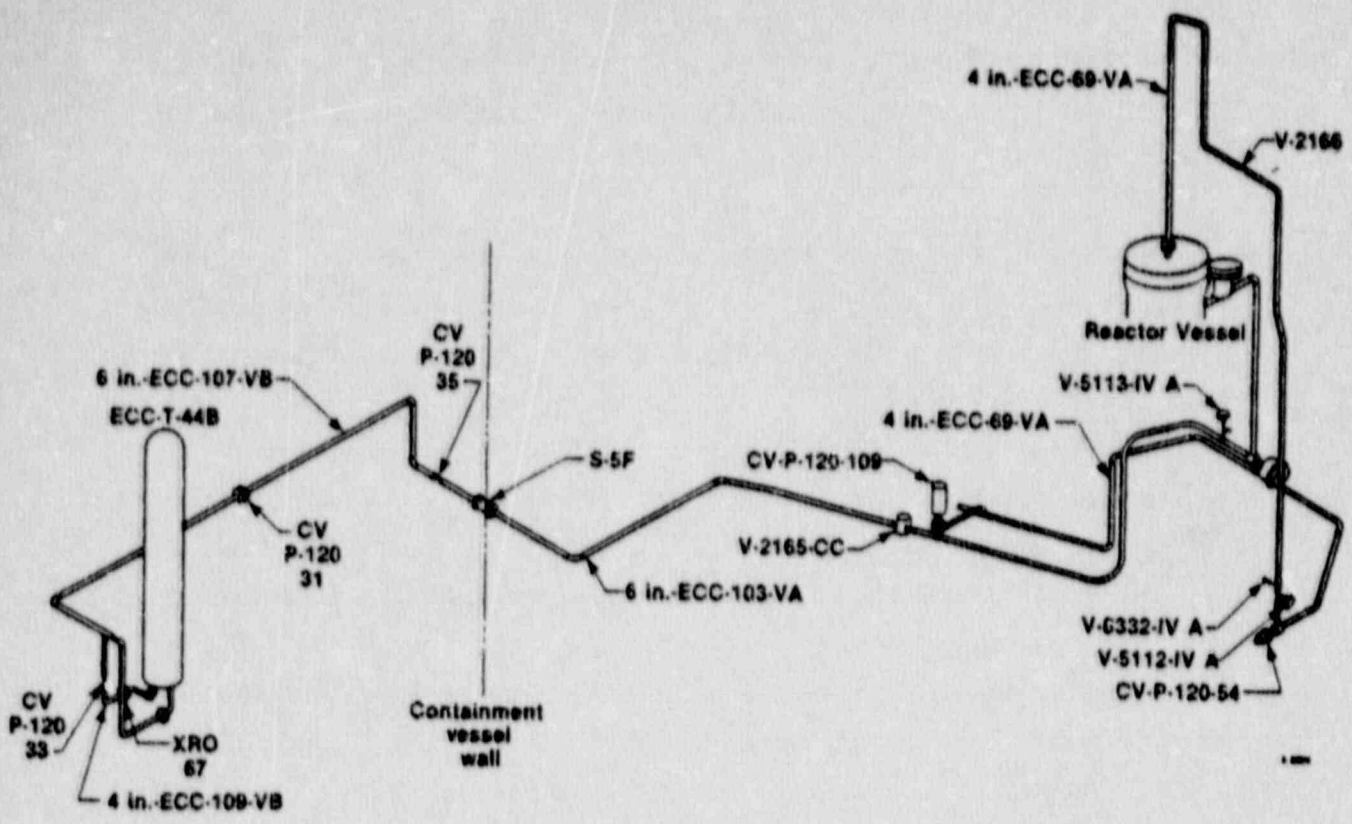

Figure 73. LP-FP-1 upper head injection piping.

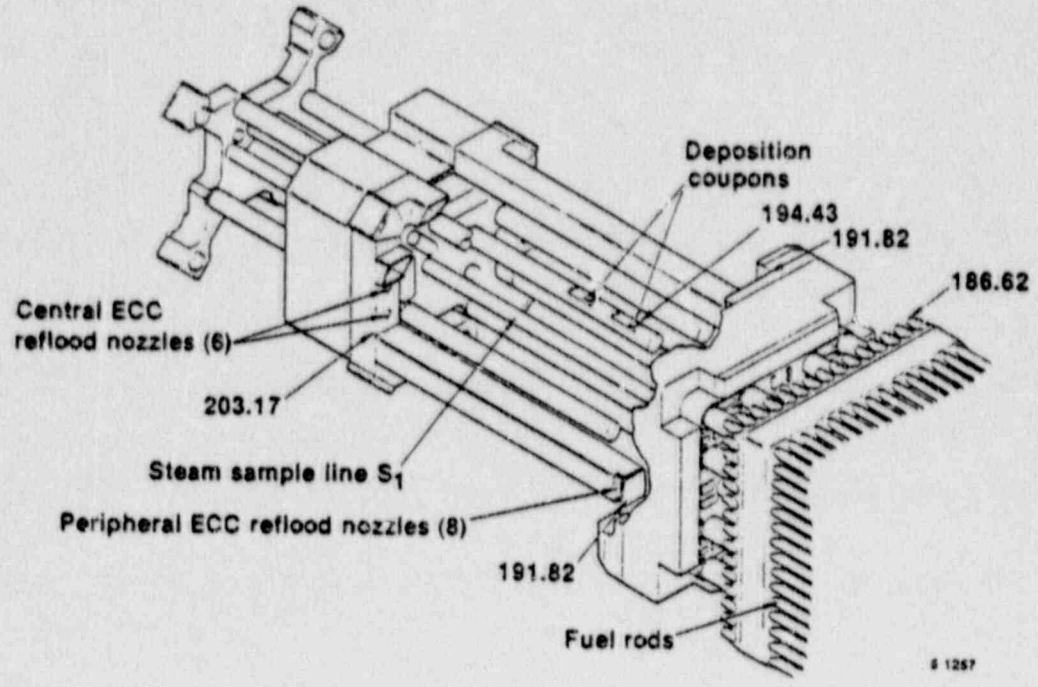

Figure 74. LP-FP-1 CFM upper structure.

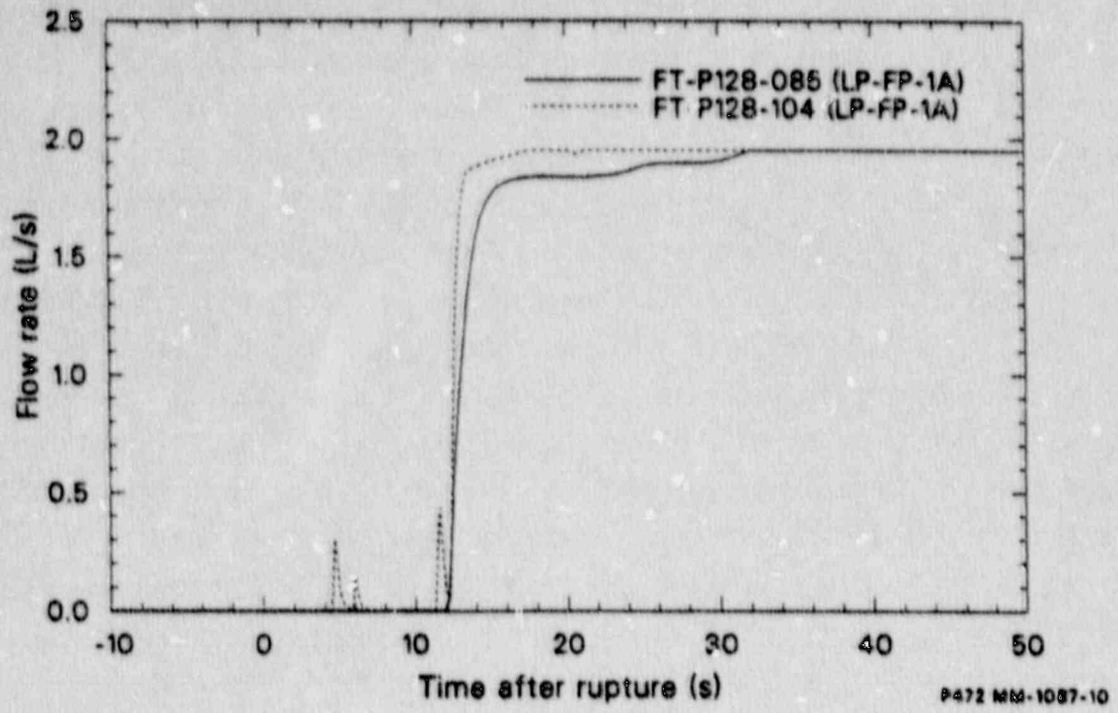

Figure 75. HPIS volumetric flow during Experiment LP-FP-1A.

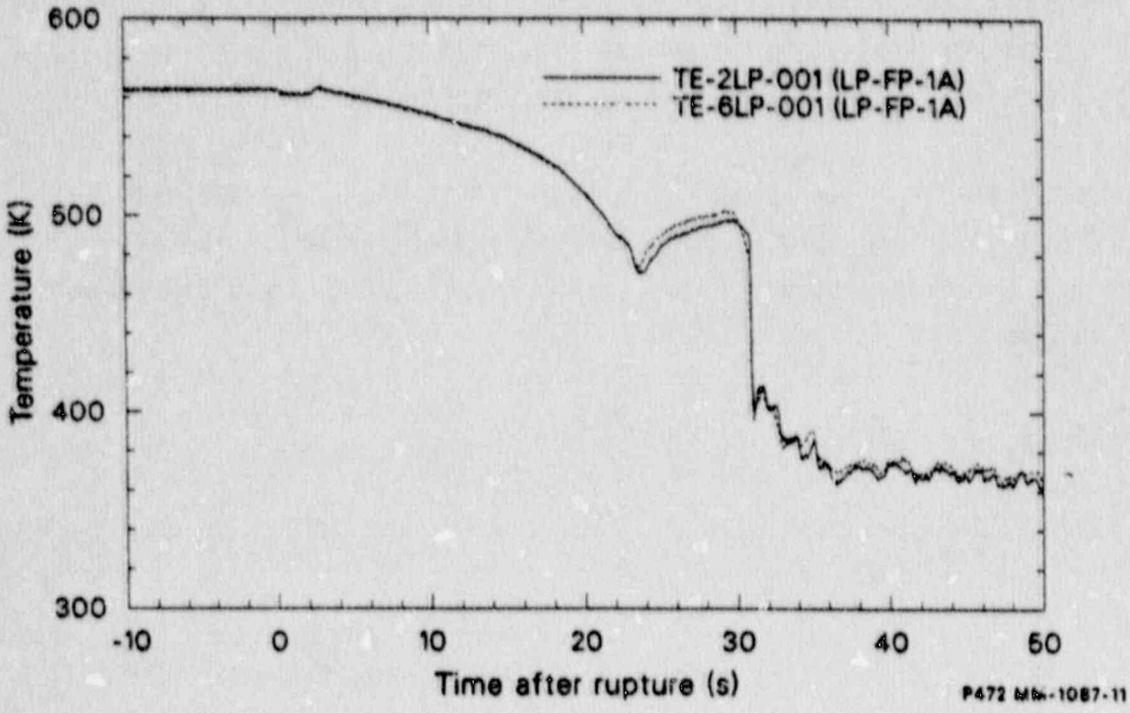

Figure 76. Liquid temperatures at the lower end boxes during Experiment LP-FP-1A.

Review of cladding temperatures throughout the core during LP-FP-1 and LP-FP-1A provides some insights on ECCS effectiveness with regard to different injection locations. Figures 77, 78 and 79 compare cladding temperatures measured at three levels during both experiments. All three figures indicate similar thermal core behavior at the three elevations for the early part of the transient. Strong differences between the two experiments begin after 22 s when the core showed more tendency to heatup in LP-FP-1A than in the LP-FP-1. The unintentional injection, explained in Section 3.6, which started early in the blowdown phase and was effective at about 24 s, is the cause of this difference. This unintentional injection penetrated the entire core causing complete quench at about 25 s (Figure 77) and 24 s (Figure 79) in the lower part and upper part of the core, respectively. In the hot region of the core (Figure 78) the unintentional injection also caused a quench; however, the quench was not complete until about 44 s. Figures 77-79 illustrate the effectiveness of upper plenum injection in mitigation of a core temperature escalation. The upper plenum injection seems to be even more effective than a full PPS action because only 200 kg (estimated) resulted in almost complete core quench within about 44 s. The short quench time in LP-FP-1 and also in case of LP-FP-1A was possible because of the low maximum temperature (less than 700 K) which was a result of the early quench phenomena described in Section 4.1.

The combined upper plenum and cold leg injection in LP-FP-1 started at 344 s when predetermined termination conditions were reached. The central fuel bundle was quenched at about 369 s (Figure 80) and the whole core was quenched at about 374 s (Figure 81).

In summary, the conclusions are:

1. The ECCS configuration in LOFT has significant effect on core quench but not on lower plenum refill

2. Early quench phenomena reduced the time of complete core quench by about 30%

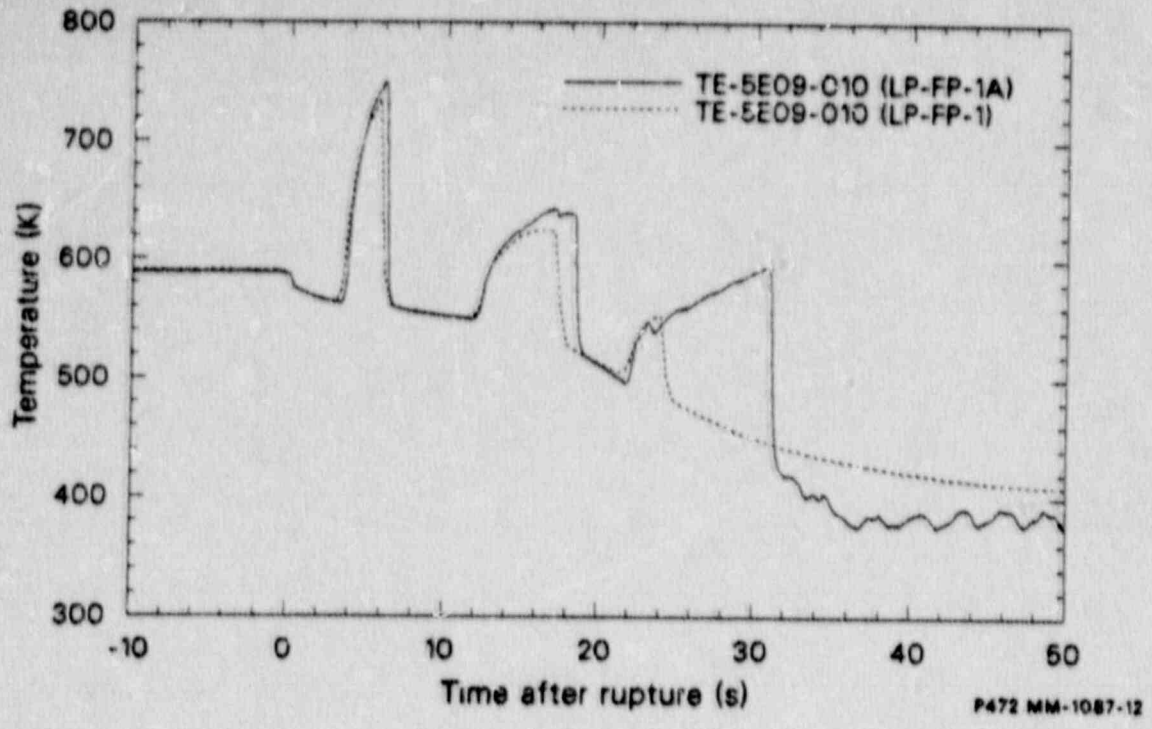

Figure 77. Cladding temperatures at the lower core region during Experiments LP-FP-1 and LP-FP-1A.

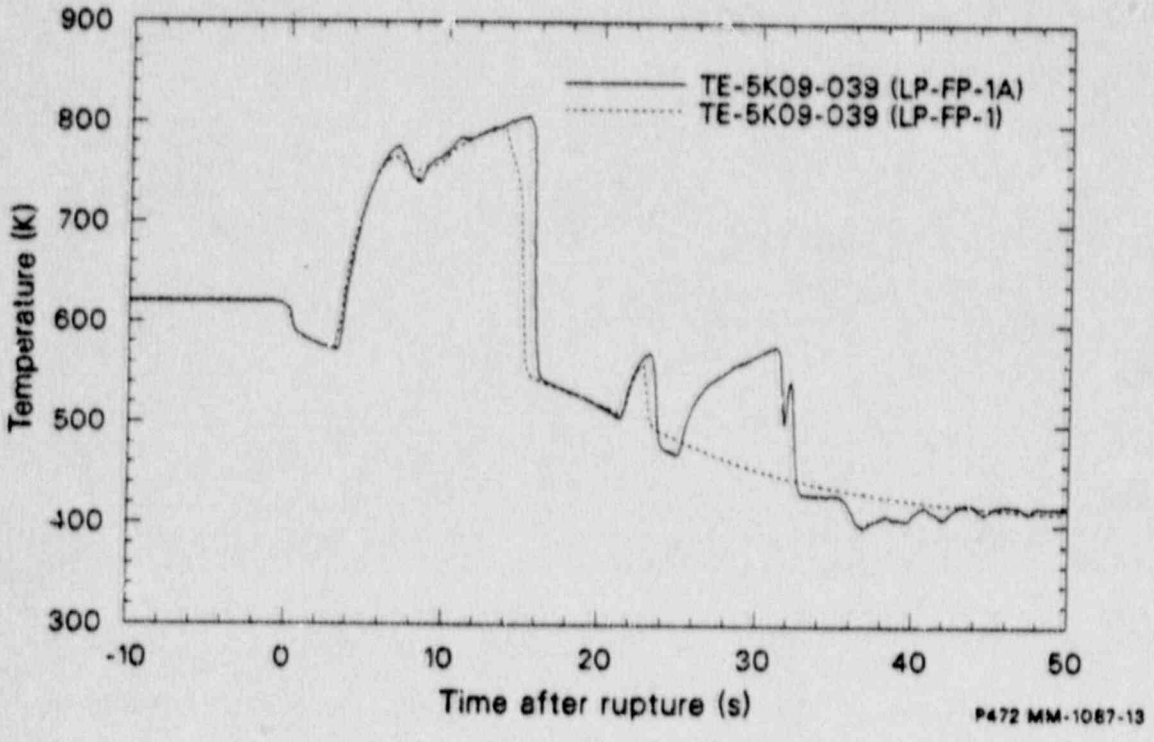

Figure 78. Cladding temperatures in the upper core region during Experiments LP-FP-1 and LP-FP-1A.

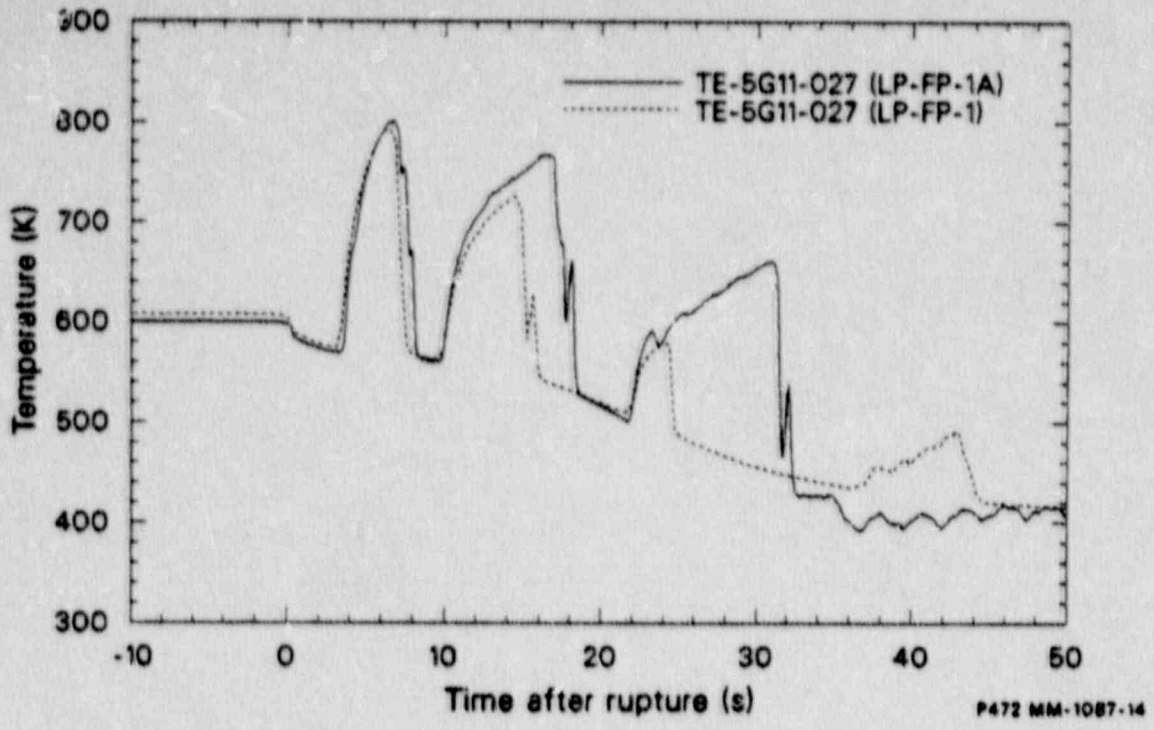

Figure 79. Cladding temperatures in the central core region during Experiments LP-FP-1 and LP-FP-1A.

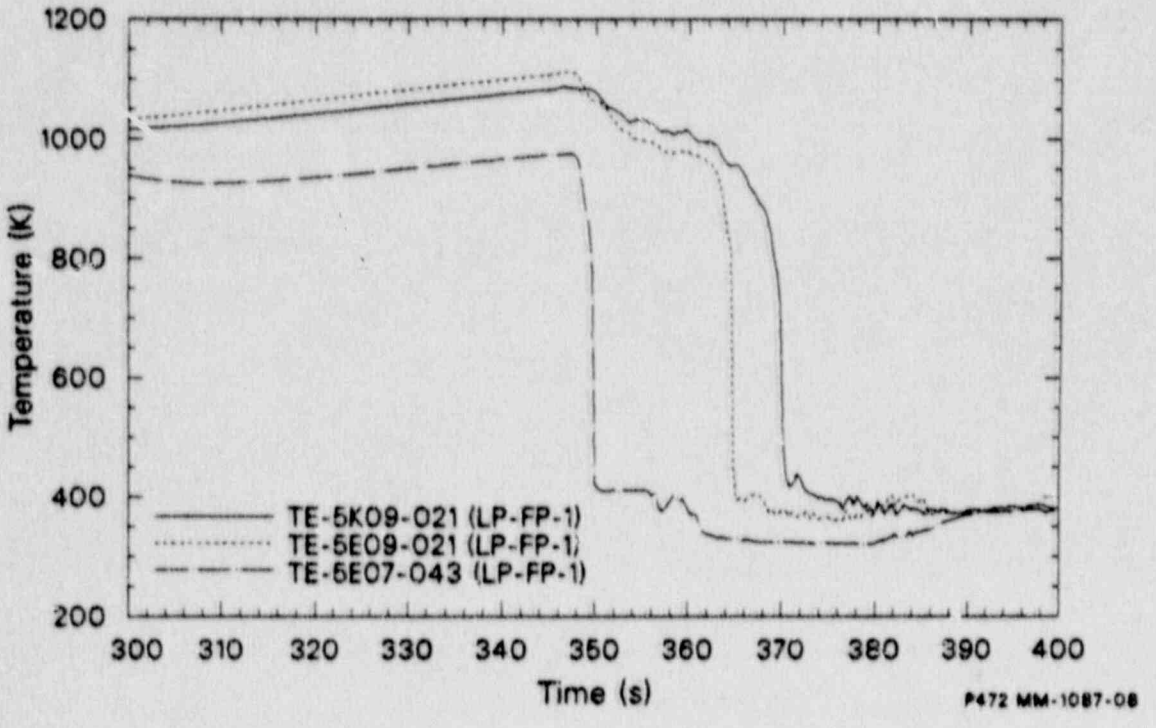

Figure 80. Cladding temperatures in the central fuel element during Experiment LP-FP-1.

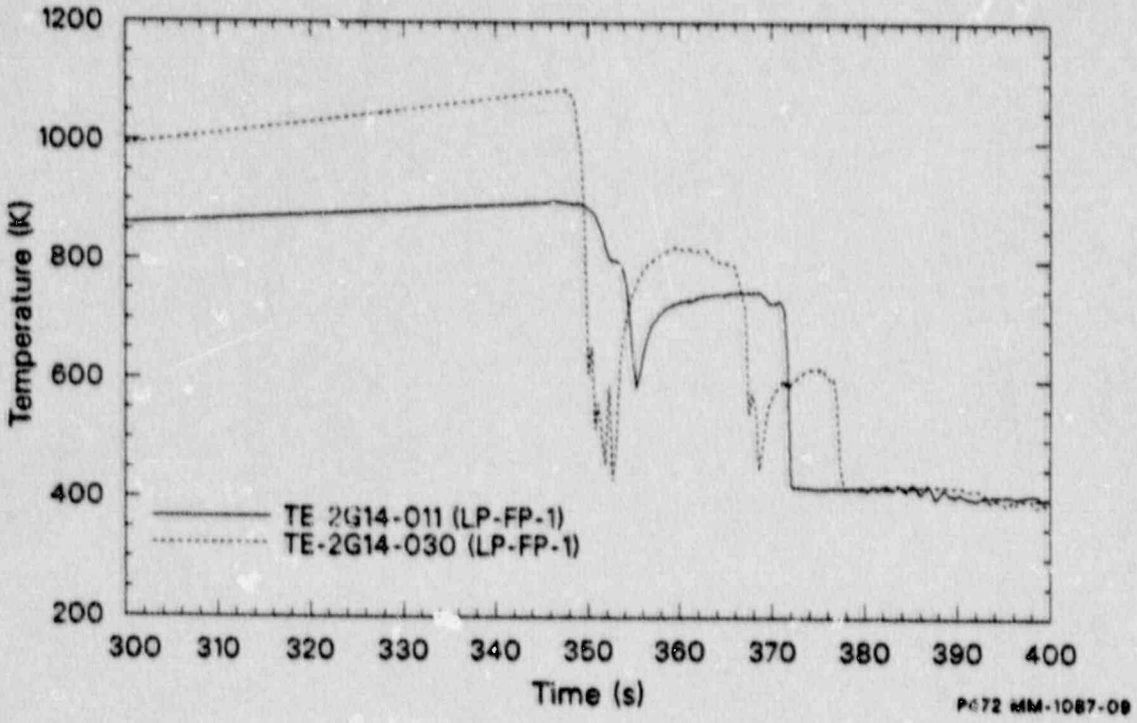

Figure 81. Cladding temperatures in a peripheral bundle during Experiment LP-FP-1.

3. The shortest quench time was achieved during PPS operation which involved a higher net rate of accumulator injection

4. Upper plenum injection is highly effective (about 200 kg of unintentionally injected water quenches 80% of the core)

5. Upper plenum injection reduced the final quench time in LP-FP-1 by about 30%.

5. SUMMARY AND CONCLUSIONS

Forty-four experiments were completed in the LOFT facility over a nine year period ending with a severe fuel damage experiment in July 1985. These experiments were conducted at typical initial and boundary conditions associated with loss of coolant accidents and anticipated transients in commercial PWRs. The research program included six nuclear large break LOCA experiments, the primary objective of which was to obtain data on LOCA phenomena and system response for a range of initial and boundary conditions which could be used for reactor system code development and assessment. The objectives, design, and principal results of the nuclear large break experiments are described. The important thermal-hydraulic phenomena measured in the large break transients and their significance are discussed in the principal areas of analysis that have been undertaken. The principal finding from the large break experiments is that, for the degrees of severity in initial and boundary conditions, the measured fuel cladding temperatures remained well below the peak cladding licensing limit temperatures.

The data obtained from the LOFT large break LOCA experiments provided new insight into phenomena associated with the large break LOCA. One of the most important phenomena, observed for first time in the LOFT transients, is fuel cooling/cladding quench during blowdown. This phenomenon is very important to the degree of transient severity because it removes a large part of the stored energy from the fuel early in the transient. The cooling/quench phenomena was determined to be caused by system hydraulics in response to the operational characteristics of the primary coolant pumps relative to the transition from subcooled to saturated choked flow at the break. The significant finding was that the cooling/quench phenomena would occur in all conditions except for a pump trip concurrent with break initiation and decoupling from the flywheels. Similar limiting conditions are expected to be required to suppress the phenomena in commercial PWRs.

Separate effect experiments in other facilities and analysis of LOFT data showed conclusively that the blowdown cooling/quench in LOFT large break LOCA experiments is real. However, the thermocouples do reduce the blowdown peak cladding temperature because of an induced delay to DNB. Fin cooling

subsequent to DNB was not found to adversely affect measurement accuracy. In contrast, surface cladding thermocouples are recognized to have noticeable effects on reflood quenching which occurs at much slower rates compared to the observed quenching during blowdown.

Examination of the LOFT large break LOCA experiments provided important insight on emergency core cooling (ECC) performance during large break transients. In general, the experiment results have shown that the ECCS operation even in degraded conditions was effective in core quench and transient recovery. The hot wall delay time was at most 2 s. Only a small part of the ECC water is lost through downcomer bypass to the broken loop cold leg indicating that the "downcomer bypass", which is one of the concerns in licensing, is not of concern. Cooling phenomena during blowdown can reduce the time to final quench by about 30% because the reflood quench is strongly dependent on cladding temperature levels at the end of the refill phase. Experiment LP-FP-1 which included upper plenum ECC injection showed that ECCS mode is highly effective and that relatively small amounts of water can quench the core.

6. REFERENCES

1. C. L. Nalezny, "Summary of Nuclear Regulatory Commission's LOFT Program Experiments", NUREG/CR-3214, EGG-2248, July 1983.

2. D. L. Reeder, "LOFT System and Test Description (5.5-Ft Nuclear Core LOCEs)", NUREG/CR-0169, EGG-2037, March 1983.

3. C. L. Nalezny, "Summary of the Nuclear Regulatory Commissions LOFT Program Research Findings", NUREG/CR-3005 EGG-2231, April 1985.

4. L. J. Ybarrondo et al., "Examination of LOFT Scaling", Proceedings of ASME Winter Annual Meeting, New York, New York, November 17-22, 1974.

5. P. A. Harris et al., "Power Ascension Test Series L2, LOFT Experiment Operating Specification", Vol. 2, NE L2 Series, Rev. 2, July 1978.

6. M. McCormic-Barger, "Experiment Data Report for LOFT Power Ascension Test L2-2", NUREG/CR-0492, TREE-1322, February 1979.

7. W. H. Grush, et al., "Results and Predictions of Scaled, Nuclear Large Break Loss-of-Coolant Experiments", ASME Winter Meeting, November 16-21, 1980, Chicago, Illinois, (80-WA/HT-49).

8. P. G. Prassinos, B. M. Galusha, D. B. Engleman, "Experiment Data Report for LOFT Power Ascension Experiment L2-3", NUREG/CR-0792, TREE-1326, July 1979.

9. J. C. Lin, "Posttest Analysis of LOFT Loss-of-Coolant Experiment L2-3", EGG-LOFT-5075, March 1980.

10. P. D. Bayless and J. M. Divine, "Experiment Data Report for LOFT Large Break Loss-of-Coolant Experiment L2-5", NUREG/CR-2826, EGG-2210, August 1982.

11. P. N. Demmie, T. H. Chen, S. R. Behling, " Best Estimate Predictions for LOFT Experiment L2-5", EGG-LOFT-5869, May 1982.

12. E. M. Feldman, "OECD LOFT Project Experiment Specification Document Cold Leg Large Break Experiment LP-02-6", OECD LOFT-T-3402, July 1983.

13. J. P. Adams, K. G. Condie and D. L. Batt, "Quick-Look Report on OECD LOFT Experiment LP-02-6", OECD LOFT-T-3404, October 1983.

14. K. G. Condie, P. N. Demmie, E. W. Coryell, "Best Estimate Prediction for the OECD LOFT Project Large Cold Leg Break Experiment LP-02-6", OECD LOFT-T-3403, September 1983.

15. J. C. Birchley, "OECD LOFT Project Experiment Specification Document for Cold Leg Large Break Experiment LP-LB-1",OECD LOFT-T-3502, December 1983.

16. J. P. Adams, J. C. Birchley, "Quick-Look Report on OECD LOFT Experiment LP-LB-1", OECD LOFT-T-3504, February 1984.

17. V. T. Berta, E. W. Coryell, "OECD LOFT Project Experiment specification Document Fission Product Experiment LP-FP-1", OECD LOFT-T-3702, October 1984.

18. A. B. Wahba, "Thermal-Hydraulic EASR of OECD LOFT LP-FP-1", OECD LOFT-T-3709, November 1986.

19. E. W. Coryell, H. G. Glaeser, "Best Estimate Prediction for OECD LOFT Project Fission Product Experiment LP-FP-1", OECD LOFT-T-3703, October 1984.

20. J. P. Adams et al., "Quick-Look Report on OECD LOFT Experiment LP-FP-1", OECD LOFT-T-3704, March 1985.

21. J. P. Adams, "Monitoring PWR Reactor Vessel Liquid Level with SPNDs during LOCAs", Proceedings of the Topical Meeting on Advances in Reactor Physics and Core Thermal Hydraulics, Kiamesha Lake, New York, Sept. 22-24 1982, NUREG/CP-0034, Vol. 2, August 1982.

22. J. P. Adams and V. T. Berta, "Monitoring Reactor Vessel Liquid Level with a Vertical String of SPNDs", ANS Winter Meeting, San Francisco, California, 1983.

23. S. N. Aksan, "Evaluation of Analytical Capability to Predict Cladding Quench", EG&G-LOFT-5555, August 1982.

24. R. A. Nelson, "Forced-Convective Post-CHF Heat Transfer and Quenching", Journal of Heat Transfer, Vol. 104, February 1982.

25. R. C. Gottula, J. A. Good, "The Effects of Cladding Surface Thermocouples on the Behavior of an Electrical Heater Rod", EG&G Idaho Report LO-00-80-115, 1982.

26. R. C. Gottula, "Effects of Cladding Surface Thermocouples and Electrical Heater Rod Design on Quench Behavior", NUREG/CR-2691, EG&G-2186, February 1984.

27. R. C. Gottula, M. L. Carbonneau, E. L. Tolman, "An Assessment of LOFT Fuel Rod Quench Behavior Based on Electric Rod Quench Tests," Proceedings of the International Symposium on Fuel Rod Simulators-Development and Application, Gaithersburg, Tennessee, USA, October 1980, (Conf-801091, May 1981).

28. S. N. Aksan, E. L. Tolman, R. A. Nelson, "Application of Analytical Capability to Predict Rapid Cladding Cooling and Quench During the Blowdown Phase of a Large Break Loss-of-Coolant Accident", Proceedings of the Second International Topical Meeting on Nuclear Reactor Thermal-Hydraulics (Vol. 3), Santa Barbara, CA, January 11-14, 1983.

29. T. R. Yackle, "An Assessment of the Influence of Surface Thermocouples on the Behavior of Nuclear Fuel Rods During a Large Break LOCA", The 8th Water Reactor Safety Research Information Meeting, Gaithersburg, Maryland, USA, NUREG/CP-0023, Vol. 4, October 1980.

30. R. W. Garner, P. E. MacDonald, "Power Burst Facility Thermocouple Effects Test Results Report, Test Series TC-1, TC-2, and TC-3", NUREG/CR-2665, EGG-2190, June 1987.

31. R. W. Garner, "PBF Thermocouple Effects Tests, Test Series TC-4, Quick Look Report", EGG-TFBP-5465, August 1981.

32. D. S. Seegmiller, "LOFT F1 and F2 Bundle Thermocouple Perturbation Analysis", EG&G Idaho Internal Technical Report LO-14-82-082, Released Report RE-A-82-044, USNRC-P394, February 23, 1983.

33. H. G. Kraus, "COUPLE/MOD5, A General Purpose Two-Dimensional Finite Element/Finite Difference Heat Conduction Code", RE-A-82-035, EG&G Idaho, December 1981, EG&G Idaho, Inc.

34. J. J. Pena, "Post Experiment Analysis of the OECD LOFT Experiment LP-02-6, OECD LOFT-T-3408", May 1985.

35. T. D. Knight, "TRAC Analysis of The OECD LOFT Experiment LP-02-6", OECD LOFT-T-3409, October 17, 1985.

36. R. C. Gottula, K. G. Condie, R. K. Sundaram, S. Neti, J. C. Chen, R. A. Nelson, "Forced Convective, Nonequilibrium, Post-CHF Heat Transfer Experiment Data and Correlation Comparison Report", NUREG/CR-3193.

37. S. R. Fisher et al., "RELAP4/MOD6: A Computer Program for Analysis of Nuclear Reactors and Related Systems, Users Manual," CDAP-TR-003, January 1978.

38. E. L. Tolman, M. L. Carboneau, "Comparison of Semiscale MOD-1 and LOFT Large Break Loss-of-Coolant Experiments. A Case for Nuclear Experiments", ANS Winter Meeting, San Francisco, California 1981.

39. H. Grutter et al., "NEPTUN Bundle Reflooding Experiments: Test Facility Description", EIR Report No. 386, Wurenlingen, March 1980.

40. S. N. Aksan, "NEPTUN Bundle Boil-off and Reflood and Experimental Program Results", The 10th Water Reactor Safety Research Information Meeting, Gaithersburg, Maryland, USA, NUREG/CP-0041, Vol. 1 (1982).

41. M. Richner, "Comparison of NEPTUN-I and NEPTUN-II Reflooding Experiments: External Thermocouple Effect", (In German) EIR Internal Report, (TM-32-87-06) Wurenlingen, May 1987.

42. C. Vitanza et al., "Blowdown/Reflood Tests With Nuclear Heated Rods (IFA-511.2)" OECD Halden Reactor Project, HPR-248, May 1986.

43. T. Johnsen, C. Vitanza, "Blowdown/Reflood Tests With Semiscale Heaters (IFA-511.3, Data Collection)", OECD Reactor Project, HWR-17, May 1981.

44. T. Johnsen, C. Vitanza, "Results of LOCA Tests With Semiscale Heaters (IFA-511.5)", OECD Halden Reactor Project HPR-313, May 1984.

45. C. Vitanza, T. Johnsen, "Results of Blowdown/Reflood Tests With REBEKA Electric Simulators (IFA-511.4, July 2)", OECD Halden Reactor Project, HWR-85, May 1983.

46. P. Ihle, K. Rust, "PWR Reflood Experiments Using Full Length Bundles of Rods With Zircaloy Claddings and Alumina Pellets (Results of the SEFLEX Program)", Proceedings of Third International Topical Meeting on Reactor Thermal Hydraulics, Newport, Rhode Island, USA, October 15-18, 1985 (Vol. 1).

47. S. N. Aksan et al., "Boil-off Experiments With the EIR-NEPTUN Facility: Analysis and Code Assessment Overview Report", EIR Report No. 623, September 1987.

APPENDIX A

CODE CALCULATIONS

APPENDIX A

CODE CALCULATIONS

The predictions for LOFT large break LOCA experiments (discussed in the section "LOFT Nuclear Large Break Experiments") were performed using codes of the earlier generation such as RELAP4/MOD6, RELAP5/MOD1 or TRAC-PD2. Although, these codes are currently being used in specific applications they do not represent the current knowledge in reactor safety. In this section we present examples of the application of current advanced thermal-hydraulic codes for analysis of LOFT large break LOCA experiments. We understand that these thermal-hydraulic codes will continue to be refined and maintained in the future. These codes are: DRUFAN, RELAP5/MOD2 and TRAC-PF1/MOD1.

A few relatively recent calculations for LOFT large break LOCA experiments were selected and are briefly discussed to illustrate performance of these codes. Table A1 shows which codes were applied to pre- and post-experiment analyses of LOFT large break experiments, and Table A2 summarizes performance of the current codes in presented calculations. Additional information on code performance in simulation of the large break LOCA can be found in Reference A1 which provides review of analyses of Experiment LP-02-6 with RELAP5/MOD2, TRAC-PD2/MOD1, DRUFAN-2 and TRAC-PF1/MOD1 codes.

A1. The Thermal Hydraulic Code DRUFAN-02

The Code DRUFAN has been developed in the Gesellschaft fur Reaktorsicherheit (GRS) mbH, Germany for the simulation of LWR reactors. The code is applied to the analysis of large, medium sized and small breaks and selected transients.

The physical system is described by "lumped parameter" control volumes which are connected by flow paths. Also, valve, pump, accumulator, steam generator and pressurizer models are available for simulation. The numerical method used in DRUFAN is the lumped parameter approach. The ordinary differential equation system of the thermo- and fluid-dynamic model is based

TABLE A1. CODE APPLICATION TO LOFT LB EXPERIMENTS

	L2-2		L2-3		L2-5		LP-02-6		LP-LB-1		LP-FP-1	
	P	PA	P	PA	P	PA	P	PA	P	PA	P	PA
RELAP4/MOD6	X		X			X						X
RELAP5/MOD1					X	X						
TRAC-PD2						X	X	X	X		X	
DRUFAN-02				X	X	X	X			X	X	X
RELAP5/MOD2								X		X		X
TRAC-PF1/MOD1								X		X		X

P - Predictions

PA - Postexperiment Analyses

TABLE A2. PERFORMANCE OF CURRENT THERMAL-HYDRAULIC SYSTEM CODES

	PSC	Break Mass Flow	Blowdown Quench	PCT	Reflood Quench	ECC
DRUFAN-02 L2-5	Pressure: Good ILCL Flow: RCP:	Subcooled cold leg break flow underpredicted. HL break flow initial 2-phase flow underpredicted. Effects of intact loop draining into upper plenum (increase of break flow) not calculated.	Top-down quench not calculated. Effects in peripheral Bundles not calculated.	Satisfactory		
RELAP5/MOD2	Pressure: Good ILCL Flow: Initially underpredicted (5s). RCP: Calculated coastdown speed deviates from measured.	Good. Shows osccilations during accumulator injection.	Bottom-up quench calculation only using reflood option. Quench not as complete as in experiment. No rapid return to DNB. No heatup in upper part of core. Top-down quench too early; too much water kept above the core.	Good with good timing.	At lower elevation correct timing and rate, delayed at PCT elevation.	Initial injection rate good. Later overpredicted.
TRAC-PF1 MOD1 LP-02-6	Pressure: Good ILCL Flow: Initially underpredicted (5s). RCP: Initial condition speed too high. Later coastdown overpredicted.	Good	No bottom-up quench, only some cooling in lower core. Top-down quench: Some cooling and quenching calculation in upper core, not as complete as in experiment. Mostly missing in peripheral bundles.	Blowdown PCT quite correct. Reflood PCT overpredicted significantly.	Reflood quench delayed and lower temperature than measured.	Accumulator empties earlier than in experiment calculation injection. Condition results in PCS pressure drop and overprediction of accumulator flow.

on the conservation laws for vapor mass, liquid mass, overall energy and overall momentum. The liquid and vapor phases are treated as a homogeneous mixture, or in the case of mixture level-tracking as a nonhomogenous mixture [A2].

The velocity difference of the liquid and vapor phase may be determined by a drift flux model. The differential equations are integrated by an explicit-implicit integration method with automatic control of time step, order of consistency and local discretization error [A3].

The entire range from subcooled liquid to superheated vapor including nonequilibrium effects is simulated by assuming either the liquid or vapor phase to be saturated.

The table for the determination of critical discharge rate at the break is calculated by a one-dimensional nonequilibrium model which is based on the same four conservation equations used for the "lumped parameter" control volumes. This model takes into account the geometry of the discharge flow path [A3].

For the simulation of structures, electrical heaters and fuel rods a heat conductor model and point neutron kinetics model are used. The heat transfer coefficients coupling the structure and thermal hydraulic model are determined by a comprehensive heat transfer package. The heat transfer package also contains a set of critical heat flux correlations.

The LOFT input model was developed for the L2-3 post experiment calculation and was then used for prediction of L2-5 and LP-02-6. The primary and secondary loops of LOFT were simulated by 79 control volumes, 98 junctions and 118 heat conductors. All parts of the LOFT facility except the blowdown suppression tank were simulated. The LOFT core was simulated by two parallel channels. The hot channel simulated the central region and included two heat conductors with a radial power factor of 1.4 and 1.2. The second channel simulated all fuel rods outside the central region and included two heat conductors with the power factors 1.0 and 0.75. Cross flow was allowed

between the two parallel channels and was simulated by horizontal junctions. The heat generation in the active core was determined by a point neutron kinetic model. A value of 6000 W/m^2K was used for the gap conductance.

The upper plenum was divided into three levels and represented by 4 control volumes. The central part was simulated by two parallel control volumes to account for differences in geometry above the fuel bundles. The bypass between the downcomer and the upper plenum was modelled allowing flow of 5% of the total steady state loop flow.

Two parallel channels were used to represent the nonuniform transient behavior of the fluid in the downcomer. Each channel was divided into four axial cells connected by vertical junctions. Cross flow was permitted between the parallel channels through four horizontal junctions. The fluid between the core filler pieces was represented by one cell, which admits a core bypass of 6% of the steady state flow.

The inner and outer heat structures were modelled. The heat losses on the primary side were assumed to be equally distributed and totaled 150 kw. All essential parts and structures of the LOFT steam generator were modelled. The total heat loss through the outer structures was 50 kW. The heat generation of the primary coolant pumps was also taken into account.

The pressurizer was simulated by one control volume and a second control volume simulated the surge line. The broken loop nodalization included the steam generator and pump simulators. The critical discharge rate was determined by the 1-D (BIASI) discharge model.

DRUFAN-02 was used for pre and post-experiment calculations of the large break LOFT experiments. Experiment L2-5 was chosen to be international standard problems No. 13 (ISP 13). DRUFAN-02 was used for the blind calculations [A4]. The agreement between measured and calculated peak clad temperature was satisfactory as shown in Figure A1. Also good agreement was formed by comparing other thermal hydraulic parameters such as system pressure (Figure A2) and break flow (Figures A3 and A4). However,

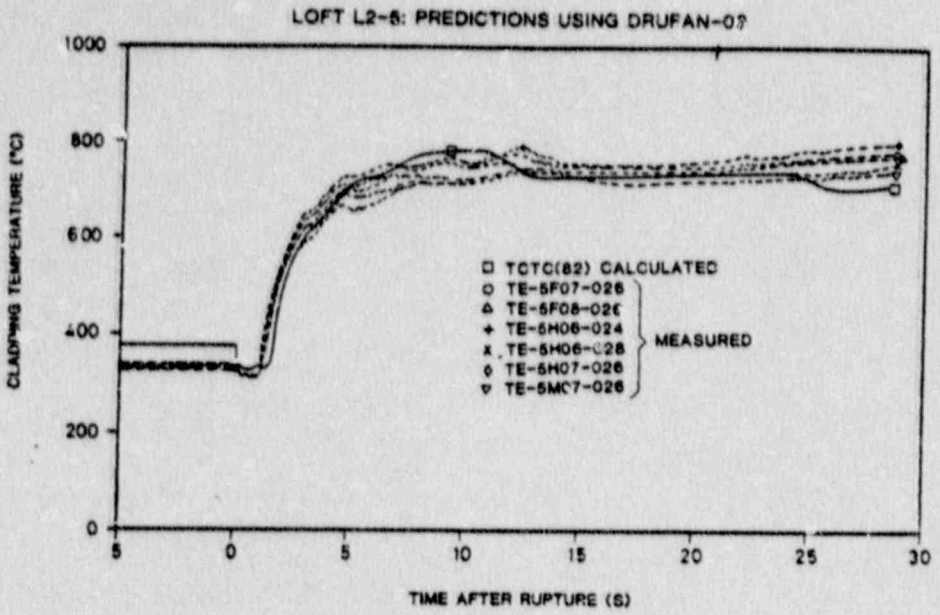

Figure A1. Measured and calculated with DRUFAN-02 peak cladding temperatures for Experiment L2-5.

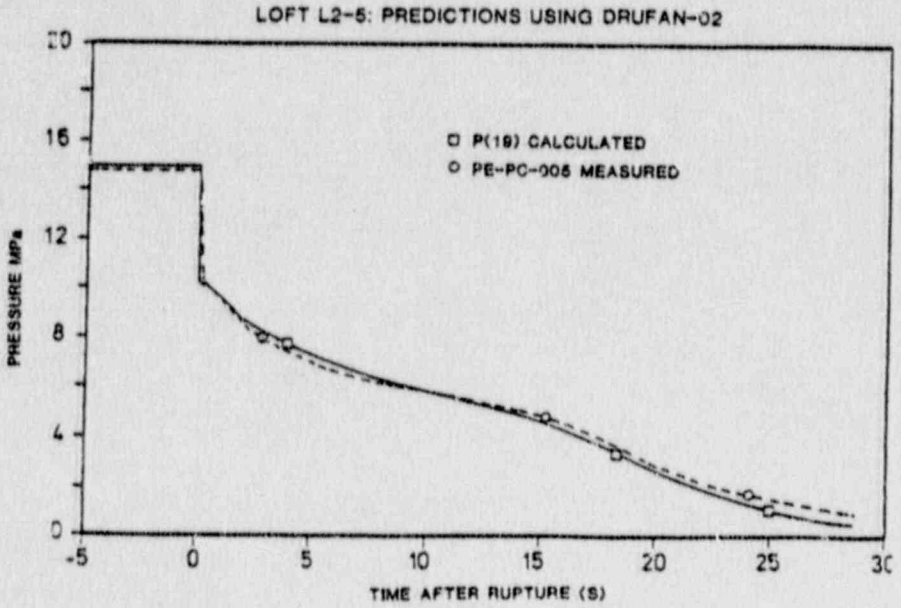

Figure A2. Measured and calculated with DRUFAN-02 primary system pressure for Experiment L2-5.

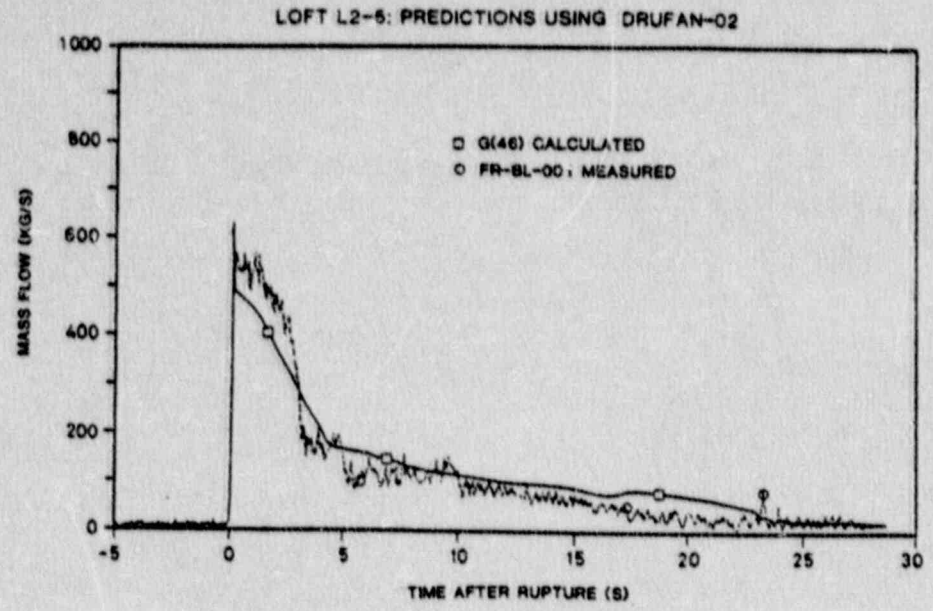

Figure A3. Measured and calculated with DRUFAN-02 cold leg break flow for Experiment L2-5.

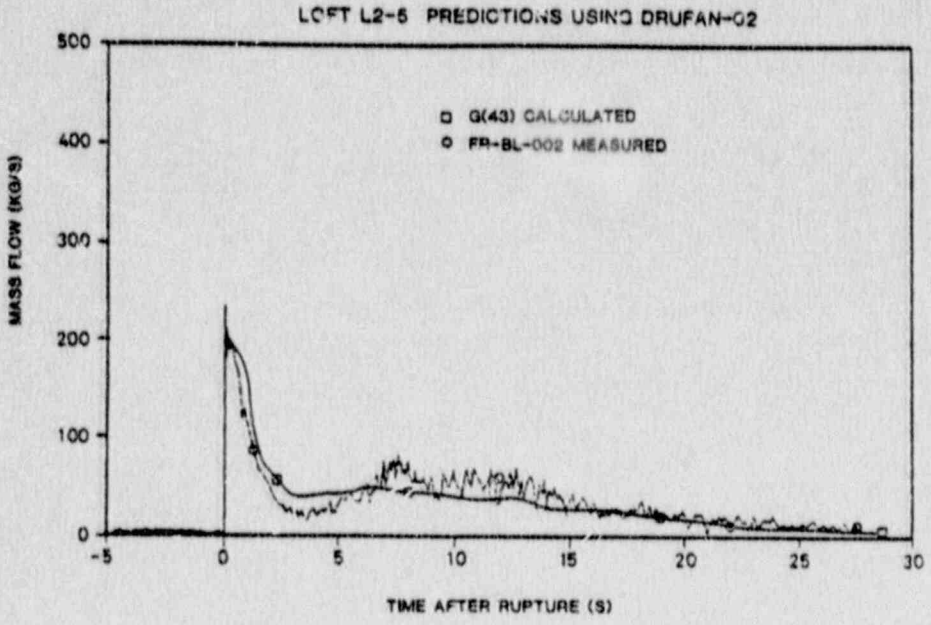

Figure A4. Measured and calculated with DRUFAN-02 hot leg break flow for Experiment L2-5.

multidimensional phenomena due to quench processes could not be calculated. Also rewetting time and subsequent CHF did not agree consistently with measured values specially in the peripheral bundles.

A2. RELAP5/MOD2

The RELAP5/MOD2 code, developed at the Idaho National Engineering Laboratory, is a best-estimate thermal-hydraulic system code for simulation of a variety of hydraulic and thermal transients in both nuclear and nonnuclear systems involving steam-water-noncondensible fluid mixtures [A5].

The RELAP5/MOD2 hydrodynamic model is a one dimensional, transient two-fluid model for flow of a two-phase steam-water mixture that can contain a noncondensible component in the steam phase and/or a nonvolatile component in the liquid phase. The basic field equations for the two-fluid nonequilibrium model consist of two phasic continuity equations, two phasic momentum equations, and two phasic energy equations. The system model is solved numerically using a semi-implicit finite difference technique. For steady state and very slow transient there is a user option for a nearly-implicit finite difference technique which allows violation of material Courant limit.

The code includes many generic component models from which general systems can be simulated. The component models include pumps, valves, pipes, heat structures, reactor point kinetics, electric heaters, jet pumps, turbines, separators, accumulators, and control system components. In addition special process models are included for effects such as form loss, flow at an abrupt area change, branching, choked flow, boron tracking, and a noncondensible gas.

The first independent application of RELAP5/MOD2 for analyses of a LOFT experiment was for post experiment calculations of Experiment LP-02-6 [A6]. Code version 36 was used. In these calculations the input model was used based on a RELAP5/MOD1 model for predictions of this experiment. This model included a split downcomer and split core channel for better simulation of the 3-D effects strongly present in a large break LOCA. The parallel

channels were connected with cross flow junctions. The gap conductance model was used only for the prepressurized fuel rods in the center fuel module. Recorded setpoints and initial conditions were used in this analysis.

Figure A5 shows the calculated and measured primary system pressure. The calculated pressure follows the measured pressure, relatively close although it is lower than the measured during initial 10 s of the transient and higher in the latter part of the depressurization. The code calculated a period of positive core flow during the blowdown. However, the balance of flows in the broken loop cold leg and the intact loop cold leg indicates a possible smaller flow through the core than in the experiment which is attributed to a less-than-measured calculation of the early intact loop mass flow rates. The blowdown bottom-up quench was predicted by the code however not to the extent as measured in the experiment. The cladding at the hot elevation was cooled rather than quenched (Figure A6). The reason may be the lower mass flow rate calculated during that time or that the film boiling correlation used is not valid for low quality flows. The code also calculated the top-down quench but earlier than measured. It was concluded that the CCFL conditions are not adequately modeled by the code. The calculation places too much liquid on the top of the core which acts to prevent cladding heatup in the upper part of the core.

A3. TRAC-PF1/MOD1

The TRAC-PF1/MOD1 code was developed at Los Alamos National Laboratory under the sponsorship of the U.S. NRC. TRAC-PF1 is the successor of the TRAC-PD code.

TRAC-PF1/MOD1 is a best-estimate computer code for analysis of postulated accidents in light water reactors. The code [A7] features a three dimensional treatment of the reactor vessel and associated internals, two phase nonequilibrium hydrodynamic models, flow regime dependent constitutive relations, optional reflood tracking capability for both bottom-reflood and falling-film quench fronts, and consistent treatment of entire accident scenarios, including the generation of consistent steady state conditions.

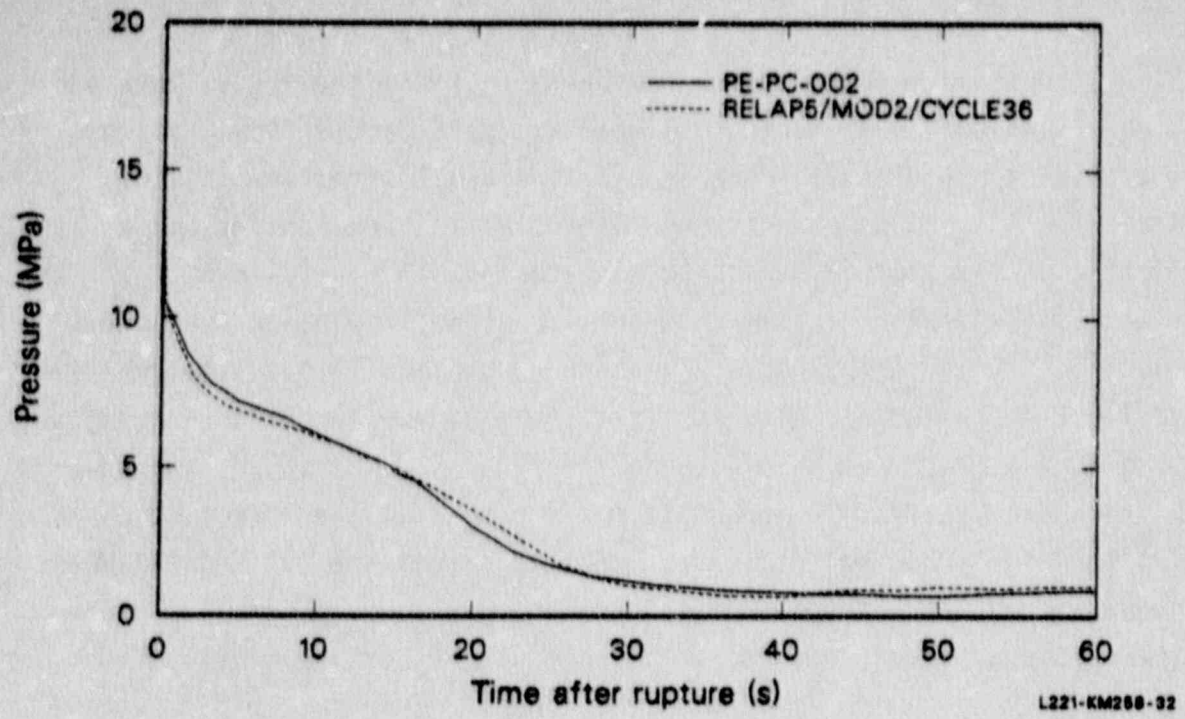

Figure A5. Measured and calculated with RELAP5/MOD2 primary system pressure for Experiment LP-02-6.

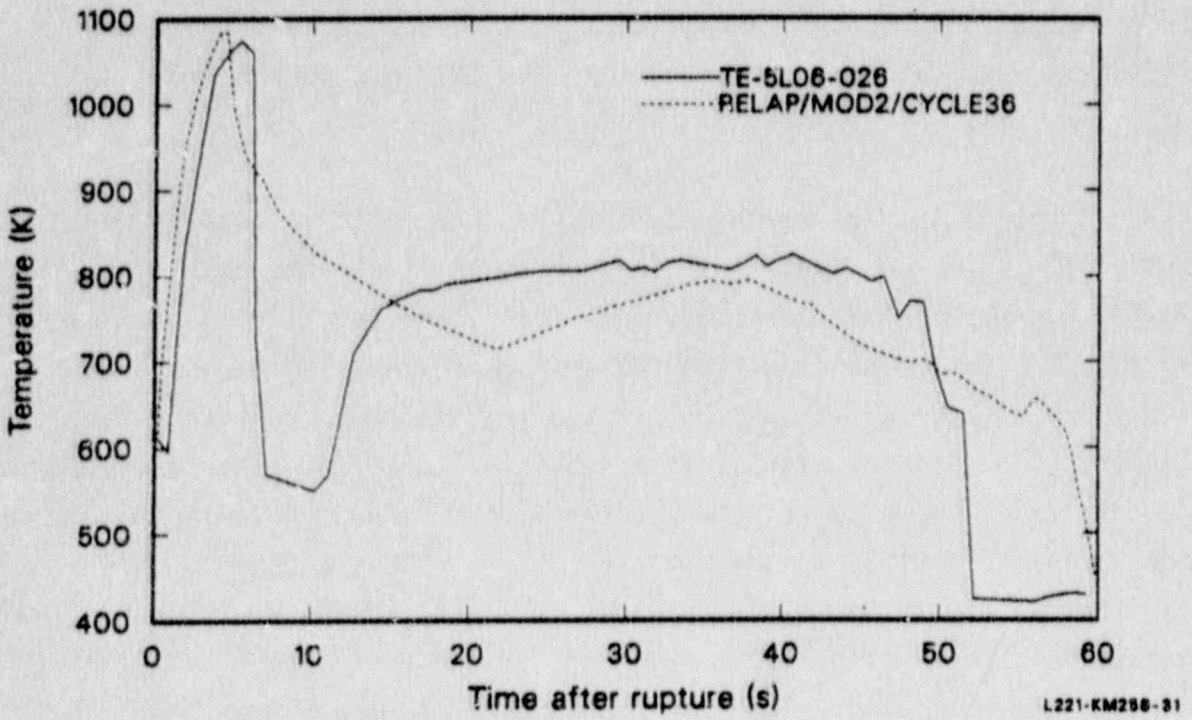

Figure A6. Measured and calculated with RELAP5/MOD2 peak cladding temperatures for Experiment LP-02-6.

The hydrodynamic model is a two-fluid, six equations model in both one- and three-dimensional components. The partial differential equations are solved by finite differences. The stability-enhancing two-step (SETS) numerical algoritnm is used in the one dimensional hydrodynamics and permits this portion of the fluid dynamics to violate the material Courant condition. This technique permits large time steps and, hence, reduced running time for slow transients. The three-dimensional vessel option uses semi-implicit differencing. The finite-difference equations for hydrodynamic phenomena form a system of coupled, nonlinear equations that are solved by a Newton iteration procedure. The heat-transfer equations are treated using a semi-implicit differencing technique. Reactor components in TRAC-PF1/MOD1 consist of accumulators, breaks, fills, cores, pipes, pressurizers, plenums, steam generators, tees, turbines, valves and vessels with associated internals.

The calculations of Experiment LP-02-6 presented here were performed at the Los Alamos National Laboratory and are documented in Reference A8. The input model used in these analyses was adopted from the TRAC-PD2 input model used in pre-experiment calculations with code required modifications and measured initial conditions. Code version 12.0 was used on CDC-7600 computer.

The code calculated the primary system pressure quite well as shown in Figure A7. The cold leg break flow also agrees well with the data (Figure A8). However, the break mass flow rate increase calculated after 40 s as result of nitrogen injection and system pressure increase was not measured. The peak cladding temperature was calculated to contain fewer cooling effects during the transient as shown in Figure A9. The code was not able to calculate the early bottom-up quench. The final quench is calculated to occur later and from lower temperatures than in the experiment. The inability to calculate the rapid quenching during blowdown is attributed [A8] to limitations in heat transfer correlations in the code. Figure A10 shows the measured and calculated cladding temperatures in bundle 4 in which the top down quench was most effective. The comparison indicates that TRAC was also not able to calculate this phenomenon.

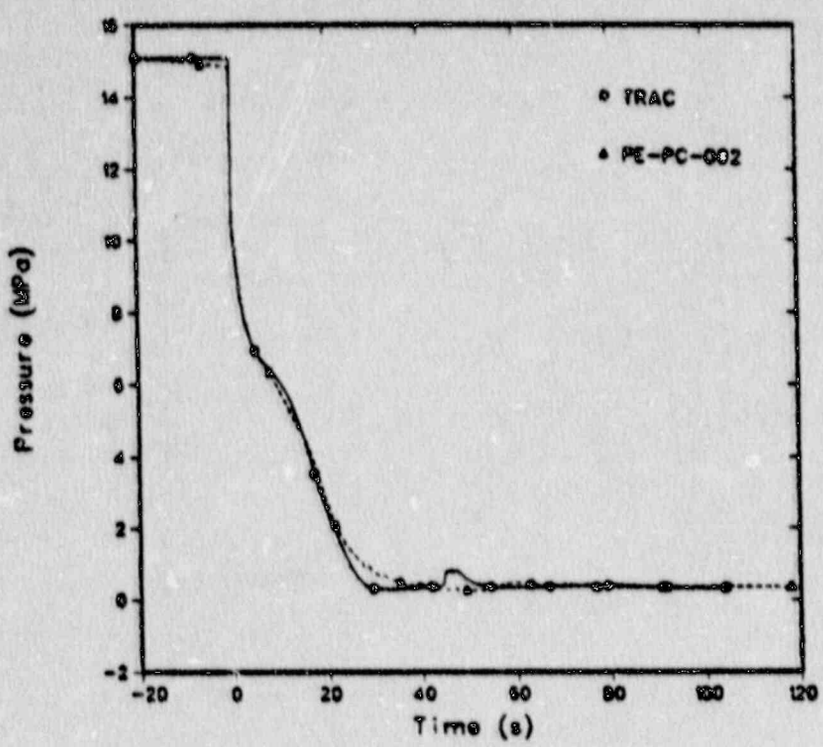

Figure A7. Measured and calculated with TRAC-PF1/MOD1 primary system pressure for Experiment LP-02-6.

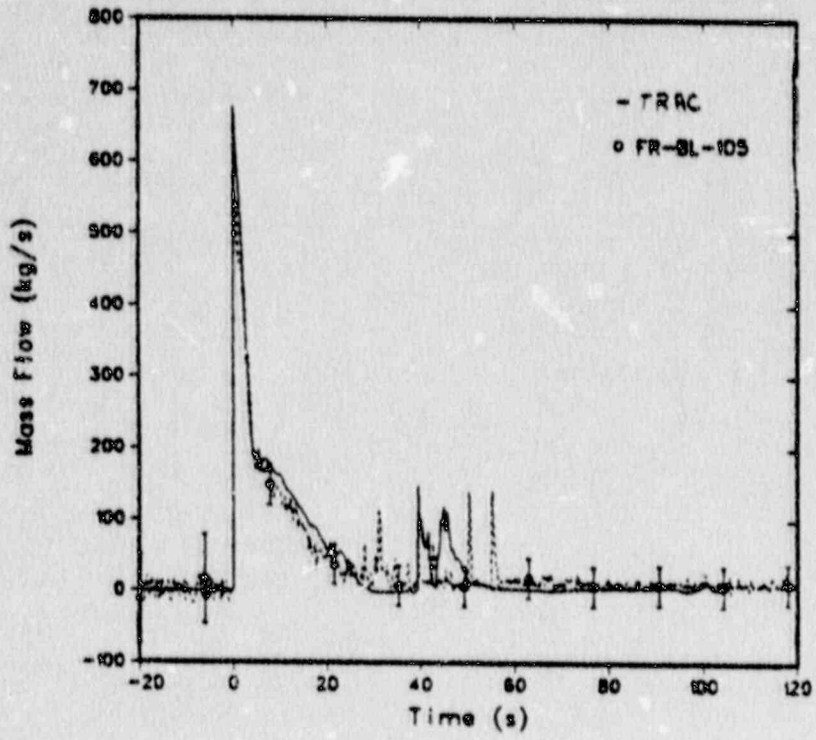

Figure A8. Measured and calculated with TRAC-PF1/MOD1 cold leg break flow for Experiment LP-02-5.

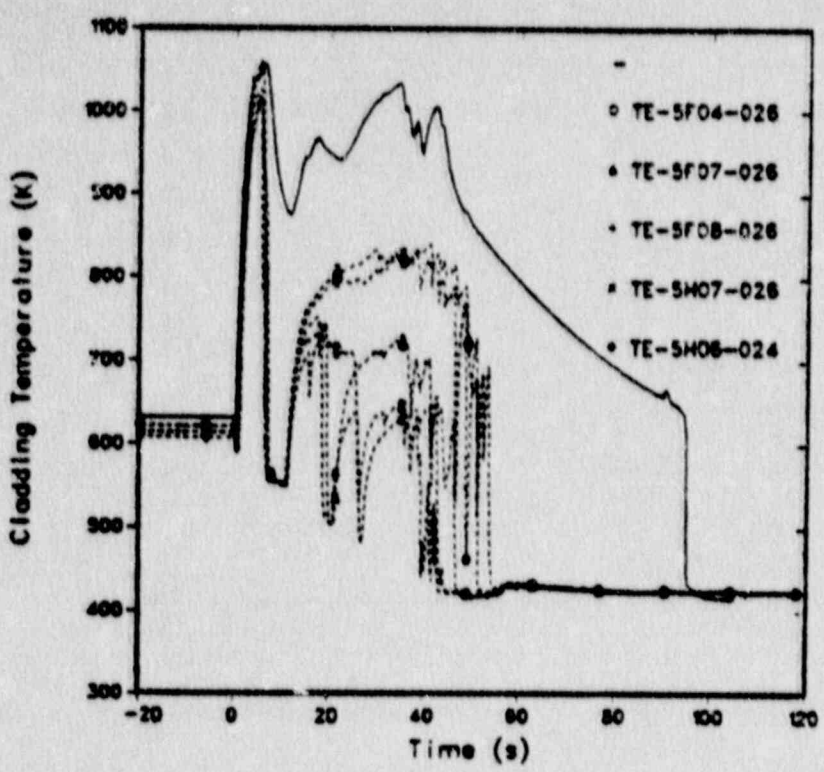

Figure A9. Measured and calculated with TRAC-PF1/MOD1 peak cladding temperatures for Experiment LP-02-6.

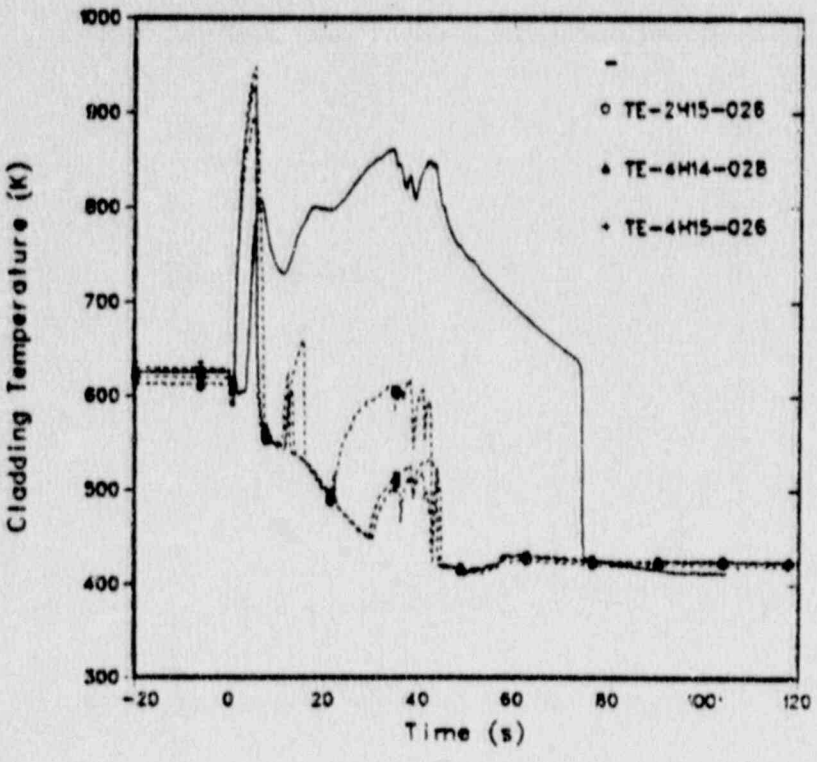

Figure A10. Measured and calculated with TRAC-PF1/MOD1 cladding temperatures in peripheral bundles for Experiment LP-02-6.

In summary, the most advanced thermal-hydraulic systems codes perform in an acceptable manner in a macroscopic sense. That is, parameters such as system pressure and break flow are well-calculated. However, in a microscopic (or localized) sense, the codes do not do as well although, in general, the trends in the calculations indicate that the phenomena in question, such as fuel cladding cooling/quench phenomena, are being sensed however incorrectly in magnitude. These codes are projected to be able to calculate the significant phenomena in a large break LOCA with improved models for phenomena such as post-CHF heat transfer and forced convective cooling.

APPENDIX A
REFERENCES

A1. S.Guntay, "A Comparative Analysis on OECD-LOFT Experiment LP-02-6", OECD LOFT-T-3410, November 1987.

A2. F. Steinhoff, "DRUFAN-02 Interim Program Description Part 1", GRS-A-685, March 1982.

A3. M. J. Burwell et al., "DRUFAN-01/MOD2 Volume III", GRS-A-846, July 1983.

A4. J. D. Burt, S. A. Crowton, "International Standard Problem 13 (LOFT Experiment L2-5)", EGG-NTAP-6276, April 1983.

A5. V. H. Ransom, et al.,"RELAP5/MOD2 Code Manual, Volume 1: Code Structure, Systems Models, and Solution Methods", NUREG/CR-4312, August 1985.

A6. J. J. Pena, "Postexperiment Analysis of the OECD LOFT Experiment LP-02-6", OECD LOFT-T-3408, May 1985.

A7. "TRAC-PF1/MOD1: An Advanced Best-Estimate Computer Program for Pressurized Water Reactor Thermal-Hydraulic Analysis", NUREG/CR-3858, July 1986.

A8. T. D. Knight, "TRAC Analyses of LOFT LP-02-6", LA-UR-85-3723, October 1985.

NRC FORM 335 (2-89) NRCM 1102, 3201, 3202

U.S. NUCLEAR REGULATORY COMMISSION

BIBLIOGRAPHIC DATA SHEET

(See instructions on the reverse)

1. REPORT NUMBER (Assigned by NRC, Add Vol., Supp., Rev., and Addendum Numbers, if any.)

NUREG/IA-0028
OECD LOFT-T-3900

2. TITLE AND SUBTITLE

Review of LOFT Large Break Experiments

3. DATE REPORT PUBLISHED

MONTH: October YEAR: 1989

4. FIN OR GRANT NUMBER

5. AUTHOR(S)

S. M. Modro, S. N. Aksan, V. T. Berta, A. B. Wahba

6. TYPE OF REPORT

7. PERIOD COVERED (Inclusive Dates)

8. PERFORMING ORGANIZATION – NAME AND ADDRESS (If NRC, provide Division, Office or Region, U.S. Nuclear Regulatory Commission, and mailing address; if contractor, provide name and mailing address.)

Austrian Research Center Seibersdorf
A-2444 Seibersdorf, Austria

Idaho National Engineering Laboratory
Idaho Falls, ID 83415

Paul Scherrer Institute
CH-5303 Wurenlingen, Switzerland

Reactor Safety Corporation
Gesellschaft fuer Reaktorsicherheit
Porschungsgelaende, 8046 Garching
The Federal Republic of Germany

9. SPONSORING ORGANIZATION – NAME AND ADDRESS (If NRC, type "Same as above"; if contractor, provide NRC Division, Office or Region, U.S. Nuclear Regulatory Commission, and mailing address.)

Office of Nuclear Regulatory Research
U. S. Nuclear Regulatory Commission
Washington, D.C. 20555

10. SUPPLEMENTARY NOTES

11. ABSTRACT (200 words or less)

Six non-nuclear and five nuclear large break loss-of-coolant experiments were performed in the Loss-of-Fluid-Test (LOFT) PWR facility at the Idaho National Laboratory. These experiments provided a large amount of data necessary for evaluation and refinement of reactor system computer codes and had major impact on the understanding of large break loss-of-coolant accidents. An overview of these nuclear large break experiments performed under NRC and OECD LOFT programs is given and the major research results are presented.

12. KEY WORDS/DESCRIPTORS (List words or phrases that will assist researchers in locating the report.)

Loss-of-Fluid Test (LOFT)
Organization for Economic Cooperation and Development (OECD)

13. AVAILABILITY STATEMENT

Unlimited

14. SECURITY CLASSIFICATION

(This Page) Unclassified

(This Report) Unclassified

15. NUMBER OF PAGES

16. PRICE

NRC FORM 335 (2-89)

UNITED STATES
NUCLEAR REGULATORY COMMISSION
WASHINGTON, D.C. 20555